Adsorption and desorption processes on polymers in aquatic systems

Dissertation

zur Erlangung des akademischen Grades eines
Doktors der Naturwissenschaften
- Dr. rer. nat –

vorgelegt von

Tobias Horst Uber

geboren in Frankfurt am Main

Lehrstuhl für Instrumentelle Analytische Chemie

der

Universität Duisburg-Essen

2019

DOI: 10.17185/duepublico/70287
URN: urn:nbn:de:hbz:464-20190820-144916-4

Die vorliegende Arbeit wurde im Zeitraum von Juni 2013 bis Dezember 2018 im Arbeitskreis von Prof Dr. Torsten C. Schmidt am Institut für Instrumentelle Analytische Chemie der Universität Duisburg-Essen durchgeführt.

Tag der Disputation: 16.07.2019

Gutachter: Prof. Dr. Torsten C. Schmidt

Prof. Dr. Franziska Träger

Vorsitzende: Prof. Dr. Mathias Ulbricht

Danksagung

Mein besonderer Dank gilt Herrn Prof. Dr. Torsten Schmidt von der Universität Duisburg-Essen, als Erstgutachter. Er hat es mir ermöglicht, die vorliegende Arbeit mit größtmöglichem, wissenschaftlichem Freiraum anzufertigen. Ebenso gilt meine höchste Dankbarkeit Frau Prof. Dr. Sibylle Planitz von der Westfälischen Hochschule, als Betreuerin dieser Arbeit. Ihre langjährige Begleitung in der Wissenschaft, beginnend mit der Bachelorarbeit, über die Betreuung Ihrer Praktika, führte letztendlich zu dieser vorliegenden Doktorarbeit. Zusätzlich danke ich Frau Prof. Dr. Träger von der Westfälischen Hochschule, die aufgrund unvorhergesehener Umstände als Zweitgutachterin einspringen konnte.

Ein großer Dank gilt Dr. Thorsten Hüffer von Universität Wien, dessen exzellente Anmerkungen und Korrekturen einen großen Einfluss auf die Kapitel 3 und 4 dieser Arbeit haben. Ebenso danke ich Dr. Florian Metzelder, dessen Kommentare and Anmerkungen einen großen Teil zu der Fertigstellung von Kapitel 5 lieferten.

Weiterhin danke ich allen Mitarbeitern der Westfälischen Hochschule in Recklinghausen, die mir immer ein offenes Ohr geschenkt haben und in der Kaffeeküche oft Kuchen zur Verfügung stellten. Ganz besonders möchte ich mich hier bei Heiko Tewes, Daniel Junghans und Dr. Ingo Tausendfreund bedanken.

Des Weiteren danke ich der Firma Axel Semrau und allen aktuellen Mitarbeitern, die mich herzlich in Ihrem Kreis aufgenommen haben. Ausdrücklich möchte ich hier Titus Breski danken, dessen Bachelorarbeit ich betreuen durfte. Die Diskussionen mit Ihm lieferten viele Ansätze zu dieser Arbeit.

Ich danke Dr. Marc Wiechers für die mittlerweile mehr als zehnjährige Begleitung und für die konstruktiven Diskussionen. Ich danke ganz besonders meiner Frau Melanie. Ihre Begleitung und Motivation in den letzten sechs Jahren führte letztendlich dazu, dass diese Arbeit fertig gestellt wurde.

Ich danke weiterhin meiner Mutter Beate, ohne die ich es wahrscheinlich niemals so weit in der Welt gebracht hätte. Vielen Dank Mutti! Ebenso danke ich meiner ganzen Familie, speziell auch meinen Schwestern Laura und Anna-Marie sowie meinem Vater Jörg, seiner Frau Moni und meinem Stiefvater Uli, die immer stets zu mir gehalten haben. Ebenso danke ich all meinen Freunden für Ihre Unterstützung der letzten Jahre und das regelmäßige Erkunden zu dem Stand der Doktorarbeit.

Summary

The sorption behaviour of high-density polyethylene (HDPE) and some other plastic materials in the aquatic environment with non-ionic organic compounds has already been studied to some degree although there is not yet a systematic approach to determine the sorption properties for a larger compound set. With the steady increase of interest on plastic materials in the environment, especially due to micro plastic particles (MP) or the great garbage patches, an increased demand for estimating sorption behaviours of those materials is mandatory. This is not only the case for HDPE but also for other plastic materials such as polystyrene (PS), low-density polyethylene (LDPE) or polyacrylate (PA). To this end, this thesis aims at a systematic investigation of sorption behaviour of selected plastic materials by use of probe sorbates in an aquatic environment.

Sorption batch experiments with HDPE material used for water pipes and selected probe sorbates were carried out in a three-phase system (air/HDPE/water) covering an aqueous concentration range of at least three orders of magnitude. Sorption in the concentration range below 10^{-2} of the aqueous solubility was found to be nonlinear and the Freundlich model was used to account for this non-linearity. Multiple regression analysis (MRA) using the determined distribution coefficients and literature-tabulated sorbate descriptors rendered robust ppLFER models for all three concentration levels. Sorption was found to be dependent on polymer density and crystallinity by the ppLFER model and the derived ppLFER model described sorption more accurately than commonly used single-parameter predictions (spLFER). A comparison of predicted data to experimental data from literature and this work demonstrated the strength of the ppLFER, based on the training set over several orders of magnitude.

Batch experiments with PS were done with the same experimental approach but isotherms were evaluated with additional sorption models. The Freundlich fit rendered again the most robust data and it was shown that sorption of organic compounds to PS foil in water is nonlinear and that absorption is the dominant sorption mode. The properties directing the sorption to PS are impacted by non-specific and specific interactions. The specific interactions are driven mainly by the bipolarity/polarizability and it is shown to be influenced by the aromatic π-π-interactions of PS with the sorbates. As with other non-polar plastics, sorption is also driven by hydrophobic interactions.

A novel approach to determine distribution data is the inverse liquid chromatography (ILC) that was applied to HDPE. This is one of the first times the sorption behaviour of an environmentally relevant plastic material is investigated applying the ILC approach. The packed ILC columns rendered robust data that are comparable to data generated with the batch approach. The distribution coefficients from aged HDPE material were investigated under salty and salt-free conditions. The sorption strength for non-polar compounds did not change for aged HDPE compared to new HDPE material, whereas sorption for polar compounds did decrease significantly. Ionic strength of the eluent had a minor effect on sorption for both groups. The work showed that the ILC approach to investigate sorption properties under environmentally relevant conditions is promising and represents a feasible alternative to batch experiments.

This thesis demonstrates that a systematic approach to determine sorption behaviour with the help of probe sorbates renders robust results into molecular interactions with plastic materials in water. It also shows the benefit when using the ILC approach over the batch approach, in terms of easy variability of experimental conditions and time spent.

Zusammenfassung

Das Sorptionsverhalten von hochdichtem Polyethylen (HDPE) und einigen anderen Kunststoffen in der aquatischen Umwelt mit nicht-ionischen organischen Verbindungen wurde bisher nur teilweise untersucht. Eine systematische Herangehensweise, um die Sorptionseigenschaften für ein großes Substanzset zu bestimmen, existiert bisher nicht. Durch das immer weiter steigende Interesse an Kunststoffen in Wasser, speziell aufgrund der Thematik um Mikroplastik (MP) oder den „Müllstrudeln“ in den Ozeanen, ist das Abschätzen des Sorptionsverhaltens von Kunststoffen in Wasser von großem Interesse. Dies ist nicht nur der Fall für HDPE, sondern auch für andere Kunststoffe wie Polystyrol (PS), niedrigdichtem Polyethylen (LDPE) oder Polyacrylat (PA). Zu diesem Zweck ist das Ziel dieser vorliegenden Arbeit eine systematische Untersuchung des Sorptionsverhaltens ausgewählter Kunststoffe in der wässrigen Umwelt mithilfe einiger Modellsubstanzen.

Batchexperimente mit HDPE, welches für den Bau von Trinkwasserleitungen verwendet wird, und ausgewählten Modellsubstanzen wurden in einem Drei-Phasen-System (Luft/HDPE/Wasser) durchgeführt. Der gewählte Konzentrationsbereich verlief dabei über drei Dekaden, beginnend bei zwei Dekaden unterhalb der wässrigen Löslichkeit der Sorbate. Die Sorption innerhalb dieses Konzentrationsbereichs war nichtlinear, und das Freundlich-Modell wurde verwendet, um diese Nicht-Linearität zu berücksichtigen. Eine multiple Regressionsanalytik (MRA) mithilfe der bestimmten Verteilungskoeffizienten und Literatur-Deskriptoren der Sorbate lieferten ein robustes Modell nach der Poly-Parameter-linearfreien Energiebeziehung (ppLFER-Modell) bei allen drei Konzentrationsbereichen. Das Sorptionsverhalten anhand des berechneten ppLFER-Modells in diesem Bereich war abhängig von der Dichte und Kristallinität des Kunststoffes. Das Abschätzen der Verteilungskoeffizienten mithilfe des ppLFER-Modells war zudem wesentlich genauer als das Abschätzen anhand eines Ein-Parameter-Modells (spLFER). Ein direkter Vergleich von experimentellen, abgeschätzten und Literaturdaten demonstrierte die Stärke des ppLFER-Modells.

Sorptionsdaten für PS wurden anhand des gleichen experimentellen Vorgehens bestimmt, jedoch wurden die Daten mithilfe weiterer Sorptionsmodelle ausgewertet. Das Sorptionsmodell nach Freundlich lieferte die robustesten Daten und zeigte, dass die Sorption an PS nichtlinear verlief und Absorption der dominierende Sorptionsmodus ist. Die bestimmenden Sorptionseigenschaften bei Sorption an PS sind nicht-spezifische und spezifische Interaktion. Dabei werden die spezifischen Interaktionen größtenteils von der

Bipolarität/Polarisierbarkeit beeinflusst. Dabei spielen größtenteils die aromatischen π-π-Wechselwirkungen von PS und den Sorbaten eine Rolle. Wie mit anderen unpolaren Kunststoffen wird die Sorption an PS ebenso von hydrophoben Wechselwirkungen beeinflusst.

Eine neuartige experimentelle Methode zur Bestimmung von Sorptionskoeffizienten ist die Inverse Flüssigchromatografie (ILC), welche für den HDPE-Kunststoff verwendet wurde. Dies ist eine der ersten Studien, die das Sorptionsverhalten eines umweltrelevanten Kunststoffes mit Hilfe der ILC untersuchen. Die gepackte ILC-Säule generierte robuste und vergleichbare Daten zu den Batchexperimenten, und es konnten die die Sorptionseigenschaften von gealtertem HDPE in salzhaltigem und salzfreiem Wasser untersucht werden. Die Sorptionsstärke von unpolaren Substanzen änderte sich im Vergleich zu neuem HDPE nicht, wohingegen sich die Sorptionsstärke für polare Substanzen signifikant reduzierte. Die ionische Stärke des Eluenten hatte hingegen keinen signifikanten Einfluss auf polare oder unpolare Substanzen. Generell zeigte die Untersuchung mithilfe des ILC-Ansatzes eine elegante Alternative, um Sorptionseigenschaften in umweltrelevanten Umgebungen zu untersuchen und zeigte eine vielversprechende Alternative zu Batchexperimente.

Diese Arbeit demonstrierte, dass ein systematischer Ansatz zur Untersuchung des Sorptionsverhaltens mithilfe von Modellsubstanzen einen robusten Einblick in die molekularen Interaktionen von Kunststoffen in der wässrigen Umwelt liefert. Ebenso zeigte die Bestimmung von Sorptionseigenschaften mithilfe des ILC-Ansatzes eine robuste, variable und einfache Alternative.

Table of Contents

Table of contents

Chapter 1 General Introduction

1.1 Plastic Materials

1.1.1 Theoretical Background on Plastic Materials

Plastics are polymeric materials consisting mainly of carbon (C) and hydrogen (H) [1]. The term *plastic* exhibits from the Latin word *plastein* (to form, to shape) which represents the simple handling and processability. The plastic material itself is an organic polymer synthesized out of monomers or prepolymers [2, 3]. The basic units are monomer molecules that are linked by polymerization, leading to oligomers or prepolymers *(oligos = few*) and then to polymers (*poly = many*). According to IUPAC the term polymer is a synonym for a macromolecular substance, consisting of many macromolecules (=polymer molecules) [4]. Organic macromolecules consist of many different base units which are formed by different chemical or biological reactions (synthesis) from the base compounds (e.g monomers) (Figure 1-1). The synthesis reaction of polymers is mainly induced by catalysts or initiators and heat. In general, polymers can be of natural or synthetic origin. Prominent examples for natural polymers are natural rubber (NR), cellulose and amylose. They are used commercially as plastic materials either directly (NR latex) or after treatment with some chemical modifications (e.g. vulcanized natural rubber NR)[5].

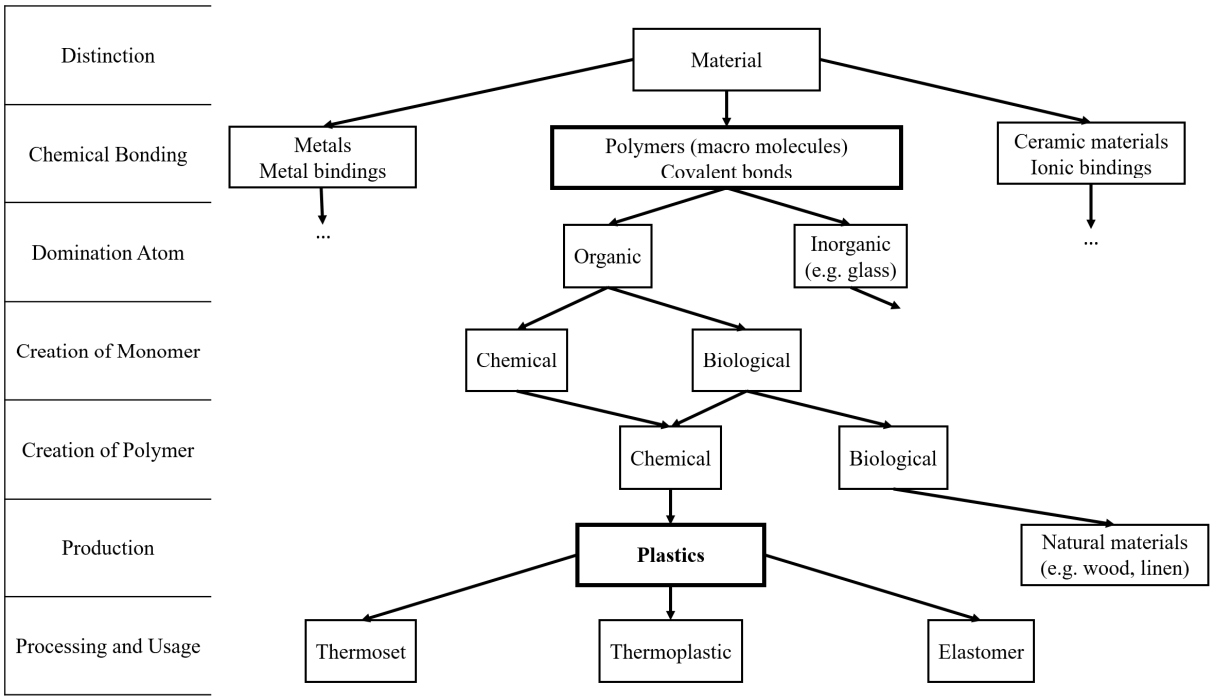

Figure 1-1 - Classification of plastic in contrast to other material classes [3]**.**

In different languages, the terms *plastic* and *polymers* are often used as synonyms which can lead to confusion. The monomers, prepolymers and polymers are basically raw materials for plastic production. In short, plastic is a polymer that is synthesised, modified used as a (technical) material. Normally additives are incorporated to give the desired properties of colour, strength, etc.)

Polymers themselves can be separated into three major groups depending on their mechanical and thermal properties: *thermoplastics*, *thermosets* and *elastomers* (Figure 1-1)[4].

Thermoplastics are the most widely used group of polymeric materials. On a molecular level they consist of unconnected long chains of linear or branched macromolecules (Figure 1-2 a). At high temperatures the cohesive forces between the chains are overcome and they form a melt that can be shaped into any form during cooling. This process can in theory be repeated any number of times. Every time the material is heated up, breaking of the polymer chains will occur. The group of thermoplastics is further divided into completely amorphous and partially crystallized polymers. All thermoplastics are hard, brittle and solid below their glass transition temperature (T_g), where chain mobility is not possible. Above T_g the chains gain mobility and start to move, thus softening the material. Amorphous polymers will be used at temperatures above T_g (Figure 1-3). Examples are polystyrene (PS), polymethylmethacrylate (PMMA) and polyvinylchloride (PVC) [6, 7].

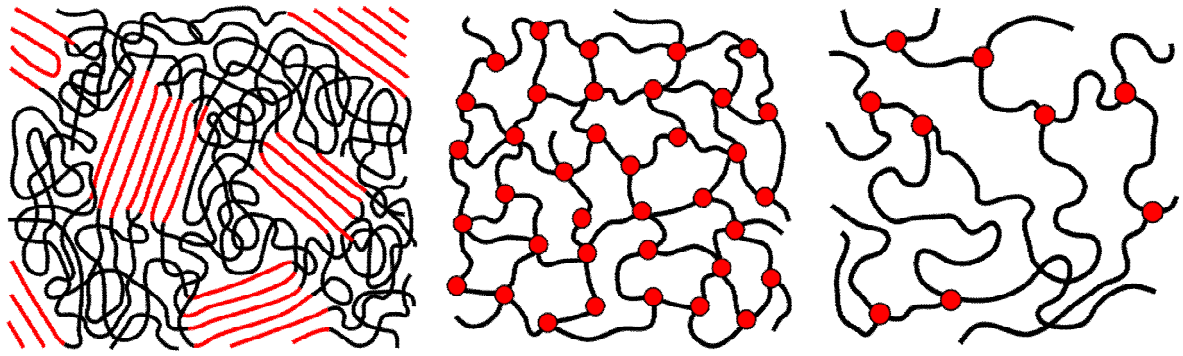

a **b** **c**

Figure 1-2 - Different groups of plastics, based on their monomeric units. a) partially crystalline Thermoplastic with amorphous and crystalline areas b) Thermosetting resin c) Elastomer.

Partially crystalline polymers still retain highly ordered areas of quasi-crystallinity at temperatures above Tg, that will remain stable until a melting temperature T_m is reached. They thus exhibit flexibility and strength combined in the area between T_g and T_m, their primary usage temperature. Prominent examples for partially crystalline thermoplastics are the polyolefines (PE, PP), polyethyleneterephthalate (PET) and the polyamides (PA)

Thermosetting resins are polymerised out of low-molecular weight components, each monomer containing more than 2 crosslinking functions, thus leading to highly crosslinked materials (Figure 1-2 b). The final form is determined during the polymerisation or hardening step and can only be modified by machining (e.g. milling, planing, turning, grinding). As a thermoset is mainly a single macromolecule reheating does not lead to reshaping of the material. High temperatures will lead to chain breakage and thereby to decomposition. Thermosetting resins are very brittle and hard materials (Figure 1-3). Prominent examples for thermosetting resins are polyurethane (PUR) or unsaturated polyester resins (UP) [7].

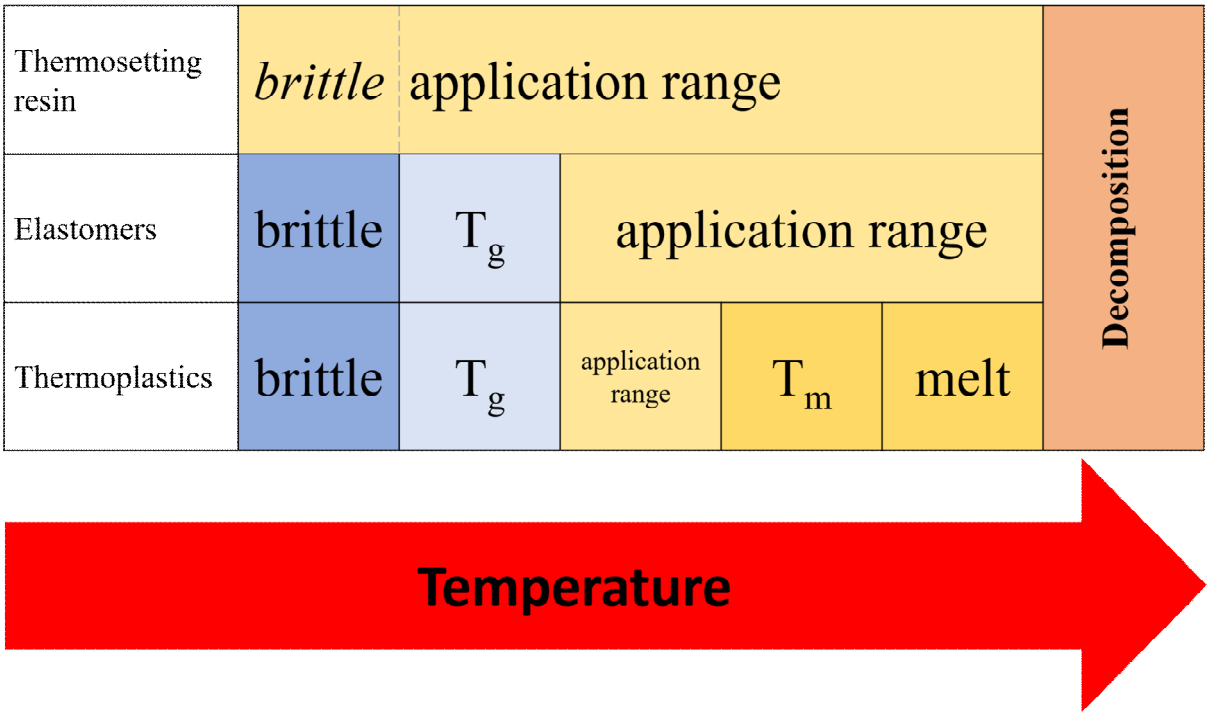

Figure 1-3 - Thermal properties of plastic materials. T_g represents the glass transition temperature and T_m the melting temperature.

Elastomers too are crosslinked, but the crosslink density is much lower than for thermosets. They are used at temperatures above T_g, when the amorphous parts move freely, thereby making the material quite soft and flexible. The crosslinks limit maximum displacement and cause the elasticity. Those materials can undergo massive deforming by pull- and push-forces and will go back to their initial form afterwards without any tear. (Figure 1-2 c). Below T_g the elastomers loose that elastic ability (Figure 1-3). Prominent examples are natural rubber (NR) or butadiene rubber (BR). The mechanical properties are highly influenced by the amount of crosslinking (vulcanization) [7].

1.1.2 Plastic materials in the economy

The use of plastics has dramatically increased in the last 50 years due to a number of features: integrated production methods (1 step), low cost of material, very good specific properties, such as strength per volume, low electric conductivity, very good variability of properties by polymer variation and use of additives. Plastic materials are being used as a substitute for wood, metal, stone, glass and ceramic. For many applications plastics have already been incorporated to substitute the predominant materials for more than hundred years [8, 9]. Figure 1-4 shows the production volume of plastic material, steel and aluminium from the 1950th until 2010. The production volume of plastic materials had a steady increase. Before the 1950s, plastics were mainly products for special applications. Baekeland with the discovery of bakelit [10] or Staudinger with the finding, especially for the thermoplastics, that plastics are made of longer chains consisting of macromolecules [11] are few examples for the research before the 1950s on plastics. The second world war did increase the development of new plastics materials since there was a need to preserve natural resources. Nylon, a polymer used for parachutes, ropes or body armor was developed by Wallace Carothers in 1935. Plexiglas, poly(methyl methacrylate) (PMMA), proved to be a very efficient substitute for conventional glass to be used in aircraft windows. In the united states the plastic production increased during World war II by 300 % [12]. Polytetrafluoroethylene (Teflon), a plastic developed for the nuclear weapon industry, was approved for food applications in the 1960s generating all kinds of non-stick cookware [9, 13]. It was a non-conductor of electricity, immune to bacteria and it was slippery. After world war two, those properties were the ones that brought it to almost every household in one way or another. The well-known Tupperware, made of polyethylene, is another prominent example that has been in household kitchens for over 70 years, and also became more and more famous after world war two [14].

By changing the main resource for plastic production from coal to petrochemical resources in the mid-1950s the plastic production and development got a major push. From the high demand for heating oil, which as a side product from refining gives lighter fuel fractions that are used mainly for ethylene production, plastic production was cheap. Especially the thermoplastics PP, PE, PS and PVC did benefit from the change to a different resource for plastic production. Today roughly 5 % of the world's petroleum production is converted into polymer materials [1]. With the switch to a different source, developments in the field of synthetic polymers, especially plastics, increased steadily. There is a considerable potential for new applications of plastics that will bring benefits in the future, e.g. as novel medical

applications, in the generation of renewable energy and by reducing energy used in transport [15].

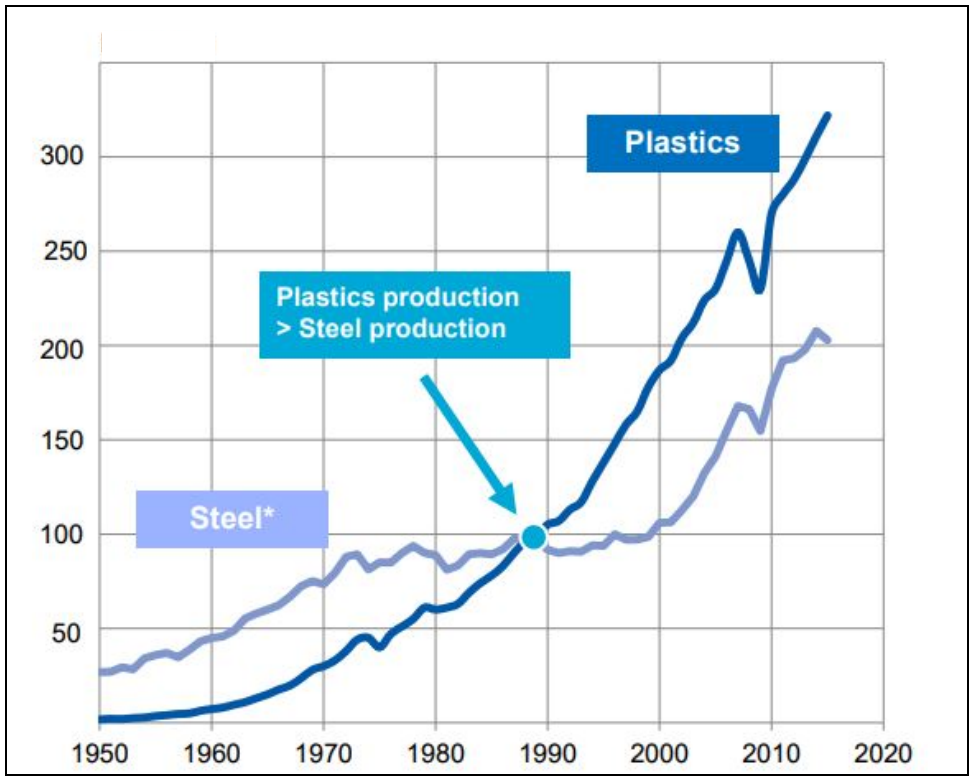

Figure 1-4 - Global production volume (Mio. m^3) of polymers, steel and aluminium from 1950 to 2015 [7, 16]**.**

One of the big advantages of plastic materials is that mass production of all kinds of different forms is easy to achieve. The only bigger investment that needs to be done is the initial development of a certain polymer that can be used to create the plastic material. The reduced costs for plastic materials can lead to more availability of commodities for many different demographic groups.

1.1.3 Technical applications

The main use of plastic has changed over time, from supplementing basic materials (e.g. plexi glass for conventional glass) to convenience products (e.g. cups, cutlery). As Figure 1-5 shows for Europe in 2015 most of the plastic that is produced is designed as packaging material or for construction purposes. It is either PE (low-density, high-density, linear low-density or medium-density) and PP for packaging or expanded PS (PS-E) or PVC for the construction industry. Those fields comprise almost 60 % of the used plastics in Europe and are also the main source for environmental litter [17]. Depending on the application requirements, the plastic material can be designed for food packaging (according to health standards), for the pharmaceutical industry (i.e. blood samples), or as a very durable and protecting packaging

material against shock or weather impact (in the electronic industry). A large fraction is used for all kinds of end products, e.g. polyacrylate (PA) or polyoxymethylene (POM) as gear wheels, PE as foils or cutlery. In the car industry polyamide 66 (PA 66) is used for tires, polyurethane (PU) foam as cushion material [18]. In any case, the plastic material is designed to be very durable even under degrading conditions, e.g., in the environment from sun light (UV-rays). This is indicated in Figure 1-5 with the average lifespan of the material class once in the environment. Besides the packaging and construction industry, plastic materials have been used for many other day to day products like convenience products. In different lotions and toothpastes, plastic particles were added for cleaning functionality [19]. Those additive fillers have already been banned in many countries worldwide due to their possible side effects to the environment [20, 21]. The plastic industry tries to overcome the environmental impact of plastic materials in several ways.

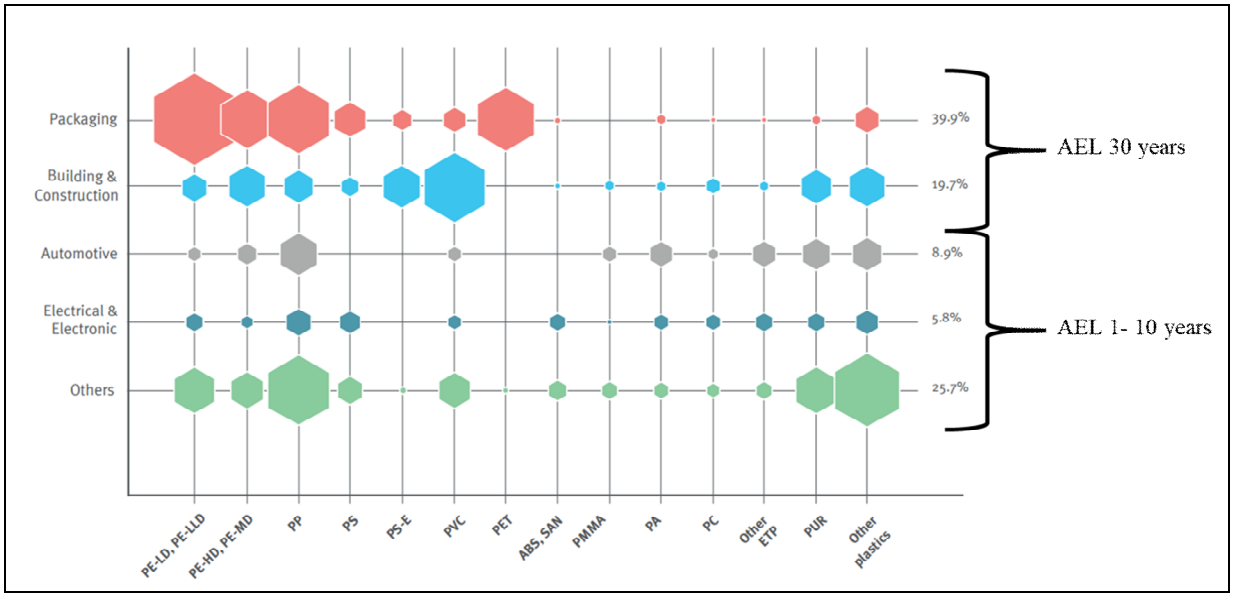

Figure 1-5 - European plastic demand in 2015 by industrial branch [7]**. AEL represents the average environmental lifespan of the plastic material group in the environment.**

1.1.4 Plastic waste in the environment

Handling plastic waste

With the high demand for new plastic materials to deliver a cheaper substitution for conventional materials like metal or ceramics, there comes also an ecological cost. Be it the "free" cost of use of air, water and land due to industrial parks producing plastic materials, but also the high energy consumption in the production, use and disposal of plastics [1]. But compared to other industrial branches (i.e. transportation, industry or residential &

commercial), the energy data are in favour for the plastic industry as are the amounts for air and water employed in the production and the use and disposal of plastics [22]. This is demonstrated in Figure 1-6 by data from the U.S. energy consumption. Especially the disposal of plastics in Europe has seen drastic changes in the recent years. Almost 70 % of the plastic waste from 2014 was recovered through recycling and energy recovery whereas only 30 % still went to landfills [7]. With more countries within Europe exhibiting a landfill ban, this number will be further decreased.

There are environmental concerns to plastics that are undeniable, including possible harmful effects by the plastic itself, the polymer used or any by-products from either production or combustion. Polymerisation reactions are rarely complete and unreacted residual monomers can be found in the resulting plastic material [23]. Using landfills as a disposing method will contain many of those effects but it is estimated that roughly 1 million tons of plastic are disposed into the high seas annually [1] resulting in an estimated 5 trillion plastic pieces [24]. There are several ways to overcome this. The most important one is to enhance the post-consumer recycling to prevent disposal into the seas and in general a proper waste management. This faces many issues, e.g. unsorted recycled polymers represent a mixture of different polymers which might need different treatment. Separating those mixtures is sometimes overcome by density separation but needs further improvement [25, 26]. Another approach would be to promote the use of biodegradable plastics. They are made of biodegradable polymers like cellulose, poly(lactic acid) or contain starch [22]. Once in the environment, as landfill or disposed in the oceans, degradation of biodegradable plastics occurs through hydrolysis, UV radiation or by bacteria [27, 28]. The downside is, that biodegradation is generally slow and thus will take up much landfill space and therefore is also not the general solution to overcome the amount of plastic waste.

Recycling involves many (costly) steps, from separating household plastic waste to refurbish the material. The costs for recycling vary between 35 % and 80 % of the costs of the virgin material. And this accounts only for thermoplastics since they can be reshaped. Thermosets cannot be recycled. However, after fine grinding they can be added to virgin resins as fillers between 15 % - 30 % without significant physical change of the end product [1]. A good example where recycling of plastic products does work very well, are the reusable high-density polyethylene (HDPE)- or Polyethylene terephthalate (PET)-bottles. The bottles demonstrate very well the value plastic waste can have, when properly recycled. Due to recycling the energy that was used for production can be spread over multiple lifetimes of the final plastic bottle [22]. Another good example are car tires that are being used as a fuel for the

concrete production. There, the tires are introduced at very high temperatures where they will combust and act as fuel for the concrete manufacturing. To date, tires are one of the most powerful alternative fuels, because of their low moisture levels and very high energy content above 30 MJ kg^{-1} [29].

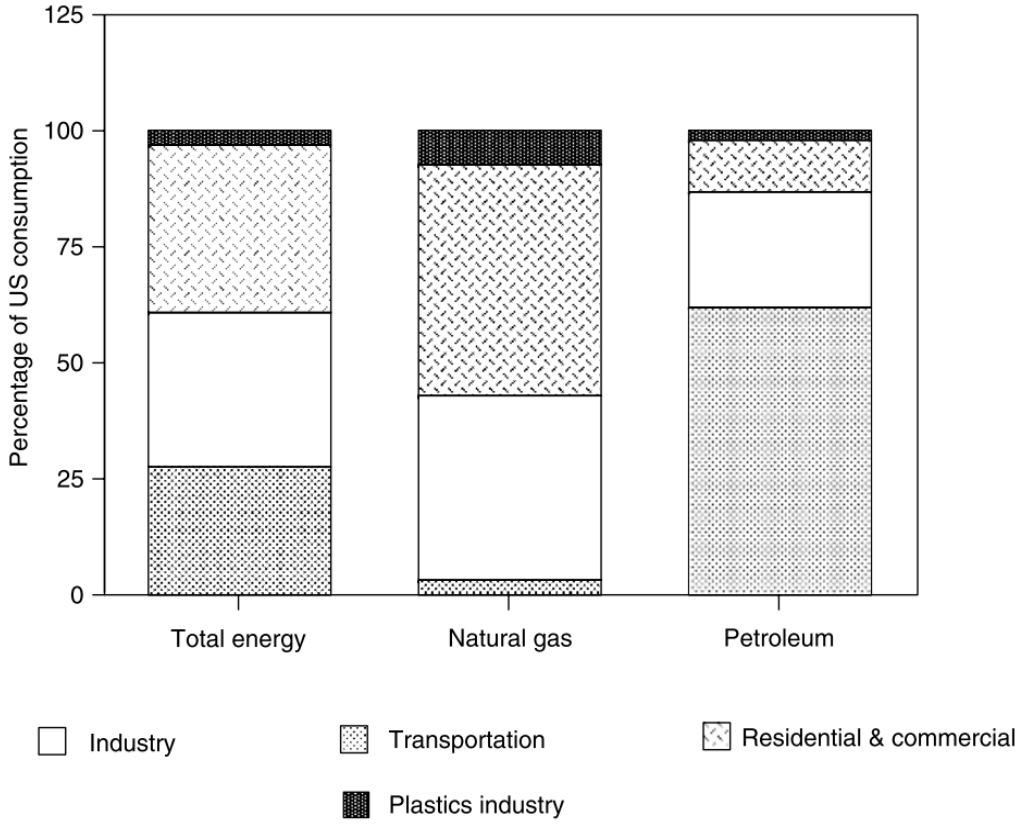

Figure 1-6 - Estimated energy consumption by U.S. plastics industry relative to that by other sectors (based on Plastics and the Environment, 1998) [22].

Plastic waste in the oceans

Despite recycling, which is demonstrating a good alternative for used plastic materials, an increasing problem worldwide is the disposal of plastic materials into the environment, either into domestic rivers, forests or into the oceans. There have been many reports in the last 30 years on the occurrence of multiple floating plastic objects in the oceans, accumulating into *islands*. In contrast to the common opinion those *garbage patches* are not real islands only consisting of plastic waste. Rather, in these regions there is an exceptionally high relative concentration of plastic materials, chemical sludge and other debris [22, 30]. This waste is trapped by the currents in the ocean gyres. Those gyres are in every ocean and are induced by the ocean currents (Figure 1-7). The biggest *garbage patch* has a size as big as china and has

been described in 1988 by the National Oceanic and Atmospheric Administration of the united states. There the discoveries of enormous stretches of floating debris in regions governed by oceans current were reported by several researchers [31].

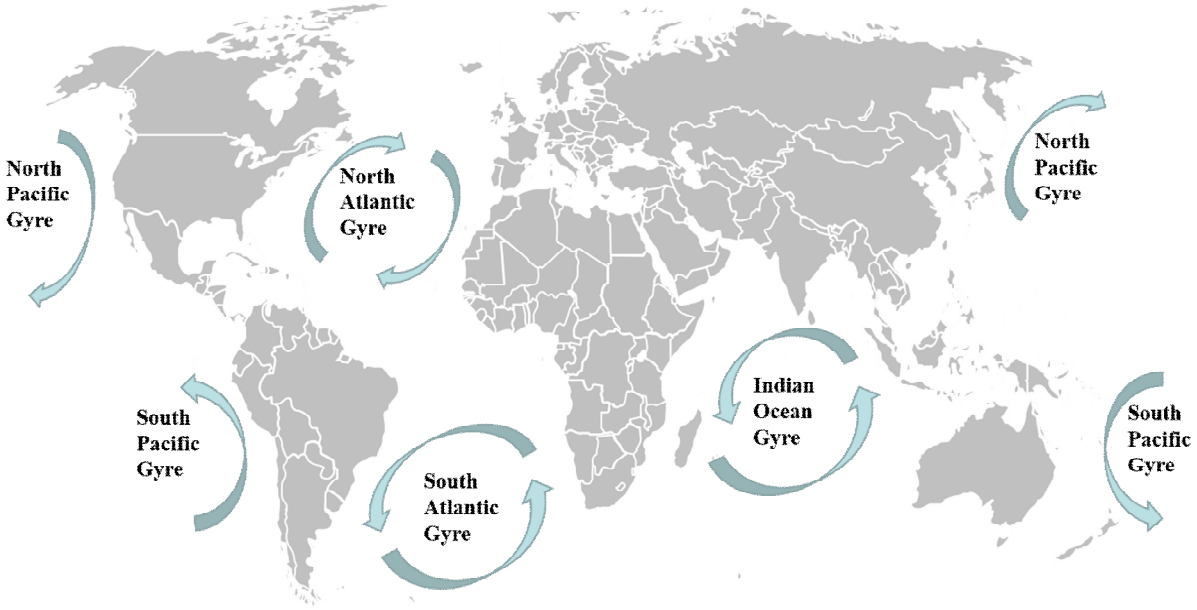

Figure 1-7 – Schematic locations of the major garbage gyres of the world's oceans.

It is not only the visible plastic particles that are floating in the oceans. Plastic pieces and particles below the water surface, floating or on the ground are also of major concern. It has been reported that the mean abundance for plastic pieces of the biggest *garbage patch* is about 334271 pieces per km^2 or 5114 g per km^2 and most of its particles are actually beneath the water surface [32]. Furthermore, smaller plastic particles barely visible for the human eye are a much greater threat to the marine ecosystem. More than 90 % of plastic pollution is actually made up of particles smaller than a fingernail [33]. As stated above, plastic is not biodegradable, but it is UV- and mechanical stress-degradable. Through degradation those plastic particles will get smaller over time, and eventually end up in the small micro meter size. Those particles are then called *micro plastics* and the discussion on the threat of these *micro plastic particles* (MP) is ongoing [34]. Besides degradation of plastic waste (primary MP), the convenience product industry is another source of the MP (secondary MP), e.g. cosmetic products [35], as stated above. In the US, according to Gouin et. al. [36], an estimate on daily emission of microbeads for hand wash alone, would be about 1 gram per capita, per year. This would lead to roughly 300 tons a year of MP flushed into the sewage plants. Discussions are on the actual capability of sewage plants not being able to filter those MP from the water [37, 38]. As is evident from Figure 1-8, the interest in microplastics in the environment has seen a drastic increase in the last seven years. Especially their sorption behaviour in the environment is of

major interest. Initial considerations suggested that persistent organic pollutants (POP) could be transported by these particles through sorption all the way into the human food chain [30, 39–45]. Recent studies claimed that the threat for accumulation in the food chain is neglectable [46, 47] but other studies demonstrate a transport of PAHs by polyethylene [48]. In general, the threat of MP in the environment can't be neglected, and as other effects than accumulation in the food chain have not been investigated enough yet [49].

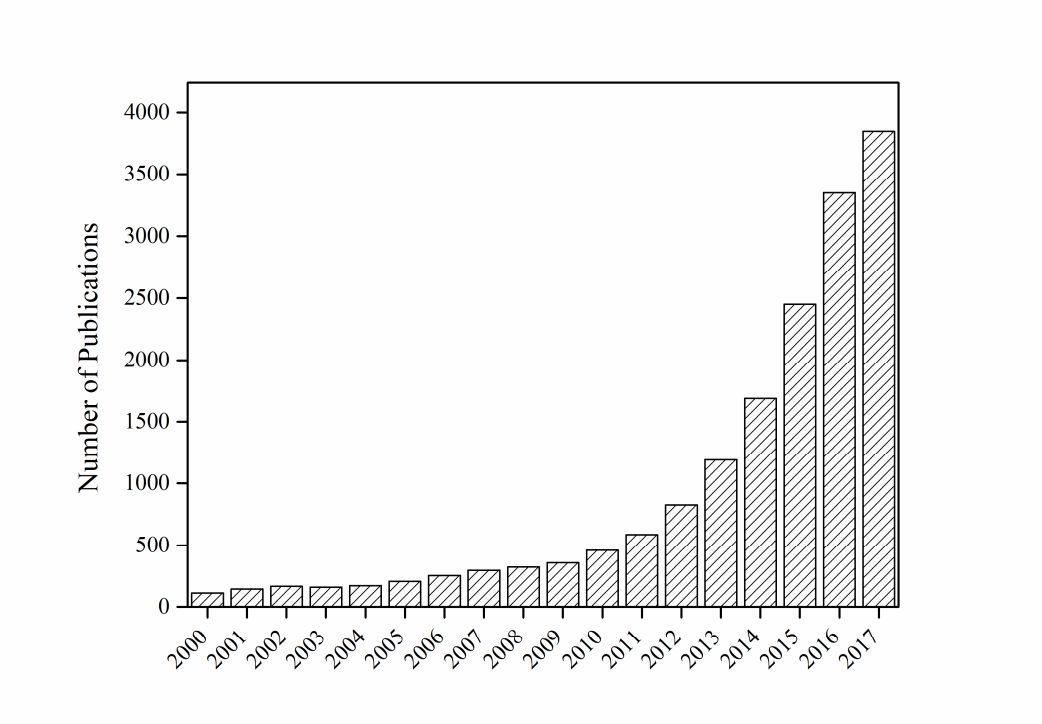

Figure 1-8 - Number of publications on "microplastics in the environment" between the year 2000 and 2017. Data was gathered from Google Scholar August 31st, 2018.

An increased knowledge on the sorption behaviour plastics in water can help to bring about a better understanding to improve sorption assessment for plastics in the environment (e.g. plastic waste and MP) and also technical applications (e.g. water pipes). In order to achieve an improved understanding, further insight into underlying mechanisms affecting sorption behaviour is necessary.

1.2 Theoretical Background on Sorption

1.2.1 General sorption mechanism

The distribution of a compound *i* (sorbate) between phase *a* and phase *b* (sorbents) is defined as sorption, where one is a solid (e.g. plastic) and the other can be either liquid or gaseous (e.g. water). The sorption mechanism itself consists of *ad*- and *ab*-sorption and can be followed by *a de*-sorption mechanism. It is *ad*-sorption when the molecular interaction to a phase is only to its surface (Figure 1-9.I), *ab*-sorption when the molecules of compound *i* move into the phase (*a* or *b*) by either spontaneous formation of cavities, defects within the structure or open voids (Figure 1-9.II). It is *de*-sorption when the connection that was formed during *ad- or ab*-sorption, is disconnected and the molecule *i* goes back into its origin phase *(*Figure 1-9.*III)*. The process of *ad*- or *ab*-sorption and *de*sorption is specified as sorption [50].

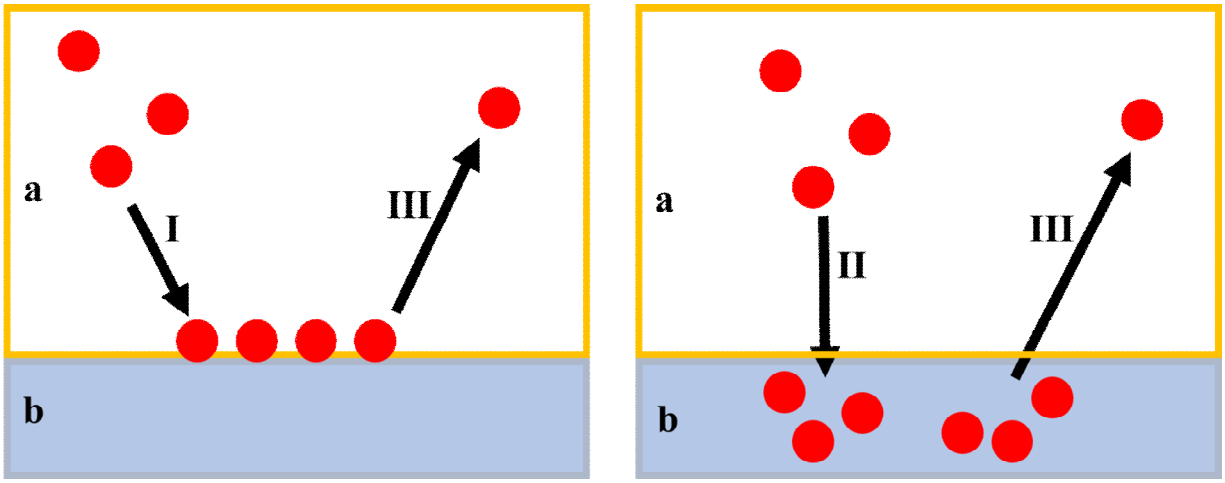

Figure 1-9 - Differences of *ad*sorption (I), *ab*sorption (II) and *de*sorption (III) between phases *a* and *b*.

1.2.2 Sorption

The process of *ad-/ab*sorption and *de*sorption will always depend on the total sorbate concentration in the solid ($C_{i,s}$) and the sorbate concentration in the solution ($C_{i,w}$) at a constant temperature [50]. To mathematically describe the *equilibrium* distribution of a chemical between those two phases at a constant temperature, the distribution coefficient (K_d) is calculated as the ratio between $C_{i,s}$ and $C_{i,w}$:

$$K_d = C_{i,s}\ C_{i,w}^{-1} \qquad \text{(Eq. 1-1)}$$

To generate data for the calculation of K_d, usually *sorption isotherms* are gathered from experimental investigations of distribution coefficients within a specified concentration range.

1.2.3 Determining distribution coefficients

Batch approach

One approach to generate sorption isotherms are batch experiments, where a certain amount of sorbate is spiked to a mixture of the two phases of interest (i.e. plastic and water). Sometimes this is also done with a third phase being air. Then the mixture is brought to equilibrium conditions at a constant temperature, usually by over-head shaking for several days. The amount of the sorbate in the water and solid phase is either determined via chromatographic experiments for both phases (GC, LC), or one can be calculated via mass balance. The concentration data $C_{i,w}$ and $C_{i,p}$ are then plotted against each other and fitted to a *sorption model*. If sorption would be linear, K_d is constant and independent of concentration, otherwise non-linear sorption is present and K_d is concentration dependent and determined by a higher order sorption model. Several of these sorption models exhibit many different approaches. The ones applied in this work are presented in the next section.

Inverse liquid chromatography

A more novel experimental approach to determine distribution coefficients is the inverse liquid chromatography (ILC). Inverse chromatography, mostly gas chromatography, has already been applied to several compounds to determine sorption parameters [51]. In the past years, an increasing number of ILC experiments were undertaken to determine distribution coefficients [52, 53]. Figure 1-10 shows a typically instrument setup for ILC experiments. There, the sorbent is packed into a LC column, and then flushed with a liquid medium (i.e. water). Depending on the sorption strength of the sorbent and material properties (i.e. soft materials can lead to compression of the particles), the sorbent material needs to be mixed with inert material, to avoid irreversible sorption and to decrease the experiment time. Once the column is under equilibrium conditions, the sorbates are injected onto the column. The detection is then done via different detectors like UV-vis (UV) or refractive index (RI). From the retention time of the sorbate, the retention time of a non-retained tracer and the column dimensions, the distribution coefficient can be calculated. Details on the different calculation approaches can be found in the literature [54] and are also explained in Chapter 5.

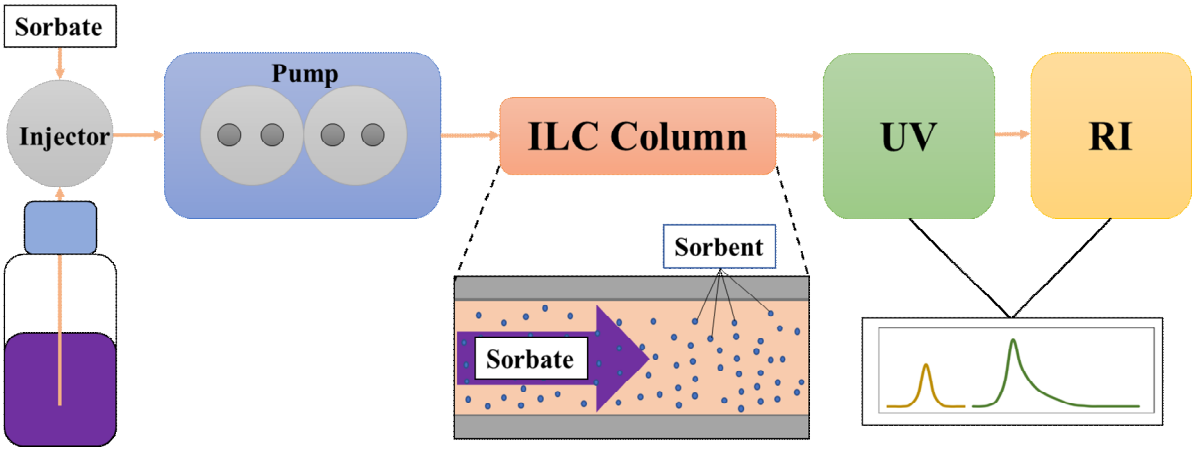

Figure 1-10 - Scheme of an experimental set up for inverse liquid chromatography (ILC) with a UV-detector (UV) and a refractive index detector (RI).

1.2.4 Sorption models

Linear sorption

The simplest approach to describe the sorption is the assumption that the affinity for both sorbent phases is consistent over the observed concentration range (Equation 1-2). The so called linear sorption is commonly used to describe sorption in the case of complicated sorption mechanisms, but where simple calculations are sufficient, even at very low concentrations. [50].

$$C_{i,s} = a \cdot C_{i,w} \qquad \text{(Eq. 1-2)}$$

Freundlich model

The non-linear model that has been frequently incorporated in statistics on sorption relevant data is the assumption by *Freundlich* (FM). There, the assumption is that there is unlimited sorption capacity and that the availability of sorption sites is equal over the observed concentration range. The relationship can be described as follows [50]:

$$C_{i,s} = K_{i,F} \cdot C^{ni}_{i,w} \qquad \text{(Eq. 1-3)}$$

where $K_{i,F}$ is the Freundlich coefficient for the corresponding sorbate (i), usually expressed in the units of $C_{i,s}$ and $C_{i,w}$ $[(\mu g\ kg^{-1})\ (\mu g\ L^{-1})^{1/n}]^{-1}$ and n is the Freundlich exponent [-]. For ease of fitting experimental data to the model, there is also a linearized version of the model:

$$\log C_{i,s} = n_i \cdot \log C_{i,w} + \mathrm{Log}\ K_{i,F} \qquad \text{(Eq. 1-4)}$$

If in any case the Freundlich exponent n =1, sorption would be linear (see Equation 1-2)[50]. The value of n will also indicate the general linearity of the isotherm. A high deviation from 1 (negative or positive) will reflect the degree of isotherm nonlinearity [50].

Langmuir model

Another common non-linear model to describe sorption is the *Langmuir Model* (LM). It describes sorption based on the formation of a monolayer on the sorbent surface and with that a limited number of free sorption sites. The relationship via the LM is described as follows [50]:

$$C_{i,s} = \frac{Q_0 \cdot K_{i,L} \cdot C_{i,w}}{1 + K_{i,L} \cdot C_{i,w}} \qquad \text{(Eq. 1-5)}$$

where Q_0 is the adsorbed capacity [$\mu g\ kg^{-1}$] and the Langmuir constant $K_{i,L}$ is a fitting parameter. For ease of fitting, the LM can also be brought into its linear form [50] with the help of a Langmuir plot:

$$\frac{C_{i,w}}{C_{i,s}} = \frac{1}{Q_0} C_w + \frac{1}{K_{i,L} \cdot Q_0} \qquad \text{(Eq. 1-6)}$$

Polanyi-Manes model

The PMM model assumes that there is a fixed space around the adsorbent surface where adsorption occurs. Every sorbate in the area around the adsorbent has a fixed adsorption potential, named as ε. That potential is dependent on the distance between the sorbate and the sorption surface and the bare nature of the adsorbent itself. Every point of the adsorbent that has the same distance to the sorption surface will have the same potential ε, leading to an equipotential adsorbent surface [55]. Those sorbate areas will enclose a volume V(ε) between itself and the surface of the adsorbent [56]. These micro volumes can affect sorption to the surface. The PMM can be applied with the following equation:

$$\log C_{i,s} = \log Q_0 + a\left(\frac{\epsilon_{SW}}{V_S}\right)^b \qquad \text{(Eq. 1-7)}$$

where Q_0 is the adsorbed capacity [μg kg^{-1}], ε_{sw} is the effective adsorption potential [kJ mol^{-1}], V_s is the molar volume of solute [mL mol^{-1}] and a [$(mL)^{b+1}$ $(mol\ J^b)^{-1}$] and b [-] are fitting parameters.

1.2.5 Calculating sorption mode

The dominant mode of sorption (*ad*- or *ab*sorption) is an important parameter to know, prior to deciding what models to apply. One approach that was applied to the data from this study is the relationship between the distribution coefficients of cyclo- and n-alkanes (K_n/K_c) published by Endo et. al. [57]:

Structurally similar molecules will behave differently, depending whether they are situated in a condensed phase (*absorption*) or attached to the surface of a solid (*adsorption*). When comparing the distribution of n- and cyclo-alkanes, it must be considered that linear alkanes have adsorption preferences to a surface, whereas not all the atoms of the cyclo-alkane will be able to interact with the surface. This is due to their non-planar configuration. Cyclo-alkanes preferably absorb into bulk phases from air because the cavity formation in the bulk phase requires a smaller amount of energy [58]. Given this, $K_n/K_c < 1$ suggests absorption as the dominant sorption mode and $K_n/K_c \geq 1$ suggests adsorption [59].

$$K_n / K_c = (K_{d,\ n\text{-alkane}} / K_{aw,\ n\text{-alkane}}) / K_{d,\ cyclo\text{-alkane}} / K_{aw,\ cyclo\text{-alkane}}) \quad \text{(Eq. 1-8)}$$

where K_d represents the distribution coefficient of the alkane and K_{aw} denotes the alkane air-water partitioning constant. Direct comparison of K_n/K_c would still include molecular interactions with water. Therefore, the equation is corrected with the air-water distribution coefficient (log $K_{a/w}$) to exclude those interactions.

1.2.6 Linear free-energy relationships (LFER)

spLFER

There have been many studies performed in the past roughly 45 years to develop quantitative models for estimating robust sorption coefficients of organic chemicals. These models are also called single-parameter linear free-energy relationships (spLFER) and they basically regress data from a single parameter (Y) of a compound i to a response variable (X) (Equation 9) [60].

$$Y_i = m\,X + b \quad \text{(Eq. 1-9)}$$

Many of them have been on soil sorption coefficients to investigate the sorption of commercial chemicals by soil and sediments [61] or in the field of drug discovery and development [62]. The most used spLFER models are based on the n-octanol/water partition coefficient (log $K_{o/w}$) or even simpler, the aqueous solubility (log S)[63].

$$\text{Log } K_d = m \log K_{o/w} + b \quad \text{(Eq. 1-10)}$$

Log $K_{o/w}$ values are available for almost all organic compounds [64] and there are still several novel publications on applications for the log $K_{o/w}$ [65, 66]. For estimating the distribution of any organic sorbate within an aqueous phase, the log $K_{o/w}$ proves to be robust compared to experimental data. Although, the log $K_{o/w}$ or spLFER models in general have a major downside being that they are mainly specific to compound classes and are prone to bad training data [63, 67–69].

ppLFER

With all these drawbacks of spLFER models there is the alternative of applying poly-parameter linear free-energy relationships (ppLFER). The most common is the linear solvation-energy relationship model (LSER) proposed by Abraham et. al. [70–72]. There the distribution of a compound *i* is described between two phases, 1 and 2 (gaseous, liquid or solid), using terms for the individual contributions of molecular interactions from the sorbates to overall sorption (solute descriptors).

$$\log K_{i,\,s/w} = e_{p/w} E_i + s_{p/w} S_i + a_{p/w} A_i + b_{p/w} B_i + v_{p/w} V_i + c_{p/w} \quad \text{(Eq. 1-11)}$$

$$\log K_{i,\,g/w} = e_{p/w} E_i + s_{p/w} S_i + a_{p/w} A_i + b_{p/w} B_i + l_{p/w} L_i + c_{p/w} \quad \text{(Eq. 1-12)}$$

where $\log K_{i,\,s/w}$ denotes the logarithmic distribution coefficient of a given sorbate (i) between the solid (s) and water (w) phases (Equation 1-11) or where the $\log K_{i,\,g/w}$ denotes the logarithmic distribution coefficient between a gas phase (g) and water phase (Equation 1-12). The capital letters represent sorbate descriptors describing how a solute behaves in the system based on its size and capability for intermolecular interactions. The descriptor E represents the excess molar refraction; S, the bipolarity/polarizability; A, the solute hydrogen (H)-bond acidity; B, the solute (H)-bond basicity; V, the characteristic McGowan volume. Descriptors are typically calculated or derived from experiments as published in multiple studies or stored in online databases for a large number of compounds [51, 71, 73, 74]. The corresponding lowercase letters denote phase descriptors and represent the differences of solute interactions with the two phases of the system. These descriptors are determined using a multiple regression analysis (MRA).

Since the ppLFERs use descriptors for all relevant molecular interactions for the sorbates and phases, their application comprises all classes of neutral organic compounds. Also, the fitting coefficients of the ppLFERs determined by multiple regression analysis (MRA) indicate the abundance of the respective molecular interaction in the considered system (i.e. strong interactions in the water or solid phase). The ppLFER models have already successfully been applied to several systems, ranging from water or air to various phases like organic solvents [75], natural organic matter, soil [76], multiwalled carbon nanotubes [77, 78], extraction phases [79] or tissue [72]. In general, it is shown by several comparisons of modelled

and experimental data, that these ppLFER models predict sorption better than the commonly used log $K_{o/w}$.

1.3 References

[1] H.-G. Elias, *An introduction to Plastics*, 2nd ed. Wiley-VCH, 2003.

[2] H. Dominghaus, P. Elsner, P. Eyerer, and T. Hirth, *Kunststoffe*, 8th ed. Springer, 2012.

[3] E. Baur, S. Brinkmann, T. A. Osswald, and E. Schmachtenberg, *Saechtling Kunststoff Taschenbuch*, 29th ed. Carl Hanser Verlag GmbH & Co. KG, 2004.

[4] R. C. Hiorns *et al.*, "A Brief Guide to Polymer Nomenclature," in *Pure and Applied Chemistry*, vol. 84, no. 10, 2012, pp. 2167–2169.

[5] H.-G. Elias, "Polymere: Von Monomeren und Makromolekülen zu Werkstoffen. Eine Einführung," *J. für Prakt. Chemie Chem. Zeitung*, vol. 339, no. 1, pp. 203–204, Jul. 1997.

[6] C. Carraher, "Polymer Chemistry," *Polym. Chem.*, p. 850, 2003.

[7] PlasticsEurope, "Plastic - the Facts 2016," p. 38, 2016.

[8] W. Glenz, *Kunststoffe - Ein Werkstoff macht Karriere*. Hanser-Fachbuchverlag, 1989.

[9] S. Fenichell, "Plastic: The Making of a Synthetic Century," *Mater. Cult. Rev. / Rev. la Cult. matérielle; Vol. 47, Spring/Printemps 1998*, Jan. 1998.

[10] L. H. Baekeland, "Method of making insoluble products of phenol and formaldehyde," US942699, 1909.

[11] H. Staudinger, "Die Chemie der hochmolekularen organischen Stoffe im Sinne der Kekuléschen Strukturlehre. I. 12. Mitteilung," *Zeitschrift für Angew. Chemie*, vol. 42, no. 2, pp. 37–40, Jan. 1929.

[12] S. Freinkel, *Plastic: A Toxic Love Story*. 2011.

[13] F. Dakota, "Plastic Oceans: A New Way in solving Our Plastic Pollution," 2016.

[14] A. J. Clarke, "Tupperware: The Promise of Plastic in 1950s America.," *Smithson. Inst. Press*, p. 256, Sep. .

[15] R. C. Thompson, C. J. Moore, F. S. vom Saal, and S. H. Swan, "Plastics, the environment and human health: current consensus and future trends," *Philos. Trans. R. Soc. B Biol. Sci.*, vol. 364, no. 1526, p. 2153 LP-2166, Jun. 2009.

[16] G. Ehrenstein, "Technische Entwicklung ? Marktübersicht und Prognose," in *Polymer Werkstoffe*, Carl Hanser Verlag GmbH & Co. KG, 2011, pp. 1–25.

[17] G. Mehlhart and M. Blepp, "Study on Land-Sourced Litter (LSL) in the Marine Environment," Darmstad/Freiburg, 2012.

[18] A. Franck, *Kunststoff-Kompendium*, 6th ed. Vogel Business Media, 2006.

[19] I. L. N. Bråte, M. Blázquez, S. J. Brooks, and K. V. Thomas, "Weathering impacts the uptake of polyethylene microparticles from toothpaste in Mediterranean mussels (M. galloprovincialis)," *Sci. Total Environ.*, vol. 626, pp. 1310–1318, 2018.

[20] D. Carrington, "Plastic microbeads ban enters force in UK," *The Guardian*, 2018. [Online]. Available: https://www.theguardian.com/environment/2018/jan/09/plastic-microbeads-ban-enters-force-in-uk. [Accessed: 27-Aug-2018].

[21] O. Milman, "US to ban soaps and other products containing microbeads," *The Guardian*, 2015. [Online]. Available: https://www.theguardian.com/us-news/2015/dec/08/us-to-ban-soaps-other-products-containing-microbeads. [Accessed: 27-Aug-2018].

[22] A. L. Andrady, *Plastics and the environment*, vol. 51, no. 1. John Wiley & Sons, Inc.,

Hoboken, New Jersey., 1998.

[23] D. Lithner, Å. Larsson, and G. Dave, "Environmental and health hazard ranking and assessment of plastic polymers based on chemical composition," *Sci. Total Environ.*, vol. 409, no. 18, pp. 3309–3324, 2011.

[24] M. Eriksen *et al.*, "Plastic Pollution in the World's Oceans: More than 5 Trillion Plastic Pieces Weighing over 250,000 Tons Afloat at Sea," *PLoS One*, vol. 9, no. 12, 2014.

[25] S. Tall, "Recycling of Mixed Plastic Waste – Is Separation Worthwhile?," *Dep. Polym. Technol.*, vol. PhD Thesis, 2000.

[26] E. A. Bruno, "Automated Sorting of Plastics for Recycling," *Press*, pp. 3–16, 2018.

[27] D. K. A. Barnes, F. Galgani, R. C. Thompson, and M. Barlaz, "Accumulation and fragmentation of plastic debris in global environments," *Philos. Trans. R. Soc. B Biol. Sci.*, vol. 364, no. 1526, pp. 1985–1998, Jul. 2009.

[28] D. K. A. Barnes, A. Walters, and L. Goncalves, "Macroplastics at sea around Antarctica.," *Mar. Environ. Res.*, vol. 70, no. 2, pp. 250–252, Aug. 2010.

[29] N. Chatziaras, C. S. Psomopoulos, and N. J. Themelis, "Use of waste derived fuels in cement industry: a review," *Manag. Environ. Qual. An Int. J.*, vol. 27, no. 2, pp. 178–193, 2016.

[30] M. R. Gregory, "Environmental implications of plastic debris in marine settings--entanglement, ingestion, smothering, hangers-on, hitch-hiking and alien invasions.," *Philos. Trans. R. Soc. Lond. B. Biol. Sci.*, vol. 364, no. 1526, pp. 2013–2025, 2009.

[31] R. H. Day, D. G. Shaw, and S. E. Ignell, "The Quantitative Distribution and Characteristics of Neuston Plastic in the North Pacific Ocean, 1985-88," *Proc. Second Int. Conf. Mar. Debris*, no. April 1989, pp. 247–263, 1990.

[32] C. J. Moore, S. L. Moore, M. K. Leecaster, and S. B. Weisberg, "A Comparison of Plastic and Plankton in the North Pacific Central Gyre," *Mar. Pollut. Bull.*, vol. 42, no. 12, pp. 1297–1300, Dec. 2001.

[33] "Project Oceans." [Online]. Available: https://projectoceanus.wordpress.com/tag/ocean/. [Accessed: 12-Oct-2017].

[34] D. Eerkes-Medrano, R. C. Thompson, and D. C. Aldridge, "Microplastics in freshwater systems: A review of the emerging threats, identification of knowledge gaps and prioritisation of research needs," *Water Res.*, vol. 75, pp. 63–82, 2015.

[35] H. A. Leslie, "Review of Microplastics in Cosmetics," 2014.

[36] T. Gouin, N. Roche, R. Lohmann, and G. Hodges, "A Thermodynamic Approach for Assessing the Environmental Exposure of Chemicals Absorbed to Microplastic.," *Environ. Sci. Technol.*, pp. 1466–1472, Jan. 2011.

[37] M. A. Browne, T. Galloway, R. Thompson, and P. M. Chapman, "Microplastic - An Emergning contaminant of potential concern?," *Integr. Environ. Assess. Manag.*, vol. 3, no. 2, pp. 297–297, 2007.

[38] L. S. Fendall and M. A. Sewell, "Contributing to marine pollution by washing your face: Microplastics in facial cleansers," *Mar. Pollut. Bull.*, vol. 58, no. 8, pp. 1225–1228, 2009.

[39] E. L. Teuten, S. J. Rowland, T. S. Galloway, and R. C. Thompson, "Potential for Plastics to Transport Hydrophobic Contaminants," *Environ. Sci. Technol.*, vol. 41, no. 22, pp. 7759–7764, Nov. 2007.

[40] M. A. Browne, A. Dissanayake, T. S. Galloway, D. M. Lowe, and R. C. Thompson, "Ingested Microscopic Plastic Translocates to the Circulatory System of the Mussel, Mytilus edulis (L.)," *Environ. Sci. Technol.*, vol. 42, no. 13, pp. 5026–5031, Jul. 2008.

[41] E. L. Teuten *et al.*, "Transport and release of chemicals from plastics to the environment and to wildlife," *Philos. Trans. R. Soc. B Biol. Sci.*, vol. 364, no. 1526, pp. 2027–2045, 2009.

[42] Y. Mato, T. Isobe, H. Takada, H. Kanehiro, C. Ohtake, and T. Kaminuma, "Plastic resin pellets as a transport medium for toxic chemicals in the marine environment," *Environ. Sci. Technol.*, vol. 35, no. 2, pp. 318–324, 2001.

[43] J. a Ivar do Sul and M. F. Costa, "The present and future of microplastic pollution in the marine environment.," *Environ. Pollut.*, vol. 185, pp. 352–64, 2014.

[44] N. P. Ivleva, H. K. Imhof, J. Schmid, R. Niessner, and C. Laforsch, "Contamination of a Subalpine Lake with Microplastic Particles mulating in aquatic environments ; Identified & Quantified Microplastic Particles Raman Microspectroscopy Combination of Raman spectroscopy with optical microscopy Ingestion of Microplastic in," p. 95440, 2013.

[45] C. M. Rochman *et al.*, "Policy: Classify plastic waste as hazardous.," *Nature*, vol. 494, no. 7436, pp. 169–71, 2013.

[46] A. A. Koelmans, A. Bakir, G. A. Burton, and C. R. Janssen, "Microplastic as a Vector for Chemicals in the Aquatic Environment: Critical Review and Model-Supported Reinterpretation of Empirical Studies," *Environ. Sci. Technol.*, vol. 50, no. 7, pp. 3315–3326, 2016.

[47] D. Herzke *et al.*, "Negligible Impact of Ingested Microplastics on Tissue Concentrations of Persistent Organic Pollutants in Northern Fulmars off Coastal Norway.," *Environ. Sci. Technol.*, vol. 50, pp. 1924–1933, 2015.

[48] J. Kleinteich, S. Seidensticker, N. Marggrander, and C. Zarf, "Microplastics reduce short-term effects of environmental contaminants. part II: Polyethylene particles decrease the effect of polycyclic aromatic hydrocarbons on microorganisms," *Int. J. Environ. Res. Public Health*, vol. 15, no. 2, 2018.

[49] P. Jan Kole, A. J. Löhr, F. G. A. J. Van Belleghem, and A. M. J. Ragas, "Wear and tear of tyres: A stealthy source of microplastics in the environment," *Int. J. Environ. Res. Public Health*, vol. 14, no. 10, 2017.

[50] R. P. Schwarzenbach, P. M. Gschwend, and D. M. Imboden, *Environmental Organic Chemistry*, 2nd ed., no. 2. John Wiley & Sons Inc., Hoboken, New Jersey, 2003.

[51] M. H. Abraham, C. F. Poole, and S. K. Poole, "Classification of stationary phases and other materials by gas chromatography," *J. Chromatogr. A*, vol. 842, no. 1–2, pp. 79–114, May 1999.

[52] E. Bi, T. C. Schmidt, and S. B. Haderlein, "Sorption of Heterocyclic Organic Compounds to Reference Soils: Column Studies for Process Identification," *Environ. Sci. Technol.*, vol. 40, no. 19, pp. 5962–5970, Oct. 2006.

[53] E. Bi, T. C. Schmidt, and S. B. Haderlein, "Practical issues relating to soil column chromatography for sorption parameter determination.," *Chemosphere*, vol. 80, no. 7, pp. 787–93, Aug. 2010.

[54] F. Metzelder and T. C. Schmidt, "Environmental Conditions Influencing Sorption of Inorganic Anions to Multiwalled Carbon Nanotubes Studied by Column Chromatography," *Environ. Sci. Technol.*, vol. 51, no. 9, pp. 4928–4935, 2017.

[55] I. Abe, K. Hayashi, M. Kitagawa, and T. Urahata, "Application of the polanyi adsorption potential theory to adsorption of surfactants from aqueous solution on activated carbon.," *Chem. Lett.*, vol. 221, no. 12, pp. 1517–1520, 1979.

[56] L. Li, P. A. Quinlivan, and D. R. U. Knappe, "Predicting Adsorption Isotherms for Aqueous Organic Micropollutants from Activated Carbon and Pollutant Properties," *Environ. Sci. Technol.*, vol. 39, no. 9, pp. 3393–3400, May 2005.

[57] S. Endo, P. Grathwohl, and T. C. Schmidt, "Absorption or Adsorption ? Insights from Molecular Probes n -Alkanes and Cycloalkanes into Modes of Sorption by Environmental Solid Matrices," *Environ. Sci. Technol.*, vol. 42, no. 11, pp. 3989–3995, 2008.

[58] K.-U. Goss, "The Air/Surface Adsorption Equilibrium of Organic Compounds Under Ambient Conditions," *Crit. Rev. Environ. Sci. Technol.*, vol. 34, no. 4, pp. 339–389, Jul. 2004.

[59] S. Endo, P. Grathwohl, S. B. Haderlein, and T. C. Schmidt, "Characterization of sorbent properties of soil organic matter and carbonaceous geosorbents using n-alkanes and cycloalkanes as molecular probes.," *Environ. Sci. Technol.*, vol. 43, no. 2, pp. 393–400, 2009.

[60] C. Selassie and R. P. Verma, *History of Quantitative Structure-Activity Relationships*, vol. 1. 2003.

[61] A. Sabljić, H. Güsten, H. Verhaar, and J. Hermens, "QSAR modelling of soil sorption. Improvements and systematics of log KOCvs. log KOWcorrelations," *Chemosphere*, vol. 31, no. 11–12, pp. 4489–4514, 1995.

[62] W. Tong, Q. Xie, H. Hong, L. Shi, H. Fang, and R. Perkins, "Assessment of prediction confidence and domain extrapolation of two structure-activity relationship models for predicting estrogen receptor binding activity," *Environ. Health Perspect.*, vol. 112, no. 12, pp. 1249–1254, 2004.

[63] K.-U. Goss, "The octanol/water partitioning coefficient — The remedy of environmental chemistry?," *Umweltwissenschaften und Schadstoff-forsch.*, vol. 15, no. 4, pp. 273–279, 2003.

[64] R. Guicherit, D. J. Bakker, P. de Voogt, F. van den Berg, H. F. G. van Dijk, and W. A. J. van Pul, "Environmental Risk Assessment for Pesticides in the Atmosphere; The Results of an International Workshop," *Water. Air. Soil Pollut.*, vol. 115, no. 1, pp. 5–19, 1999.

[65] Q. Xiang, G. Shan, W. Wu, H. Jin, and L. Zhu, "Measuring log Kow coefficients of neutral species of perfluoroalkyl carboxylic acids using reversed-phase high-performance liquid chromatography," *Environ. Pollut.*, vol. 242, pp. 1283–1290, 2018.

[66] T. Ferrari, A. Lombardo, and E. Benfenati, "QSARpy: A new flexible algorithm to generate QSAR models based on dissimilarities. The log Kow case study," *Sci. Total Environ.*, vol. 637–638, pp. 1158–1165, Oct. 2018.

[67] T. Scior, J. Medina-Franco, Q.-T. Do, K. Martinez-Mayorga, J. Yunes Rojas, and P. Bernard, "How to Recognize and Workaround Pitfalls in QSAR Studies: A Critical Review," *Curr. Med. Chem.*, vol. 16, no. 32, pp. 4297–4313, 2009.

[68] J. Huang and X. Fan, "Why QSAR Fails : An Empirical Evaluation Using Conventional Computational Approach," pp. 600–608, 2011.

[69] M. C. Wenlock and L. A. Carlsson, "How experimental errors influence drug metabolism

and pharmacokinetic QSAR/QSPR models," *J. Chem. Inf. Model.*, vol. 55, no. 1, pp. 125–134, 2015.

[70] M. H. Abraham, "Scales of solute hydrogen-bonding: their construction and application to physicochemical and biochemical processes," *Chem. Soc. Rev.*, vol. 22, no. 2, pp. 73–83, 1993.

[71] M. H. Abraham, A. Ibrahim, and A. M. Zissimos, "Determination of sets of solute descriptors from chromatographic measurements," *J. Chromatogr. A*, vol. 1037, no. 1–2, pp. 29–47, May 2004.

[72] M. H. Abraham and H. S. Chadha, "Applications of a Solvation Equation to Drug Transport Properties," in *Lipophilicity in Drug Action and Toxicology*, Wiley-VCH Verlag GmbH, 1996, pp. 311–337.

[73] C. F. Poole, S. N. Atapattu, S. K. Poole, and A. K. Bell, "Determination of solute descriptors by chromatographic methods.," *Anal. Chim. Acta*, vol. 652, no. 1–2, pp. 32–53, Oct. 2009.

[74] K.-U. Goss and R. P. Schwarzenbach, "Linear Free Energy Relationships Used To Evaluate Equilibrium Partitioning of Organic Compounds," *Environ. Sci. Technol.*, vol. 35, no. 1, pp. 1–9, Jan. 2001.

[75] M. H. Abraham and C. Mitchell, "Hydrogen Bonding 32. An Analysis of Water-Octanol and Water-Alkane Partitioning and the AIog P Parameter of Seiler," vol. 83, no. 8, pp. 1085–1100, 1994.

[76] T. H. Nguyen, K.-U. Goss, and W. P. Ball, "Polyparameter linear free energy relationships for estimating the equilibrium partition of organic compounds between water and the natural organic matter in soils and sediments.," *Environ. Sci. Technol.*, vol. 39, no. 4, pp. 913–924, 2005.

[77] T. Hüffer, S. Endo, F. Metzelder, S. Schroth, and T. C. Schmidt, "Prediction of sorption of aromatic and aliphatic organic compounds by carbon nanotubes using poly-parameter linear free-energy relationships.," *Water Res.*, vol. 59, no. 1, pp. 295–303, 2014.

[78] K. Yang, L. Zhu, and B. Xing, "Adsorption of Polycyclic Aromatic Hydrocarbons by Carbon Nanomaterials," *Environ. Sci. Technol.*, vol. 40, no. 6, pp. 1855–1861, 2006.

[79] S. Endo, S. E. Hale, K.-U. Goss, and H. P. H. Arp, "Equilibrium partition coefficients of diverse polar and nonpolar organic compounds to polyoxymethylene (POM) passive sampling devices.," *Environ. Sci. Technol.*, vol. 45, no. 23, pp. 10124–32, Dec. 2011.

Chapter 2 Scope and Aim

Plastic materials that can be used in many different (technical) applications, while at the same time fulfilling the demands for as many mechanical properties as possible (e.g. tensile strength weight or UV-stability), are being developed at a very high rate. With the increasing variety of plastic materials comes also the need to sufficiently understand the interactions any of those materials could undergo with different non-ionic organic compounds. Whether plastics are used as a packaging material, as a deodorant agent, as a filter or as source for impact resistant materials, their variety on properties is steadily increasing. The high demand and global distribution of plastic materials, and the ever-increasing environmental disposal of plastic materials, led to the motivation for the present work.

This study aims to determine plastic sorption properties using a variety of probe sorbates with two different methodological approaches and interpreting the data with respect to the aquatic environment.

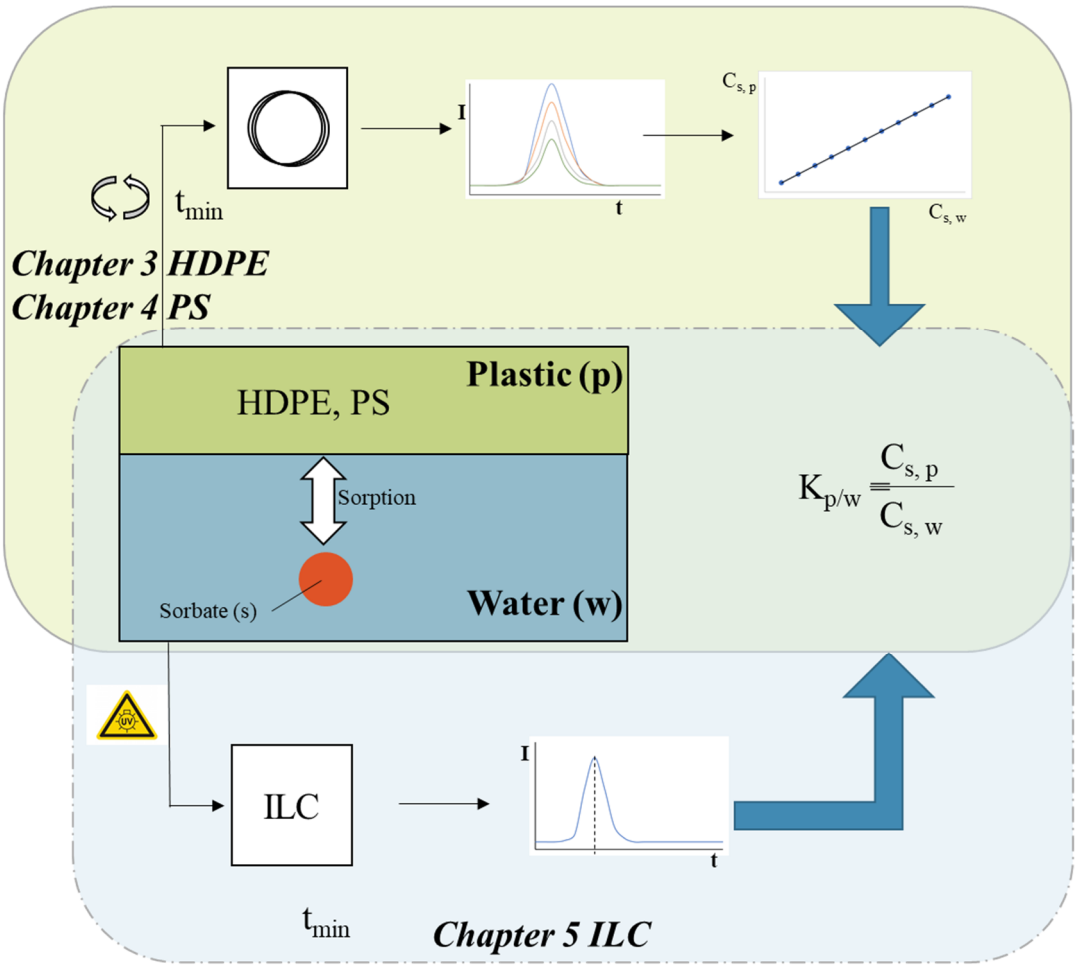

Figure 2-1 - Graphical abstract of the studies done in this work.

With high-density polyethylene (HDPE) being one of the major plastic materials produced globally, the determination of its sorption behaviour in water should be investigated in **Chapter 3**. The batch approach is applied to determine distribution coefficients for a variety of different non-ionic organic probe compounds (n-alkanes, alkenes, non-polar and polar aliphatics and aromatics). The dominant sorption mode (i.e., *ad*- or *ab*sorption) is determined by applying different sorption models and fitting sorption isotherms to the data. Further on, sorption properties are derived based on the poly-parameter linear-free energy relationship (ppLFER). Relevant sorption properties are discussed with the help of the phase descriptors and known properties of HDPE. The derived properties are also compared to other plastic materials and their sorption properties in water.

The results from Chapter 3 demonstrated very well the sorption information that could be gathered from sorption batch experiments with probe sorbates. Since HDPE is not the only plastic material relevant for environmental pollution, polystyrene (PS) is examined in **Chapter 4**. As PS is a prominent plastic material found in the environment through littering and acting as a sorbent material, its sorption properties are examined with the help of the ppLFER approach. Initially, more isotherms are fitted to the data to investigate the sorption behaviour more precisely. Further on, sorption properties are derived from the ppLFER phase descriptors. The individual phase descriptors are then compared to other data for plastic materials in the literature. Since the methodology is similar to the methodology applied in Chapter 3, a one to one comparison of the phase descriptors is done. The comparison shows differences in sorption to HDPE and PS. As the monomeric unit of PS does differ from HDPE, deviations of different phase descriptors render additional insights into the sorption behaviour by plastics in water.

Overall, the Chapters 3 and 4 showed good results for sorption on HDPE and PS, while their major downside is the amount of time and resources needed for the determination of distribution coefficients. As the set methodology to determine distribution coefficients is the batch approach, a more novel methodology is applied in **Chapter 5**. Liquid chromatography has already been applied to generate distribution data for other sorbents in a very efficient way. Using the HDPE plastic material as the stationary phase in an LC experiment can also give distribution coefficients. Once the HDPE stationary phase is characterized for LC experiments, the determination of distribution coefficients is more efficient than the batch approach. A similar compound set to Chapter 3 and 4 is then measured on the ILC column and the data is compared with each other. A one to one comparison can be done with the HDPE data in **Chapter 3** and a ppLFER is calculated.

With the results from **Chapter 3, 4** and **5** the outcomes of this study are discussed in **Chapter 6**. Lastly an outlook on potential in the field of sorption to plastic materials for future research is added.

Chapter 3 Characterization of sorption properties of high-density polyethylene using the poly-parameter linear free-energy relationships

Adapted with permission from : Uber, T. H.; Hüffer, T.; Planitz, S.; Schmidt, T. C. Characterization of sorption properties of high-density polyethylene using the poly-parameter linear-free energy relationships . *Environmental Pollution* **2019**, 248, 312-319.

 doi.org/10.1016/j.envpol.2019.02.024

3.1 Abstract

High-density polyethylene (HDPE) is a known sorbent for non-ionic organic compounds in technical applications. Nevertheless, there is little information available describing sorption to industrial HDPE for a broad range of compounds. With a better understanding of the sorption properties of synthetic polymers, environmental risk assessment would achieve a higher degree of accuracy, especially for microplastic interactions with organic substances. Therefore, a robust methodology for the determination of sorbent properties for non-ionic organic compounds by HDPE is relevant for the understanding of molecular interactions for both technical use and environmental risk assessment.

In this work, sorption properties of HDPE material used for water pipes were characterized using a poly-parameter linear free-energy relationship (ppLFER) approach. Sorption batch experiments with selected probe sorbates were carried out in a three-phase system (air/HDPE/water) covering an aqueous concentration range of at least three orders of magnitude. Sorption in the concentration range below 10^{-2} of the aqueous solubility was found to be non-linear and the Freundlich model was used to account for this non-linearity. Multiple regression analysis (MRA) using the determined distribution coefficients and literature-tabulated sorbate descriptors was performed to obtain the ppLFER phase descriptors for HDPE. Sorption properties of HDPE were then derived from the ppLFER model and statistical analysis of its robustness was conducted. The derived ppLFER model described sorption more accurately than commonly used single-parameter predictions, based i.e., on log $K_{o/w}$. The ppLFER predicted distribution data with an error 0.5 log units smaller than the spLFERs. The ppLFER was used for a priori prediction of sorption by the characterized sorbent material. The prediction was then compared to experimental data from literature and this work and demonstrated the strength of the ppLFER, based on the training set over several orders of magnitude.

3.2 Abstract Graphic

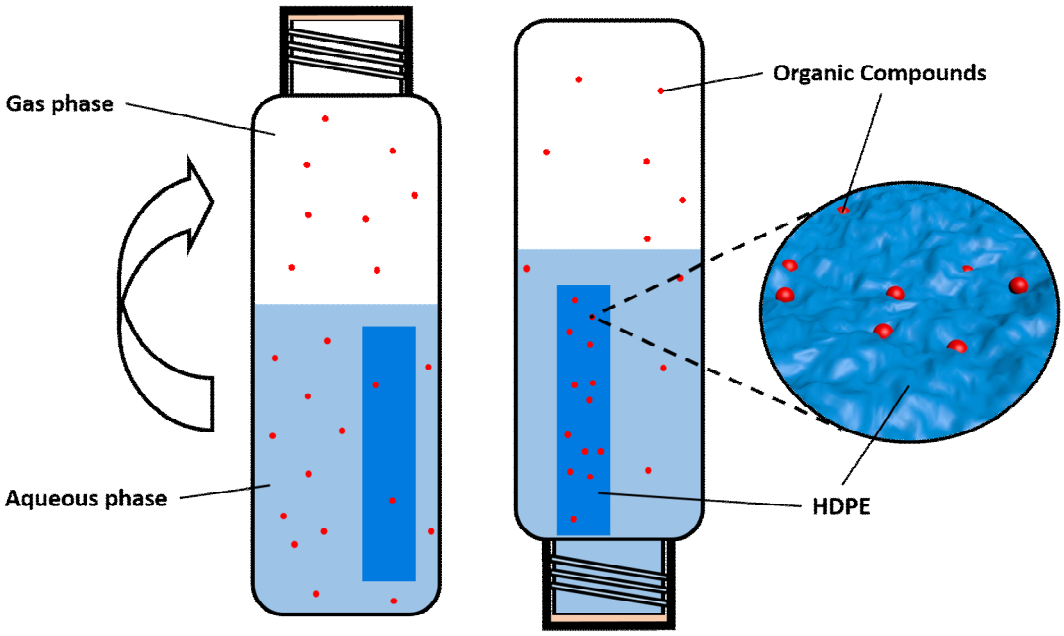

Figure 3-1 - Graphical Abstract of the studies described in this chapter.

3.3 Introduction

Today, non-polar polyethylene (PE), polypropylene (PP) and polystyrene (PS) are the most used polymeric materials [1]. The extensive usage of plastics for various applications has raised concerns over their behaviour when introduced into environmental systems, such as water bodies [2, 3]. The annual production of plastics was estimated to be 335 million tons in 2016 with an average half-life of the polymers of 450 years [4–6]. It was estimated that nearly 270,000 tons of plastic, in many different forms and sizes, were floating in the world's oceans in 2014 [7].

Most of the debris is actually present as microplastic particles (MP) [1, 8–10]. They are chemically persistent in the environment [11] and are usually between 5 mm and 1 µm in diameter. MP can be introduced into the environment by direct emissions, for example as filling materials for cosmetics [2]. Furthermore, MP can be formed in-situ in the environment as the result of weathering of larger plastic items (by UV irradiation, mechanical abrasion or biological processes) [1, 10].

It has been shown that MP can be ingested by organisms [1, 4, 12, 13]. Initial discussion on that topic suggested that MP can act as good passive samplers in organisms [2, 14, 15]. Persistent organic pollutants (POPs) might be incorporated in these MP, which can lead to a transfer of the POPs [9] into aquatic organisms. Although current studies have suggested this to be negligible and that MP does not influence the transfer of POPs into the food chain [16], the interaction of MP and (organic) substances remains an important process at their source of input into the environment and is still under discussion [17, 18].

With a production volume of about 14.5 million tons in Europe 2016 alone [6] polyethylene (PE) is one of the most used plastics and therefore one of the major plastic pollutants [6]. It can be either low-density polyethylene (LDPE) being a more amorphous, less dense polymer or high-density polyethylene (HDPE) being a more dense, crystalline and brittle polymer. LDPE is already being investigated in the literature for its sorption behaviour with polycyclic aromatic hydrocarbons and polychlorinated biphenyls [19]. HDPE has been investigated to some extent with few compounds in the literature, but not with a large set of organic compounds [20]. Applications of HDPE include packaging material (foils), plastic bottles and water pipes [21]. As the distribution rate of plastic waste in the world's oceans mounts, interaction of organic compounds with plastic will intensify.

The prediction of sorption of organic compounds by HDPE in water helps bring about a better understanding of HDPE sorption to improve risk assessment for HDPE in the

environment (e.g. plastic waste and MP) and technical applications (e.g. passive samplers and water pipes). In order to achieve this, further insight into underlying processes affecting sorption behaviour is necessary.

A common approach to predict sorption of an organic phase is based on linear free-energy relationships (LFERs) [22, 23] :

$$\log K_{i,p1/w} = a * \log K_{i,p2/w} + b \qquad \text{(Eq. 3-1)}$$

where the distribution coefficient (K) of a solute (i) between an organic phase (p_1) and water (w) is related to the partitioning of the same solute between another organic phase (p_2) and water. However, these single-parameter linear free-energy relationships (spLFER) will not serve to predict accurate $K_{i,p/w}$ values of a large variety of compounds for structurally diverse organic-water systems [22].

To understand the mechanisms of sorbent sorption behaviour, descriptors representing the sorbate and the sorbent phase need to better capture relevant molecular interactions of sorbate and phase. Abraham's solvation parameter model using poly-parameter linear free-energy relationships (ppLFER) [24–27] describe the distribution between a liquid phase (Eq. 2) and another phase (gaseous, liquid or solid) using terms for the individual contributions of sorbate (solute descriptors) and the combination of liquid and a second phase (phase descriptors) to the distribution [27 – 29]:

$$\log K_{i,\,p/w} = e_{p/w} E_i + s_{p/w} S_i + a_{p/w} A_i + b_{p/w} B_i + v_{p/w} V_i + c_{p/w} \qquad \text{(Eq. 3-2)}$$

where $\log K_{i,\,p/w}$ denotes the logarithmic distribution coefficient of a given sorbate (i) between the organic (p) and water (w) phases. The capital letters represent sorbate descriptors describing how a solute behaves in the system based on its size and capability for intermolecular interactions. The descriptor E represents the excess molar refraction; S, the bipolarity/polarizability; A, the solute hydrogen (H)-bond acidity; B, the solute (H)-bond basicity; V, the characteristic McGowan volume. Descriptors are typically calculated or derived from experiments as published in multiple studies or stored in online databases for a large

number of compounds [24, 28–30]. Clear discrimination between certain type of interactions has to be considered with caution, because of inherent correlations between the descriptors. The corresponding lowercase letters denote phase descriptors and represent the differences of solute interactions with the two phases of the system. These descriptors are determined using a multiple regression analysis (MRA). By using the lL term (hexadecane/air partition coefficient) instead of the molar volume term (vV) the model can be fitted to describe the distribution between a gas and a condensed phase [28].

The Abraham model was previously applied to distribution with hexadecane, a sorbent which is used as a model for polyethylene[31]. Recently the Abraham model was also applied to plastic materials within the discussion of sorption from organic compounds to MP like aged polystyrene [32].

In this study, a poly-parameter LFER model was developed to describe interactions of molecular probe compounds with HDPE in an aqueous system. A batch approach was used to determine sorption isotherms for selected chemical probe compounds. The derived ppLFER model was validated and analysed with statistical tests to ensure its predictability and robustness.

3.4 Materials and Methods

3.4.1 Materials

For the experiments, HDPE material which is used in fresh water pipes was chosen (Hostalen CRP 100 blue from Lyondell Basell Industries). Selected properties of the HDPE material are listed in Table 3-1 (for details of the used methods, see the appendix A3-S1). A FT-IR spectrum can be found in the appendix and showed only peaks typical for pristine PE. The PE material had a thickness of 200 µm as reported in the data sheet from the manufacturer. It was stored in a closed container and cleaned prior to the experiments with water and tissue paper to remove possible impurities on the surfaces. The probe substances for the sorption experiments were selected based on their physicochemical properties to cover a wide spectrum of solute descriptors for the ppLFER calculation and bought from Sigma Aldrich [33–35]. The substance set covered cyclic and linear alkanes, alkenes, polar and nonpolar aromatics, and polar aliphatics. Since there are no polyfluorinated compounds within the set, a ppLFER will not be adequate for such compounds. Standard solutions were prepared in methanol for volatiles and isopropanol for non-volatiles. The standard solutions were then kept in closed vials and

cooled at ~ 4 °C in a fridge to avoid evaporation. The probe substances and their corresponding physicochemical properties are listed in Table A3-1.

Table 3-1: Properties of HDPE used in this study [a].

	Material density	Molecular weight	Degree crystallinity	Melting point	Surface free energy
High-density Polyethylene (HDPE)	0.95 g cm^{-3}	5526 g mol^{-1}	70.03 %	131 °C	20.88 mN m^{-1}

[a] The properties were experimentally determined using the methods described in the appendix (A3-1).

3.4.2 Sorption batch experiments

For the sorption batch experiments, the HDPE material was placed in a 20-mL glass headspace vial with magnetic screw caps. The HDPE sheets were cut into strips of ~ 100 mg per piece (~ 3 cm^2) to fit them inside the vial. The vials were then filled with 10 mL purified water (T = 23 °C, TOC ≤ 1 ppb and σ ≤ 0.055 µS) and spiked with an equivalent of the standard solution, according to the desired concentration. The added volume of each standard was below 0.25 % (v/v) to avoid co-solvent effects from methanol or isopropanol. Initial concentrations were two orders of magnitude (*maximum*) below the aqueous solubility of the individual sorbate ($C_{i,sat}$ 10^{-2}) in line with previous sorption studies using ppLFERs. The saturation of the HDPE with water and the solvent was below 0.02 % (immersion for 24 hours) and can therefore be neglected.

The samples were shaken with an overhead shaker (Reax2, Heidolph Instruments, Germany) at ~ 1 rpm for at least 3 days to achieve sorption equilibrium. Previous studies have shown that equilibration times for polyethylene strips of 2 to 3 days are sufficient to reach equilibrium in a PE/water-system where thin polyethylene sheets were used (< 100 µm) [36]. The necessary equilibration times were determined using selected probe compounds, which indicated an equilibration time of less than 72 h (Figure A3-3).

Headspace gas chromatography coupled with a mass spectrometer (HS-GC-MS) was used for the analysis of volatile compounds (log K_{aw} > -1.70). Thermal desorption GC-MS (TDU-GC-MS) was applied for semi-volatile compounds (log K_{aw} < -1.70). For in detail description of the analytical procedure, see the appendix.

All samples were prepared in duplicates (*minimum*). The sorbate concentrations in either the aqueous or polymer phase were calculated with the aid of a mass balance approach that considered loss of analytes using spiked samples without sorbent.

After headspace analysis of the batch samples, the air concentration C_a was calculated based on the calibration curve and then converted through the air-water partitioning coefficient ($K_{a/w}$) into the aqueous concentration C_w (Eq. 3-3).

$$C_w = C_a * K_{a/w}^{-1} \quad \text{(Eq. 3-3)}$$

The solid-phase concentration C_s was then calculated from a mass balance based on the mass of the spiked sorbate m_{spiked}, fraction of the loss of the sorbate due to sorption on the surface of the vial and septum W_F, the air-volume V_a, the water volume V_w and the mass of the plastic strip m_P (Eq. 3-4).

$$C_s = [m_{spiked} - (m_{spiked} * W_F) - (C_a * V_a + C_w * V_w)] * m_P^{-1} \quad \text{(Eq. 3-4)}$$

The calculations of the distribution coefficient were based on Schwarzenbach *et al.* [22] where the sorbent concentration and the aqueous concentration were either linear fitted or log-converted and fitted to the Freundlich model equation shown in equation 3-5.

$$\log C_s = \log K_F + n \log C_w \quad \text{(Eq. 3-5)}$$

where C_s [µg kg^{-1}] and C_w [µg L^{-1}] represent the sorbed and aqueous concentration of sorbates, respectively, and K_F [(µg kg^{-1}) / (µg $L^{-1})^{1/n}$] and n [-] are the Freundlich coefficient and exponent, respectively. The isotherm fits were established using Origin software (Origin Lab Version 9.1).

3.4.3 Data analysis

The isotherm data were plotted and distribution coefficients between the sorbent and water $K_{p/w}$ [L kg^{-1}] of all compounds were calculated using the regression data for nonlinear sorption by Equation 3-6.

$$\log K_{p/w} = K_F \log C_w^{n-1} \quad \text{(Eq. 3-6)}$$

For the calculation of the ppLFER phase descriptors for sorption by HDPE in water, multiple regression analysis (MRA) was conducted using the log $K_{p/w}$ values and the sorbate descriptors (E, S, A, B and V). In the environment, organic compounds will distribute in a wide range of concentrations [37]. The analysis was performed on three concentration levels spanning three orders of magnitude at 10^{-2}, 10^{-3} and 10^{-4} of the sorbate aqueous solubility ($C_{i,sat}$) at 25 °C. The calculated HPDE-water (log $K_{p/w}$) values were additionally converted into HDPE-air distribution coefficients (log $K_{p/a}$). The distribution between the sorbent and water ($K_{p/w}$) of all compounds was interpolated at a constant sorbate loading (C_s) of 10 mg kg^{-1} on HDPE [33]. 10 mg kg^{-1} was chosen because experimental isotherm data were available for almost all compounds. Only for cycloheptane (cHep), cyclohexane (cHex), cyclooctane (cOct), 1-hexene (1Hexe) and n-propylbenzene (nPB) extrapolations for C_s had to be performed with a maximum of 0.4 log units to reach the desired concentration level. The HDPE/air distribution coefficients were calculated following the thermodynamic cycle using Equation 3-7 to investigate direct sorbate-HDPE interactions and to exclude sorbate-water-interactions.

$$\log K_{p/a} = \log K_{p/w} \log K_{a/w}^{-1} \quad \text{(Eq. 3-7)}$$

where log $K_{a/w}$ represents the air-water distribution constant (Table A3-1). MRA was carried out with the log $K_{p/a}$ values of the sorbates and their corresponding sorbate descriptors (E, S, A, B and V).

3.5 Results and Discussion

3.5.1 Sorption isotherms

All measured isotherms in this study are shown in Figure 3-2, while the fitting results with the calculated log $K_{p/w}$ values are presented in Table A3-3. Compared to other sorbents like natural organic matter (NOM) or multi-walled carbon nanotubes (MWCNTs) sorption by polyethylene is expected to be linear [9]. Linear sorption can result from a homogeneous distribution of sorption sites (e.g. nanoscale pores) in the structure of the polymer through dissolution (absorption) [38]. Given the glass transition temperature of -110 °C, at room temperature polyethylene is semi-crystalline but does contain rubbery amorphous subdomains, which exhibit a greater mobility and flexibility than glassy segments. The data were fit to the linear model and exhibited an $R^2 > 0.5$. It has been shown that internal nanoscale pores in the polymer can serve as adsorption sites where hole-filling (adsorption) leads to non-linear sorption [9]. Weber *et al.* showed that non-linear sorption behaviour of polymers can be masked at higher aqueous concentration levels by linear sorption [39]. Below 10^{-2} of the aqueous concentration level, organic compounds are sorbed mostly by sites within the polymer that show the strongest affinity for the compound (non-linear sorption). Once these sites are saturated, linear sorption to regions with lower affinity is favoured. As shown above, the data in this study was gathered below 10^{-2} of the aqueous concentration. Using the Freundlich Model resulted in better fits of the experimental data with a $R^2 > 0.94$ ($p < 0.05$). Only acetophenone (AP) and methyl phenyl ether (MPE) showed a regression coefficient $R^2 < 0.94$. The impact of the fitting error of AP and MPE on the descriptors of the ppLFER was taken into account using a sensitivity analysis for these compounds. Changes in sorption affinity (K_F) of up to ± 0.1 log units and sorption linearity (n) of up to ± 0.03 units showed no significant impact in the phase descriptors of the derived ppLFER (ANOVA test, $p > 0.05$).

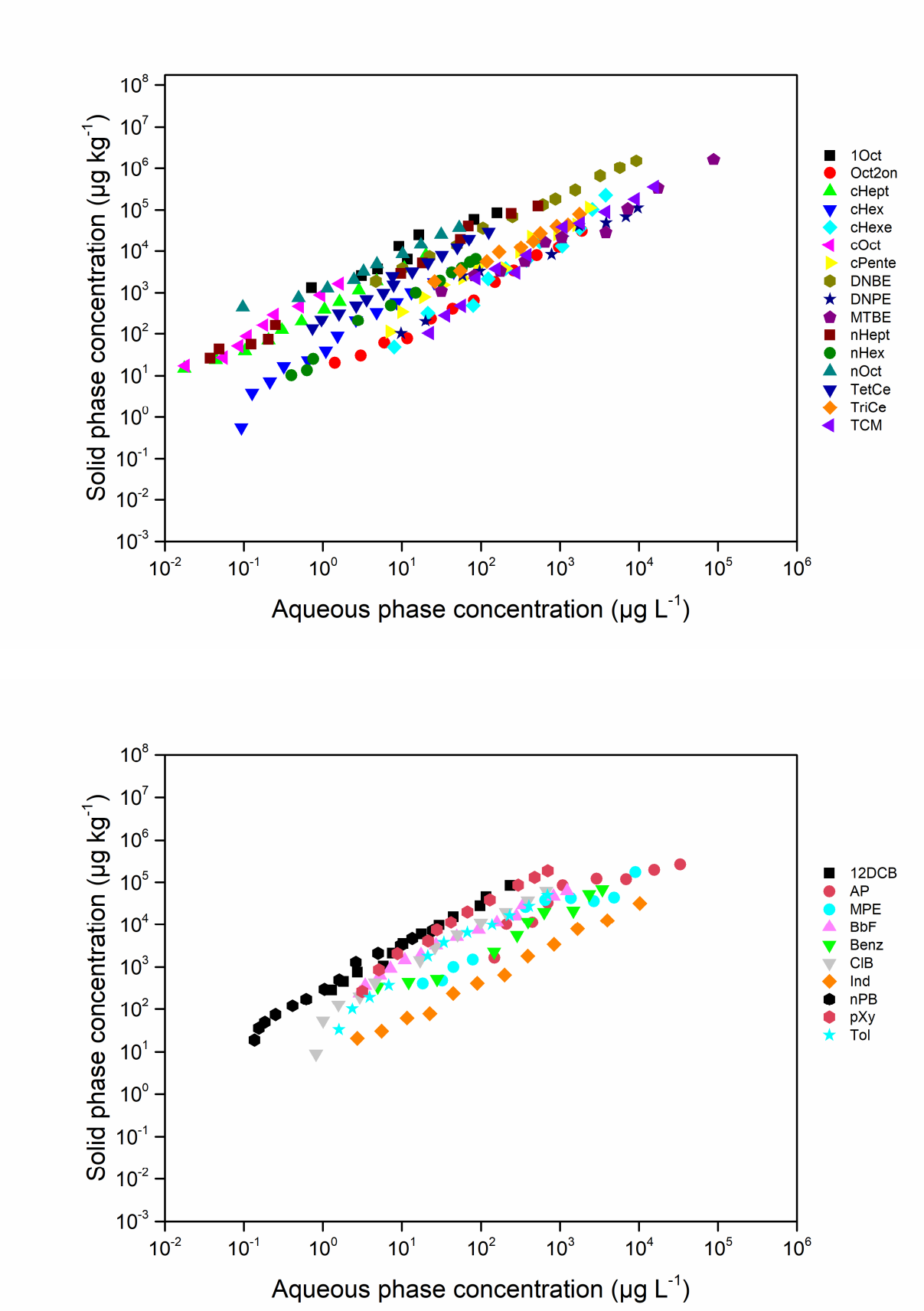

Figure 3-2 – All sorption isotherms of 16 aliphatic (top) and 10 aromatic (bottom) probe compounds used in this study. Sorbate abbreviations are given in Table A3-1.

3.5.2 Sorption mode

For the analysis of the dominant sorption mode, Endo *et al.* proposed an approach based on the ratio of the distribution coefficients for linear (K_n) and cyclic (K_c) alkanes in order to differentiate between adsorption and absorption [40]. Comparing the distribution of n- and cyclo-alkanes, linear alkanes adsorb stronger to a surface than their cyclic homologues because all carbon atoms of the planar n-alkane are able to interact with the surface. Cyclo-alkanes preferably absorb into bulk phases compared with linear alkanes because their smaller molecular volumes result in smaller energy required for the cavity formation in the bulk phase [41]. Given this, $K_n/K_c < 1$ suggests absorption as the dominant sorption mode and $K_n/K_c \geq 1$ suggests adsorption [42]. The ratios for the *n*-alkanes and cycloalkanes were calculated at an aqueous concentration of C_w 10^{-2} and resulted in K_n/K_c values for C6, C7 and C8 of 0.83, 0.56 and 0.45, respectively. This generally suggests that *ab*sorption is the dominant sorption mode for HDPE, which is consistent with previous reports, where C6 $K_n/K_c < 0.33$ were obtained for low-density polyethylene (LDPE), and K_n/K_c ratios of < 0.60 for C6, C7 and C8 were obtained for polypropylene (PP) and hexadecane [17, 40]. For LDPE, as a rubbery polymer with a lower Tg, absorption is clearly indicated by the low K_n/K_c. For HDPE, a K_n/K_c for C6 close to 1.0 indicates that the higher Tg, density and crystallinity seem to lead to an increasing contribution of adsorption. Since HDPE is a glassy polymer with amorphous segments, sorption can be described by a combination of absorption and *ad*sorption [17, 43]. The combination of a poor correlation between the experimental sorption data with the LM (assuming monolayer adsorption), the linearity of sorption isotherms obtained for many sorbates ($n > 0.9$) and K_n/K_c values < 1.0 indicated that absorption into the polymer matrix is the dominant sorption mode [44].

3.5.3 ppLFER model for sorption by HDPE in water

Phase descriptors for sorption by HDPE in water were derived from 25 experimental HDPE/water distribution coefficients (log $K_{p/w}$). The distribution data was calculated using Freundlich parameters from sorption isotherm fitting (as given in Table A3-3). The derived ppLFER descriptors are shown in Table 3-2 and the details of the statistical analysis are given in the appendix (Table A3-6 to Table A3-15). The calculated log $K_{p/w}$ values from the ppLFER model are compared with corresponding experimental log $K_{p/w}$ values in Figure 3-3 for the three concentration levels. At all three concentration levels a correlation of the experimental with calculated distribution data was obtained with an $R^2 > 0.81$ ($p < 0.05$). A deviation of the data points within the 0.3 log units deviation of the 1:1 prediction line (Figure 3-3) was obtained for

all concentration levels (RMSE between 0.27 – 0.29), which shows the robustness of the derived ppLFER model for sorption by HDPE. The compounds outside a ± 0.3 log units deviation range could not be assigned to a specific group from the data set. The 0.3 log units deviation is still within the standard error of the derived models and represent a common deviation for ppLFER modelling [45]. As proposed by Gschwend et al. [46] and others a concentration dependent ppLFER model (cdppLFER) was obtained for the data

$$\log K_{i,\,p/w} = [0.04 \log\alpha + 0.60] + [-0.09 \log\alpha + 1.93]V_i + [0.04 \log\alpha - 3.03]B_i \quad \text{(Eq. 3-8)}$$

$$+ [-0.23 \log\alpha - 3.01]A_i + [-0.11 \log\alpha - 0.37]S_i + [0.15 \log\alpha + 0.36]E_i$$

with α being the activity (α = equilibrium concentration / $C_{i,sat}$). The fitting of experimental log $K_{p/w}$ data with calculated cdppLFER data did render good correlations coefficients between 0.81 and 0.84. However, the cdppLFER did not result in significant changes in phase descriptors within the concentration range of 10^{-2} to 10^{-4} $C_{i,sat}$. Additional investigations of the cdppLFER i.e. predictability beyond this concentration is out of the scope of this manuscript and will be undertaken in the future. For easy comparison to literature, the individual ppLFER models are further on used for investigation of sorption parameters.

As can be seen in Tables A3-6 to A3-11 of the appendix the phase descriptors c, s and e render insignificant values for all concentration levels ($p > 0.05$) and should therefore have no impact on the ppLFER quality. Although, Hüffer et al. [33] demonstrated for MWCNTs that a valid prediction of sorption is difficult without taking all descriptors into account. To validate the ppLFER model derived for sorption by HDPE, a leave-many-out (LMO) approach was used for cross validation [47, 48]. The cross-validated correlation coefficients ($Q^2_{LMO\text{-}CV}$) for the three concentration levels were calculated to be > 0.85 (details in the appendix A3-4), which illustrates the robustness and predictive power of the derived ppLFER model. Scattering around the 1:1 prediction line was low (Figure 3-3) and homogeneous for all concentration levels, thus showing a good agreement with the model fit for the compound data and with previous studies [49, 50].

Table 3-2 - ppLFER descriptors for HDPE determined in this study in comparison with published ppLFER descriptors for other polymers and hexadecane.

Sorbent	e	s	a	b	v	c	R^2	N
HDPE 10^{-2}	0.06	-0.15	-2.56	-3.10	2.11	0.53	0.84	25
SE	0.64	0.71	0.82	0.70	0.40	0.44		
HDPE 10^{-3}	-0.10	-0.05	-2.33	-3.14	2.20	0.50	0.85	25
SE	0.63	0.69	0.80	0.68	0.39	0.43		
HDPE 10^{-4}	-0.25	0.06	-2.10	-3.18	2.29	0.46	0.85	25
SE	0.71	0.78	0.90	0.77	0.44	0.48		
Hexadecane[a]	0.67	-1.62	-3.59	-4.87	4.43	0.09	0.99	370
LDPE[b]	0.69	-0.15	0.00	-4.07	2.95	-0.32	0.95	98
SE	0.13	0.31	0.00	0.42	0.45	0.28		
PA[c]	0.50	-0.16	0.16	-4.00	3.28	-0.12	0.97	79
SE	0.10	0.16	0.10	0.15	0.11	0.11		
POM[d]	0.39	0.28	-0.46	-3.98	2.98	-0.37	0.99	116
SE	0.06	0.10	0.15	0.09	0.10	0.11		

HDPE: high-density polyethylene; LDPE: low-density polyethylene; PA: polyacrylate; POM: polyoxymethylene SE: Standard error of the estimates; N: Number of data points; [a] ppLFER descriptors gathered from literature [31]; [b] ppLFER calculated based on data from literature [19], [c,d] ppLFER gathered from literature [35, 49].

The here derived ppLFER for HDPE can be compared to ppLFER models derived for other polymers, in particular LDPE that consists of the same monomeric unit (-CH_2-). LDPE has more and longer side chains than HDPE, which results in lower density and crystallinity of LDPE. When ethylene is polymerized, it results in straight polymer chains from which additional chains branch out. The different branching in the molecular structure leads to a variety of structural polymer properties. LDPE has the most branching, which causes the low density leading to a less compact molecular structure. The density is usually between 0.91 – 0.93 g cm^{-3} and the crystallinity between 35 and 55 %. HDPE has minimal branching of its chain, leading to a denser, more rigid structure. It has usually a density of 0.94 – 0.97 g cm^{-3} and a crystallinity of up to 85 % [51]. The material from this study had a density of 0.95 g cm^{-3} and a crystallinity of 70 % (Table 3-1). A ppLFER with literature data in a similar concentration range as this study was generated [19]. The ppLFER for LDPE shows comparable phase descriptors with the ppLFER derived for HDPE in this study, in terms of algebraic sign and magnitude. The ppLFER for LDPE shows comparable phase descriptors with the ppLFER derived for HDPE in this study, in terms of algebraic sign and magnitude. Hexadecane (C16) has also been used to describe the sorption behaviour of polyethylene through a ppLFER (Table 3-2) and its comparison to the ppLFER shows comparable results. The domain of applicability (AD) for the ppLFER from HDPE and LDPE demonstrate the robust prediction for compounds

with A values < 0.1 [52]. For LDPE, the AD actually only accounts for compounds with A = 0 since the training set only contained compounds with zero values for H-bond acidity (Figure A3-12).

LDPE has more amorphous sites than the used HDPE [53] (LDPE has a lower crystallinity and more side branches), resulting in a higher amount of free volume within the chain network of the polymer [38]. This is also represented by the higher v descriptor of LDPE. Polymers typically have free volume (nano voids) within their polymeric structure. This results in varying amounts of sorption sites within the polymer phase for different polymers. The v value for dense polymers with short chains should be smaller than for polymers with long chains and low density [54, 55]. The comparison between the K_n/K_c results and the v-descriptor of HDPE (Table 3-2) support this assumption. Molar volume coefficients confirm this with v = 2.95 for LDPE and v < 2.29 for HDPE considering all concentration levels. Also, Figure A3-7 shows that with increasing molar volume, the log $K_{p/w}$ values strongly increase with a slope > 4.0 ($R^2 > 0.9$, $p < 0.05$). This all demonstrates that the sorption of organic compounds to HDPE positively depends on the molar volume (Figure A3-7) and consequently on the density and crystallinity of the polymer.

The large positive v-descriptors for C16 (v = 4.43) and PA (v = 3.28) [35] and the lower v-descriptor of polyoxymethylene (POM) v = 2.98 also support this observation. C16 is a liquid, PA is a common technical polymer that is classified as amorphous and POM is classified as semicrystalline [56]. Thus, the decrease in v demonstrates the impact of the polymer crystallinity.

The eE-term represents non-specific interactions, but its contribution is usually of minor importance [57]. The term is insignificant ($p > 0.05$) for HDPE when considering the standard error of the derived descriptor (Table 3-2) and can be neglected.

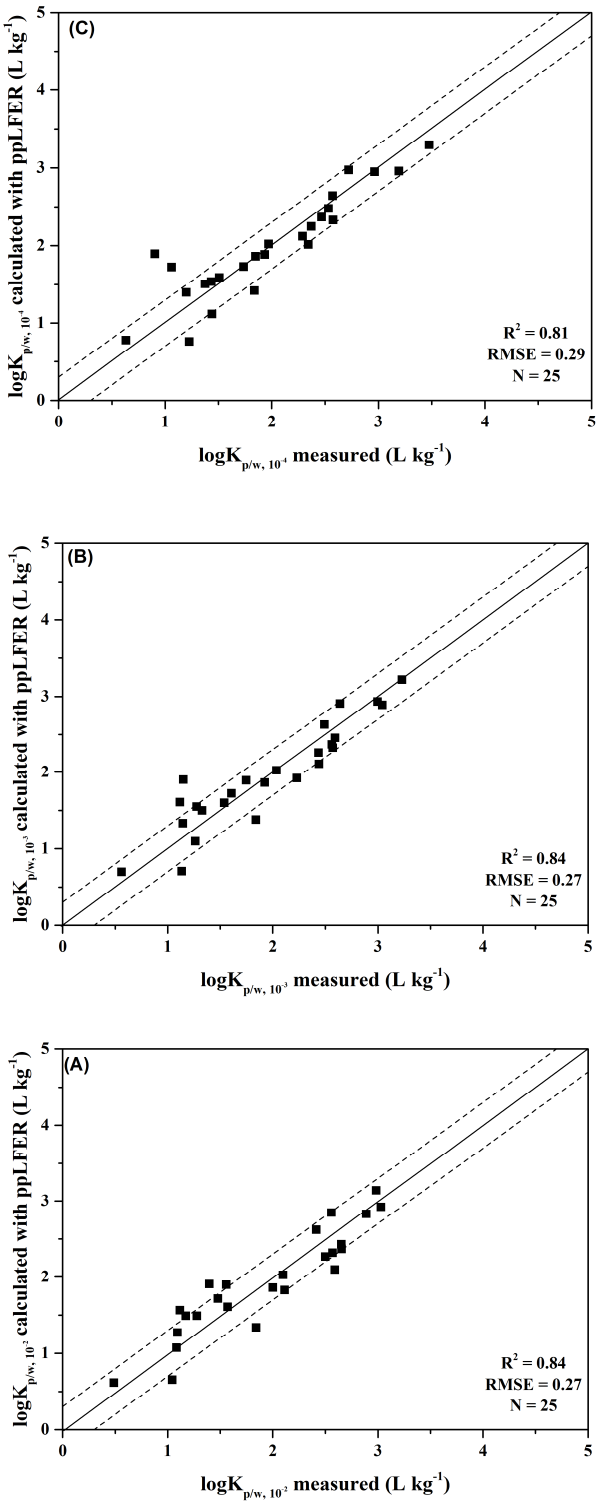

Figure 3-3 - Comparison of the calculated and measured log $K_{p/w}$ values for all compounds at the concentration levels 10^{-2} (A), 10^{-3} (B) and 10^{-4} (C) of the aqueous sorbates' solubilities. The solid lines represent the 1:1 prediction and the dashed lines represent 0.3 log units deviation of log $K_{p/w}$ values. R^2 is the regression coefficient; RMSE is the root mean squared error; N is the number of data points.

The contribution from hydrogen bond interactions (aA- and bB- term) shows significant negative values of -2.56 to -2.10 for the aA-term and -3.10 to -3.18 for the bB-term at the high and low concentration levels, respectively. Significant negative values for the aA and bB terms suggest strong interactions of the sorbates in the aqueous phase, in comparison the the plastic phase. This agrees with the polymer's nonpolar property, due to its monomer unit ($-CH_2-$). LDPE shows similar a- and b-phase descriptors (Table 3-2). PA as a structurally different polymer shows a- and b-phase descriptors close to zero which represents equal interactions in the water and polymer phase.

3.5.4 Specific and non-specific interactions

HDPE-air distribution coefficients (log $K_{p/a}$) were correlated with corresponding sorbate-descriptors given in Table A3-1, removing the influence of water to sorption. Therefore, only the contribution of non-specific (E, V and L) and specific interactions (S, A and B) to sorption of HDPE (without water) are accounted for [57]. The choice of the lL term over the vV term allows to account for interactions between the air phase and the water phase [28]. The L descriptor is not available for all compounds, therefore the MRA was performed with a confined substance set of 23 compounds from the 25 compounds above (Table A3-1 & Figure A3-11). For further analyses statistics, see the appendix (Table A3-12 and Table A3-13). To investigate the contribution of individual molecular properties to overall sorption, log $K_{p/a}$-values were plotted against the sorbate descriptors representing specific (i.e. A, B and S) and non-specific interactions (i.e. L and E) [22]. For the descriptor representing the excess molar refraction (E), the comparison with log $K_{p/a}$ showed a correlation only for the 17 nonpolar compounds ($R^2 > 0.80$, $p < 0.05$) (Figure A3-8). This can be explained by the London dispersion forces (LDF), which are part of the E descriptor but also part of the L descriptor [58]. For non-polar molecules such as alkanes and compounds with no permanent dipoles, LDF are of major importance for sorption. A correlation of the L descriptor with log $K_{p/a}$ (Figure A3-5 & Figure A3-6) for the 6 nonpolar aromatics ($R^2 > 0.96$, $p < 0.05$) supports this since the LDF are also part of the L descriptor.

The monomeric unit of HDPE ($-CH_2-$) is nonpolar; sorption behaviour should be similar to *n*-alkanes. Contributions from other than non-specific interactions should be negligible.

3.5.5 Comparison of spLFER and ppLFER

Distribution coefficients are most frequently predicted based on spLFERs with parameters for either aqueous solubility or hydrophobicity, such as the log $K_{o/w}$ or log $K_{h/w}$

where the distribution coefficient is solely based on the distribution between water and a nonpolar phase (1-octanol or hexadecane). However, the comparisons based on spLFERs must be considered with caution. Using the log $K_{o/w}$ to predict distribution for a polar solute in a system between water and 1-octanol is not accurate due to the different contributions of the solute's specific interactions [22, 59, 60]. The experimental distribution coefficients plotted against the predicted distribution coefficients for both models show an improvement in the correlation coefficient R^2 of the ppLFER model over the spLFER model (Figure 3-3 and Figure A3-11). For the ppLFER model a better regression results from using at least an $R^2 > 0.84$ compared to $R^2 > 0.75$ for the spLFER model. When considering the root-mean squared errors (RMSE) for both models, the ppLFER model shows also a lower value with 0.27 in contrast to 0.52 for the spLFER model. The data points for the spLFER model also show that the model does overpredict the distribution for the compound set whereas the ppLFER model does not. This is supported by Figure 3-4 where experimental data from literature are compared with the spLFER and the ppLFER model. As seen in Figure 3-4 the spLFER model exhibits higher log $K_{p/w}$ values for almost all compounds. The literature log $K_{p/w}$ [61] values were determined using an aqueous solution of the solute which rendered similar experimental log $K_{p/w}$ values compared to the values from this study. Experimental log $K_{p/w}$ values in this study and shown in Figure 3-4 were acquired at two orders of magnitude below the aqueous solubility of the solute. The ppLFER model does agree very well with the literature $K_{p/w}$ data.

As seen in Figure 3-4, the spLFER does overpredict the values for all compounds with an deviation of 0.75 - 1.0 log units. The ppLFER predicts the values for the same compounds with a deviation below 0.5 log units and shows to be an improvement over the spLFER model. To demonstrate that the improvement is not due to overparameterization of the ppLFER the Akaike Information criterion (AIC) was applied to the models. The AIC values indicate if the derived model is an improvement over another model fit considering overparameterization of models with more degrees of freedom.

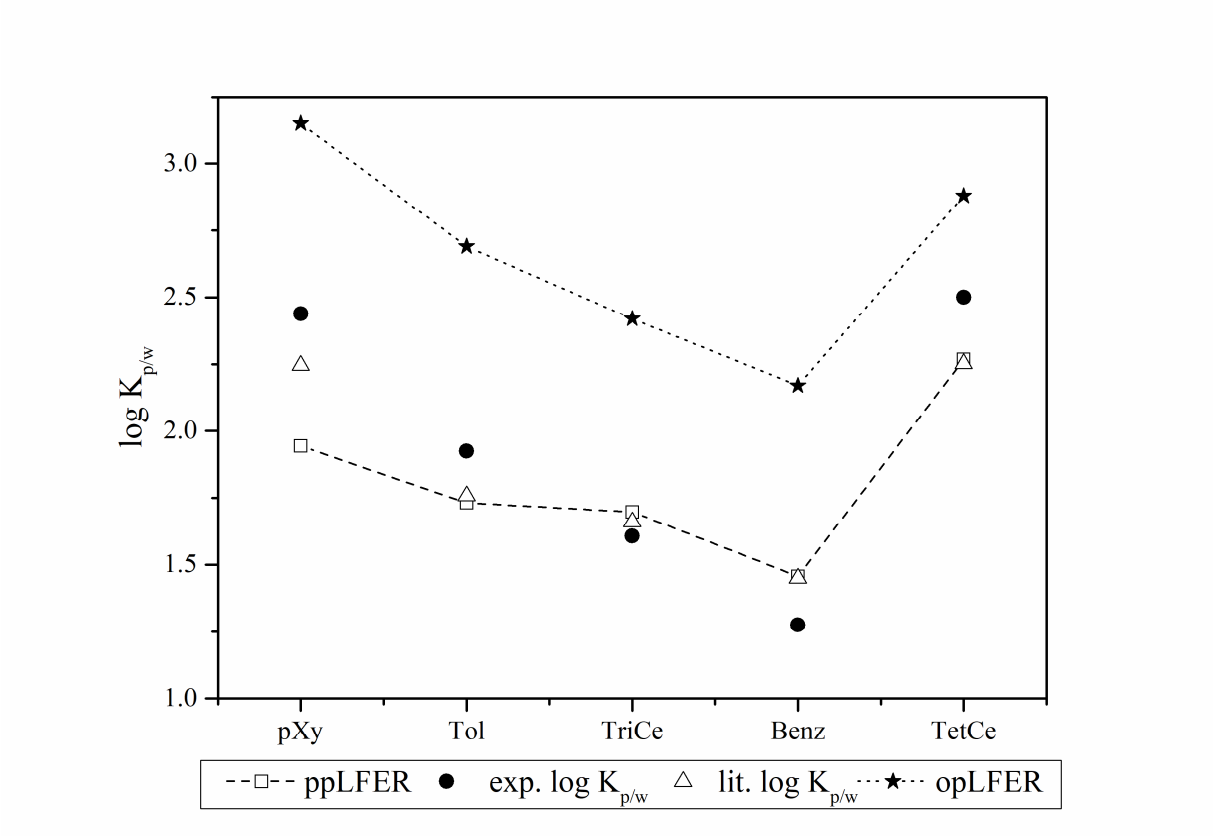

Figure 3-4 - Comparison of log $K_{p/w}$ values from literature, experimental and calculated by different models for assorted compounds. Triangles represent experimental data points from literature at a 10^{-1} below water solution of the solute. Filled dots represent data from this study at two decades below the aqueous water solubility of the solute. Stars with dotted lines represent calculated data with the spLFER model and hollow boxes represent the ppLFER model at two decades below the aqueous water solubility of the solute.

This mathematical approach has been suggested in the literature and has also been used previously to evaluate ppLFER models [33, 62]. The method is described in detail in the appendix (A3-S7); in brief, the model with the lower AIC value is supposed to be the more reliable model without overparameterization [63]. The AIC values calculated for the ppLFER model at the concentration levels $C_{i,sat}$ 10^{-2}, 10^{-3} and 10^{-4} ranged between - 66.38 and - 46.52 from high to low concentrations and for the spLFER model between -2.97 and -8.19 from high to low concentrations. This shows that the ppLFER renders an improved model for data description. Also, it is important to note that the model's capacity for accurate prediction is decidedly not due to more degrees of methodological freedom. Although HDPE is considered a nonpolar polymer, only a poor correlation was obtained with the commonly used phase partitioning predictor $K_{o/w}$, which demonstrates its limited use.

3.6 References

[1] J. a Ivar do Sul and M. F. Costa, "The present and future of microplastic pollution in the marine environment.," *Environ. Pollut.*, vol. 185, pp. 352–64, 2014.

[2] D. Eerkes-Medrano, R. C. Thompson, and D. C. Aldridge, "Microplastics in freshwater systems: A review of the emerging threats, identification of knowledge gaps and prioritisation of research needs," *Water Res.*, vol. 75, pp. 63–82, 2015.

[3] C. Wu, K. Zhang, X. Huang, and J. Liu, "Sorption of pharmaceuticals and personal care products to polyethylene debris," *Environ. Sci. Pollut. Res.*, vol. 23, no. 9, pp. 8819–8826, 2016.

[4] C. M. Rochman *et al.*, "Policy: Classify plastic waste as hazardous.," *Nature*, vol. 494, no. 7436, pp. 169–71, 2013.

[5] D. Lithner, Å. Larsson, and G. Dave, "Environmental and health hazard ranking and assessment of plastic polymers based on chemical composition," *Sci. Total Environ.*, vol. 409, no. 18, pp. 3309–3324, 2011.

[6] PlasticsEurope, "Plastic - the Facts 2016," p. 38, 2016.

[7] M. Eriksen *et al.*, "Plastic Pollution in the World's Oceans: More than 5 Trillion Plastic Pieces Weighing over 250,000 Tons Afloat at Sea," *PLoS One*, vol. 9, no. 12, 2014.

[8] F. Galgani *et al.*, "Litter on the sea floor along European coasts," *Mar. Pollut. Bull.*, vol. 40, no. 6, pp. 516–527, 2000.

[9] E. L. Teuten *et al.*, "Transport and release of chemicals from plastics to the environment and to wildlife," *Philos. Trans. R. Soc. B Biol. Sci.*, vol. 364, no. 1526, pp. 2027–2045, 2009.

[10] M. Cole, P. Lindeque, C. Halsband, and T. S. Galloway, "Microplastics as contaminants in the marine environment: a review.," *Mar. Pollut. Bull.*, vol. 62, no. 12, pp. 2588–97, Dec. 2011.

[11] V. Hidalgo-ruz, L. Gutow, R. C. Thompson, and M. Thiel, "Microplastics in the Marine Environment: A Review of the Methods Used for Identification and Quantification," *Environ. Sci. Technol.*, vol. 46, p. 3060−3075, 2012.

[12] H. K. Imhof, N. P. Ivleva, J. Schmid, R. Niessner, and C. Laforsch, "Contamination of beach sediments of a subalpine lake with microplastic particles.," *Curr. Biol.*, vol. 23, no. 19, pp. R867-8, 2013.

[13] M. R. Gregory, "Environmental implications of plastic debris in marine settings--entanglement, ingestion, smothering, hangers-on, hitch-hiking and alien invasions.," *Philos. Trans. R. Soc. Lond. B. Biol. Sci.*, vol. 364, no. 1526, pp. 2013–2025, 2009.

[14] D. Herzke *et al.*, "Negligible Impact of Ingested Microplastics on Tissue Concentrations of Persistent Organic Pollutants in Northern Fulmars off Coastal Norway.," *Environ. Sci. Technol.*, vol. 50, pp. 1924–1933, 2015.

[15] S. L. Wright, R. C. Thompson, and T. S. Galloway, "The physical impacts of microplastics on marine organisms: A review," *Environ. Pollut.*, vol. 178, pp. 483–492, 2013.

[16] A. A. Koelmans, A. Bakir, G. A. Burton, and C. R. Janssen, "Microplastic as a Vector for Chemicals in the Aquatic Environment: Critical Review and Model-Supported Reinterpretation of Empirical Studies," *Environ. Sci. Technol.*, vol. 50, no. 7, pp. 3315–3326, 2016.

[17] T. Hüffer and T. Hofmann, "Sorption of non-polar organic compounds by micro-sized plastic particles in aqueous solution.," *Environ. Pollut.*, vol. 214, no. 1, pp. 194–201, Apr. 2016.

[18] T. Hüffer, F. Metzelder, G. Sigmund, S. Slawek, T. C. Schmidt, and T. Hofmann, "Polyethylene microplastics influence the transport of organic contaminants in soil," *Sci. Total Environ.*, vol. 20, no. 657, pp. 242–247, 2019.

[19] Y. Choi, Y. M. Cho, and R. G. Luthy, "Polyethylene-water partitioning coefficients for parent- and alkylated-polycyclic aromatic hydrocarbons and polychlorinated biphenyls," *Environ. Sci. Technol.*, vol. 47, pp. 6943–6950, 2013.

[20] X. Guo, X. Wang, X. Zhou, X. Kong, S. Tao, and B. Xing, "Sorption of four hydrophobic organic compounds by three chemically distinct polymers: role of chemical and physical composition.," *Environ. Sci. Technol.*, vol. 46, no. 13, pp. 7252–9, Jul. 2012.

[21] E. Baur, S. Brinkmann, T. A. Osswald, and E. Schmachtenberg, *Saechtling Kunststoff Taschenbuch*, 29th ed. Carl Hanser Verlag GmbH & Co. KG, 2004.

[22] R. P. Schwarzenbach, P. M. Gschwend, and D. M. Imboden, *Environmental Organic Chemistry*, 2nd ed., no. 2. John Wiley & Sons Inc., Hoboken, New Jersey, 2003.

[23] K.-U. Goss and R. P. Schwarzenbach, "Linear Free Energy Relationships Used To Evaluate Equilibrium Partitioning of Organic Compounds," *Environ. Sci. Technol.*, vol. 35, no. 1, pp. 1–9, Jan. 2001.

[24] M. H. Abraham, A. Ibrahim, and A. M. Zissimos, "Determination of sets of solute descriptors from chromatographic measurements," *J. Chromatogr. A*, vol. 1037, no. 1–2, pp. 29–47, May 2004.

[25] P. Politzer and J. Murray, "Quantitative Approaches to Solute-Solvent Interactions," in *Modern Aspects of Electrochemistry SE - 1*, vol. 39, C. G. Vayenas, R. White, and M. Gamboa-Adelco, Eds. Springer US, 2006, pp. 1–63.

[26] M. H. Abraham and H. S. Chadha, "Applications of a Solvation Equation to Drug Transport Properties," in *Lipophilicity in Drug Action and Toxicology*, Wiley-VCH Verlag GmbH, 1996, pp. 311–337.

[27] M. H. Abraham, "Scales of solute hydrogen-bonding: their construction and application to physicochemical and biochemical processes," *Chem. Soc. Rev.*, vol. 22, no. 2, pp. 73–83, 1993.

[28] C. F. Poole, S. N. Atapattu, S. K. Poole, and A. K. Bell, "Determination of solute descriptors by chromatographic methods.," *Anal. Chim. Acta*, vol. 652, no. 1–2, pp. 32–53, Oct. 2009.

[29] M. H. Abraham, C. F. Poole, and S. K. Poole, "Classification of stationary phases and other materials by gas chromatography," *J. Chromatogr. A*, vol. 842, no. 1–2, pp. 79–114, May 1999.

[30] S. Endo, N. Watanabe, N. Ulrich, G. Bronner, and K.-U. Goss, "UFZ-LSER database v 2.1," *Leipzig, Germany, Helmholtz Centre for Environmental Research-UFZ. 2015*. [Online]. Available: https://www.ufz.de/index.php?en=31698&contentonly=1&lserd_data[mvc]=Public/start. [Accessed: 23-Dec-2015].

[31] M. H. Abraham and C. Mitchell, "Hydrogen Bonding 32. An Analysis of Water-Octanol and Water-Alkane Partitioning and the AIog P Parameter of Seiler," vol. 83, no. 8, pp. 1085–1100, 1994.

[32] T. Hüffer, A. K. Weniger, and T. Hofmann, "Sorption of organic compounds by aged polystyrene microplastic particles," *Environ. Pollut.*, vol. 236, pp. 474-4218–225, 2018.

[33] T. Hüffer, S. Endo, F. Metzelder, S. Schroth, and T. C. Schmidt, "Prediction of sorption of aromatic and aliphatic organic compounds by carbon nanotubes using poly-parameter linear free-energy relationships.," *Water Res.*, vol. 59, no. 1, pp. 295–303, 2014.

[34] M. Kah, X. Zhang, M. T. O. Jonker, and T. Hofmann, "Measuring and modeling adsorption of PAHs to carbon nanotubes over a six order of magnitude wide concentration range.," *Environ. Sci. Technol.*, vol. 45, no. 14, pp. 6011–7, Jul. 2011.

[35] S. Endo, S. E. Hale, K.-U. Goss, and H. P. H. Arp, "Equilibrium partition coefficients of diverse polar and nonpolar organic compounds to polyoxymethylene (POM) passive sampling devices.," *Environ. Sci. Technol.*, vol. 45, no. 23, pp. 10124–32, Dec. 2011.

[36] A. P. Tcaciuc, J. N. Apell, and P. M. Gschwend, "Modeling the transport of organic chemicals between polyethylene passive samplers and water in finite and infinite bath conditions.," *Environ. Toxicol. Chem.*, vol. 34, no. 12, pp. 2739–2749, 2015.

[37] Q. Zhao, K. Yang, W. Li, and B. Xing, "Concentration-dependent polyparameter linear free energy relationships to predict organic compound sorption on carbon nanotubes," *Sci. Rep.*, vol. 4, pp. 1–7, 2014.

[38] A. Peacock, *Handbook of Polyethylene: Structures: Properties, and Applications*. Taylor & Francis, 2000.

[39] W. J. Weber, P. M. McGinley, and L. E. Katz, "A distributed reactivity model for sorption by soils and sediments. 1. Conceptual basis and equilibrium assessments," *Environ. Sci. Technol.*, vol. 26, no. 10, pp. 1955–1962, Oct. 1992.

[40] S. Endo, P. Grathwohl, and T. C. Schmidt, "Absorption or Adsorption ? Insights from Molecular Probes n -Alkanes and Cycloalkanes into Modes of Sorption by Environmental Solid Matrices," *Environ. Sci. Technol.*, vol. 42, no. 11, pp. 3989–3995, 2008.

[41] K.-U. Goss, "The Air/Surface Adsorption Equilibrium of Organic Compounds Under Ambient Conditions," *Crit. Rev. Environ. Sci. Technol.*, vol. 34, no. 4, pp. 339–389, Jul. 2004.

[42] S. Endo, P. Grathwohl, S. B. Haderlein, and T. C. Schmidt, "Characterization of sorbent properties of soil organic matter and carbonaceous geosorbents using n-alkanes and cycloalkanes as molecular probes.," *Environ. Sci. Technol.*, vol. 43, no. 2, pp. 393–400, 2009.

[43] B. Xing and J. J. Pignatello, "Dual-Mode Sorption of Low-Polarity Compounds in Glassy Poly(Vinyl Chloride) and Soil Organic Matter," *Environ. Sci. Technol.*, vol. 31, no. 3, pp. 792–799, Mar. 1997.

[44] E. Czepirski, L., Balys, M. R., & Komorowska-Czepirska, "Some generalization of Langmuir adsorption isotherm," *J. Chem.*, vol. 3, no. 14, p. 1099–8292., 2000.

[45] F. Metzelder, M. Funck, and T. C. Schmidt, "Sorption of Heterocyclic Organic Compounds to Multiwalled Carbon Nanotubes," *Environ. Sci. Technol.*, vol. 52, no. 2, pp. 628–637, Jan. 2018.

[46] Y. H. Shih and P. M. Gschwend, "Evaluating activated carbon-water sorption coefficients of organic compounds using a linear solvation energy relationship approach and sorbate chemical activities," *Environ. Sci. Technol.*, vol. 43, no. 3, pp. 851–857, 2009.

[47] P. Gramatica, "Principles of QSAR models validation: internal and external," *QSAR Comb. Sci.*, vol. 26, no. 5, pp. 694–701, 2007.

[48] T. Scior, J. Medina-Franco, Q.-T. Do, K. Martinez-Mayorga, J. Yunes Rojas, and P. Bernard, "How to Recognize and Workaround Pitfalls in QSAR Studies: A Critical Review," *Curr. Med. Chem.*, vol. 16, no. 32, pp. 4297–4313, 2009.

[49] S. Endo, S. T. J. Droge, and K.-U. Goss, "Polyparameter Linear Free Energy Models for Polyacrylate," *Anal. Chem.*, vol. 83, pp. 1394–1400, 2011.

[50] L. Sprunger, A. Proctor, W. E. Acree, and M. H. Abraham, "Characterization of the sorption of gaseous and organic solutes onto polydimethyl siloxane solid-phase microextraction surfaces using the Abraham model.," *J. Chromatogr. A*, vol. 1175, no. 2, pp. 162–73, Dec. 2007.

[51] H.-G. Elias, *An introduction to Plastics*, 2nd ed. Wiley-VCH, 2003.

[52] K. Roy, S. Kar, and A. Pravin, "On a simple approach for determining applicability domain of QSAR models.," *Chemom. Intell. Lab. Syst.*, vol. 145, pp. 22–29, 2015.

[53] D. W. van (Dirk W. Krevelen and K. te. Nijenhuis, *Properties of polymers : their correlation with chemical structure ; their numerical estimation and prediction from additive group contributions*. Elsevier, 2009.

[54] M. H. Cohen and D. Turnbull, "Molecular Transport in Liquids and Glasses," *J. Chem. Phys.*, vol. 31, no. 5, 1959.

[55] M. S. Iotov, "Chapter 5 Methods for studying diffusion in Polymers," in *Diffusion in amorphous media*, California Institute of Technology, 1998.

[56] M. Szycher, *Szycher's Handbook of Polyurethanes*, 2nd ed. CRC Press, 2012.

[57] S. Endo, P. Grathwohl, S. B. Haderlein, and T. C. Schmidt, "Compound-Specific Factors Influencing Sorption Nonlinearity in Natural Organic Matter," *Environ. Sci. Technol.*, vol. 42, no. 16, pp. 5897–5903, Aug. 2008.

[58] T. H. Nguyen, K. Goss, and W. P. Pall, "Polyparamater Linear Free Energy Relationships for Estimation the Equilibrium Partition of Organic Compounds between Water and Natural Organic Matter in Soils and Sediments," pp. 913–924, 2005.

[59] B. Pan and B. Xing, "Adsorption mechanisms of organic chemicals on carbon nanotubes," *Environ. Sci. Technol.*, vol. 42, no. 24, pp. 9005–9013, 2008.

[60] W. Chen, L. Duan, and D. Zhu, "Adsorption of polar and nonpolar organic chemicals to carbon nanotubes," *Environ. Sci. Technol.*, vol. 41, no. 24, pp. 8295–8300, 2007.

[61] J. C. Joo, J. Y. Kim, and K. Nam, "Mass Transfer of Organic Compounds in Dilute Aqueous Solutions into High Density Polyethylene Geomembranes," *Managing*, no. February, pp. 175–183, 2004.

[62] T. Hüffer, M. Kah, T. Hofmann, and T. C. Schmidt, "How Redox Conditions and Irradiation A ff ect Sorption of PAHs by Dispersed Fullerenes (nC60)," *Environ. Sci. Technol.*, vol. 47, no. 13, pp. 6935–6942, 2013.

[63] M. Harvey and A. Christopoulos, *Fitting Models to Biological Data using Linear and Nonlinear Regression*. Oxford University Press, 2003.

3.7 Appendix

A3-S1 Procedures for determining sorption relevant properties of high-density polyethylene

The density was determined applying the displacement procedure following the DIN EN ISO 1183-1 method. The melting point was determined with the help of differential scanning calorimetry (DSC). The same instrument was applied to determine the degree of crystallinity (K %) using Equation A3-1:

$$K = (\Delta H_{melt} * 100\ \%) * (\Delta H_{literature})^{-1} \qquad \text{(Eq. A3-1)}$$

where ΔH_{melt} is the experimental determined melting enthalpy of the compound and $\Delta H_{literature}$ is the melting enthalpy from literature. ΔH_{melt} is determined by measuring the energy emission upon melting the sample.

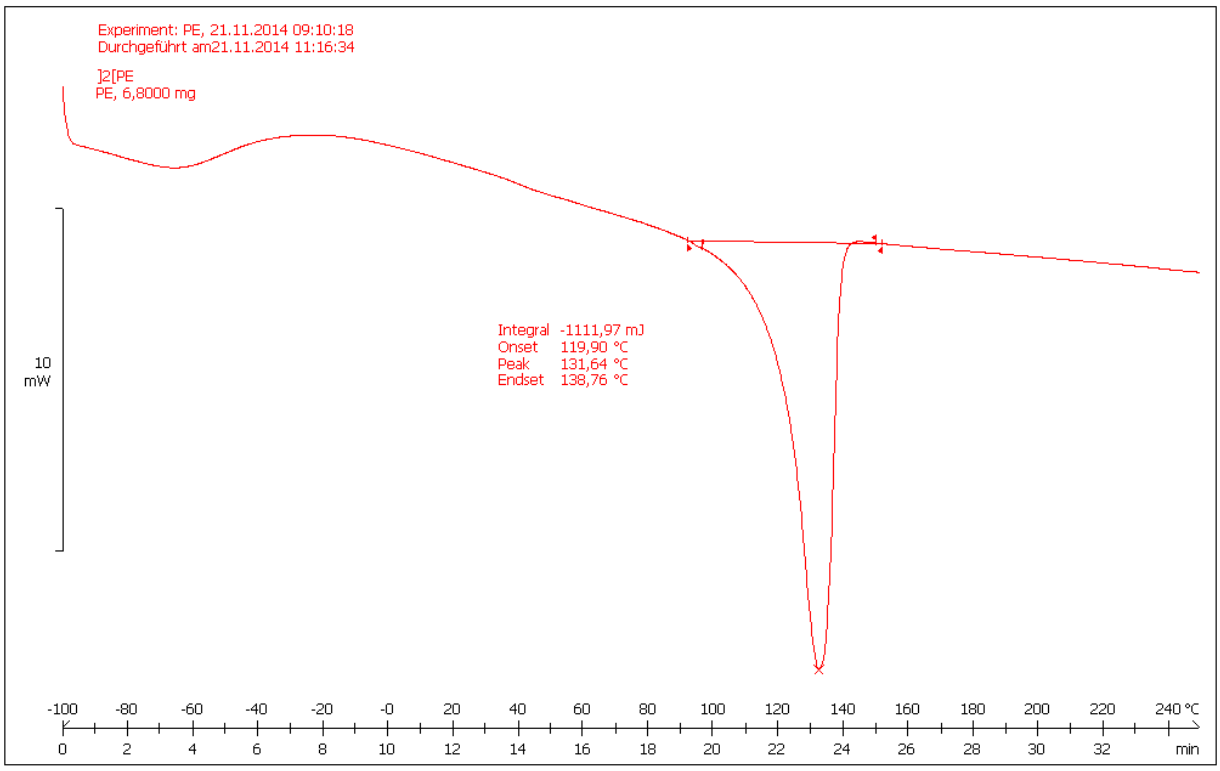

Figure A3-1 – Thermogram of the analysis of a HDPE sample from the DSC experiment.

The molecular weight was determined with a Ubbelohde apparatus, where the pressure drop within a capillary is measured when applying a laminar flow.

For the surface tension, a drop of a test substance (10 µL) was placed on the sample surface and the contact angle of each drop was measured using a sensitive and fixed camera. Surftest 4.5 was then used to calculate the surface tension in mN/m. All experiments were carried out at least three times per sample.

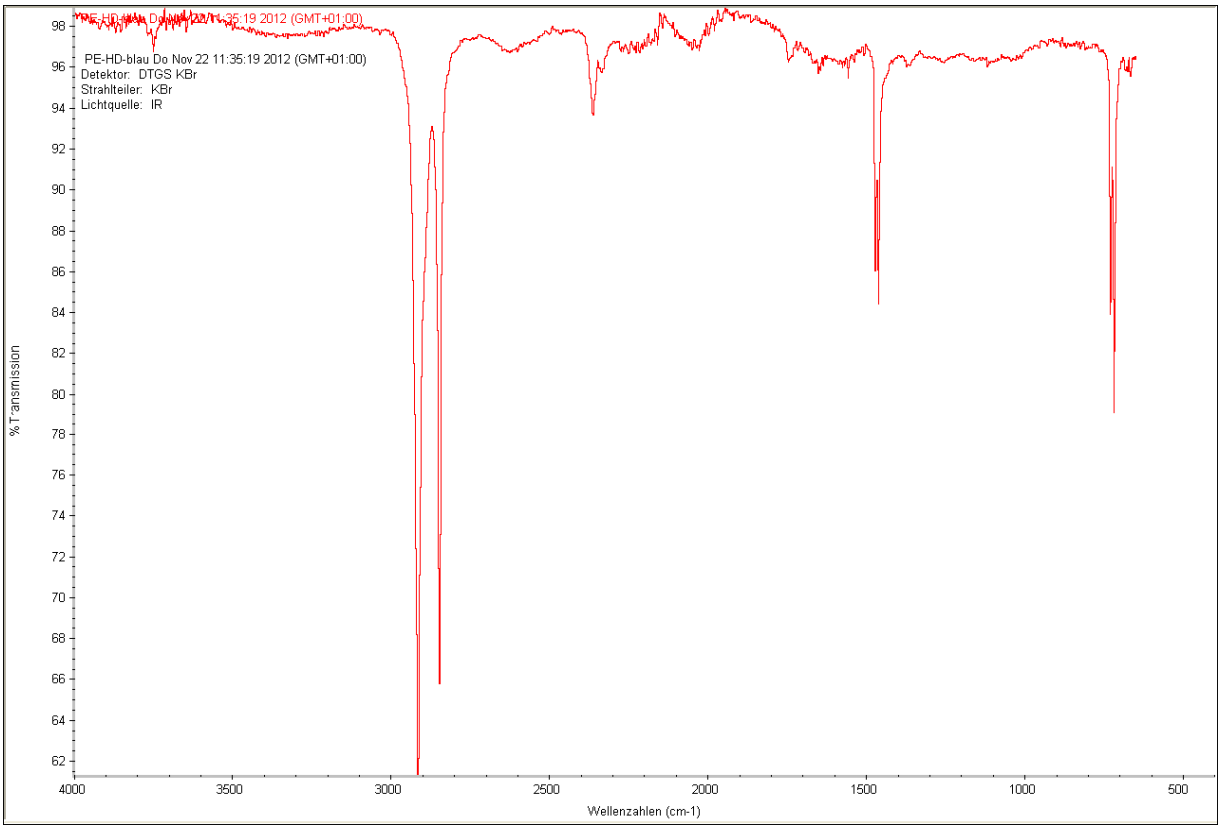

Figure A3-2 - FT-IR spectrum of the HDPE material used in this study.

FT-IR measurements were executed with the help of the IR-ATR-spectrometry. A HDPE piece was placed on an ATR crystal and was measured with a Nicolet 380 FT-IR from Thermo Scientific.

A3-S2 Experimental procedure for GC analysis

The sample vials were allowed to reach headspace equilibrium by removing them from the overhead shaker and placing them in the sample tray of the autosampler at least one hour prior to the experiment. Quantification of the sorbates was achieved using an 'Agilent Gas Chromatograph 6895' coupled to an 'Agilent Mass Spectrometer 5960'. Prior to the analysis, 12 calibration standards (in methanol) were prepared and used for quantification.

The gas-tight headspace syringe and the agitator temperature were set to 30 °C, the CIS4 was set to 250 °C with split-less injection and 2 mL min^{-1} helium gas flow. The initial GC oven temperature was set to 60 °C and increased to 140 – 200 °C at a ramp rate of 20 °C min^{-1}

depending on the substance retention. For qualification of the sorbates, the mass spectrometer used Electron Ionisation (70 eV) with the detector operating under Selected Ion Monitoring (SIM) mode using three ions for each substance.

The plastic strips were removed from the vials using forceps, dried with a tissue and transferred into a TDU-Liner (Gerstel). The liner was then placed in the sample-tray with thermal desorption performed for a duration of 5 - 15 minutes at 200 °C with a purge flow of 50 mL min^{-1} for 1.2 seconds. The GC-MS settings were identical to those of the headspace measurements. For quantification, 10 calibration standards were prepared in isopropanol and aliquots were injected into glass wool containing TDU-Liners.

A3-S3 Experimental Sorption Time

To determine the sorption time that is sufficient to reach equilibrium, HDPE strips were placed in a headspace vial with 10 mL water and were spiked with the solvent and shaken overhead. Multiple samples were prepared in order to achieve enough data points during the testing period. After a certain amount of time, a sample was removed from the overhead shaker and analyzed using HS-GC-MS. The corresponding peak areas of all samples were compared afterwards and plotted versus the exposure time.

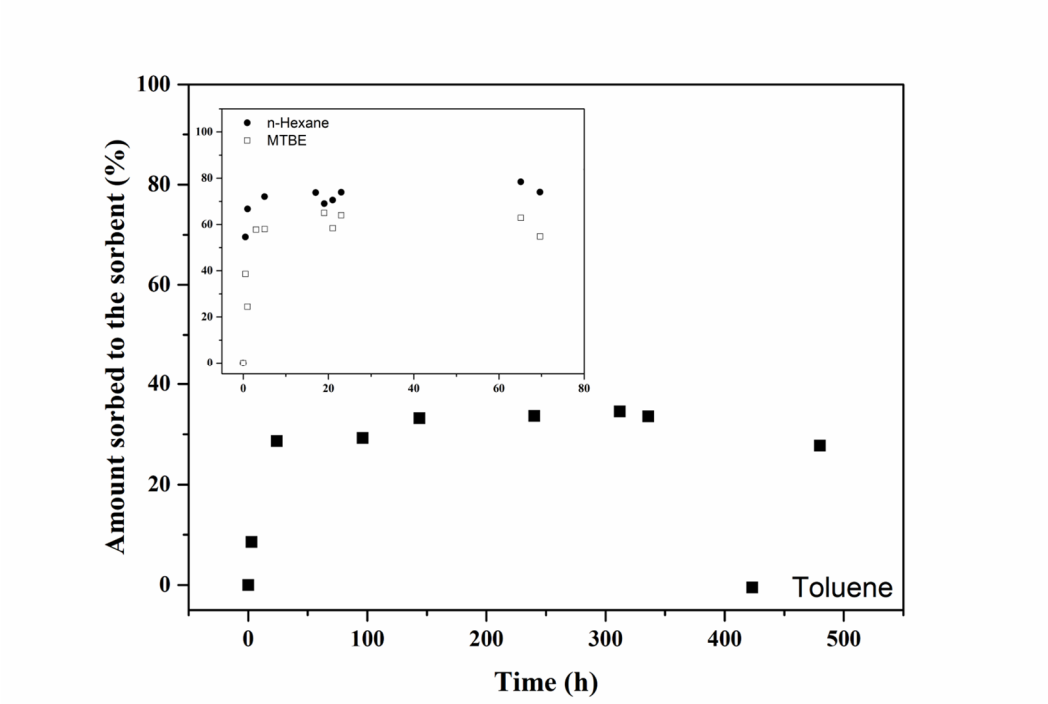

Figure A3-3 Experimental determined equilibration times in hours for toluene, n-hexane and MTBE.

Table A3-1 - Probe compounds used in this study and their corresponding sorption properties.

	Abb.	log $C_{i,sat}$	log $K_{a/w}$	log $K_{o/w}$	Method	E	S	A	B	V	L
alkanes											
Cycloheptane	cHept	1.70	3.80[a]	4.00	HS	0.35	0.10	0.00	0.00	0.99	3.70
Cyclohexane	cHex	1.74	0.89	3.44	HS	0.31	0.10	0.00	0.00	0.85	2.96
Cyclooctane	cOct	0.89	-0.68	4.45	HS	0.41	0.10	0.00	000	1.13	4.33
n-Heptan	nHept	0.53	1.84	4.66	HS	0.00	0.00	0.00	0.00	1.10	3.17
n-Hexane	nHex	0.98	1.74	3.9	HS	0.00	0.00	0.00	0.00	0.95	2.67
n-Octane	nOct	-0.18	1.95	5.18	HS	0.00	0.00	0.00	0.00	1.24	3.68
alkenes											
1-Octene	1Oct	0.61	1.41	4.57	HS	0.09	0.08	0.00	0.07	1.19	3.57
Cyclohexene	cHexe	2.33	0.27[a]	2.86	HS	0.40	0.20	0.00	0.10	0.80	3.02
Cyclopentene	cPente	2.73	-0.58	2.47	HS	0.34	0.20	0.00	0.10	0.66	2.40
halo-aliphatics											
Tetrachloroethene	TetCe	2.20	-0.27	2.88	HS	0.64	0.44	0.00	0.00	0.84	3.59
Trichloroethene	TriCe	3.10	-0.50	2.42	HS	0.52	0.37	0.08	0.03	0.72	3.00
Trichloromethane	TCM	3.90	-0.84	1.97	HS	0.43	0.49	0.15	0.02	0.62	2.48
monopolar aliphatics											
2-Octanone	Oct2on	2.95	-1.99	2.37[a]	TDU	0.11	0.68	0.00	0.51	1.25	4.28
Di-n-butyl ether	DNBE	2.48	-0.69	3.21	HS	0.00	0.25	0.00	0.45	1.30	3.92
Di-n-propyl ether	DNPE	3.69	-0.97	2.03	HS	0.01	0.22	0.00	0.44	1.01	2.80
Methyl tert-butyl ether	MTBE	4.62	-1.54	0.94	HS	0.02	0.28	0.00	0.54	0.87	2.27
nonpolar aromatics											
1,2-Dichlorobenzene	12DCB	2.19	-1.04	3.43	HS	0.87	0.78	0.00	0.04	0.96	4.16
Benzene	Benz	3.25	-0.65	2.17	HS	0.61	0.52	0.00	0.14	0.72	2.79
Benzo[b]furan	BbF	2.83	-2.34	2.67[a]	HS	0.89	0.83	0.00	0.15	0.91	-
Chlorobenzene	ClB	2.70	-0.80	2.84	HS	0.72	0.65	0.00	0.07	0.84	3.66
n-Propylbenzene	nPB	1.78	-0.40	3.69	HS	0.60	0.50	0.00	0.15	1.14	4.23
p-Xylene	pXy	2.21	-0.51[a]	3.15	HS	0.61	0.52	0.00	0.16	1.00	3.84
Toluene	Tol	2.72	-0.60	2.69	HS	0.60	0.52	0.00	0.14	0.86	3.33
polar aromatics											
Acetophenone	AP	3.74	-3.37	1.58	TDU	0.82	1.01	0.00	0.48	1.01	4.50
Methyl phenyl ether	MPE	3.02	-1.70	2.11	HS	0.71	0.75	0,00	0.29	0.92	3.89
Indole	Ind	3.28	-4.40[a]	2.14	TDU	1.20	1.12	0.44	0.22	0.95	-

Abb.: Abbreviation of compound name; log $C_{i,sat}$: saturated aqueous concentration [mg L^{-1}]; log $K_{a/w}$: logarithmic air/water partitioning constant from ref.[1, 2] unless otherwise noted; log $K_{o/w}$: logarithmic n-octanol/water partitioning constant; HS corresponds to volatile compounds where headspace analysis was used; TDU corresponds to semi-volatile compounds where the TDU-GC-MS analysis was used; [a] calculated using a combination of equations 6-15 and 6-17 from ref.[1]: $K_{a/w} = \frac{p_i[atm]}{C_{i,sat}[mol\ L^{-1}]} \cdot \frac{1}{T\ [K] \cdot R[atm\ L\ mol^{-1} K^{-1}]}$.

A3-S4 Sorption Isotherms

The data from six compounds was initially fitted to the linear model. The compounds represented different hydrocarbon classes such as aromatics, *n*-alkanes and aliphatics (Table A3-1). The isotherms agreed very well with the model ($R^2 > 0.98$, MWSE < 0.15), though when considering the whole compound set to derive the ppLFER from, an $R^2 < 0.5$ was observed for some sorbates using linear isotherms. Therefore, a model describing non-linear sorption was evaluated. The data from the six compounds was then fitted to the Freundlich model. All isotherms showed the same or better R^2 and MWSE values than the linear model. When considering the complete substance set for the ppLFER the R^2 and MWSE values were also better or the same as for the linear model. To get precise sorption data for all probe sorbates, even for substances with non-linear sorption, the Freundlich model fit was used for the complete substance set.

Table A3-2 - Comparison of two different sorption model fits to experimental data.

linear Model fit						
Sample	**a**	**SE**	**R^2**	**MWSE**	**AIC**	**N**
Benzene	2.02E+05	± 0.99	0.9786	0.1481	156.26	9
Di-n-butyl ether	1.74E+06	± 4.14	0.9932	0.1336	262.89	12
n-Hexane	7.24E+01	± 1.22	0.9977	0.0055	87.42	8
Chlorobenzene	9.41E+01	± 0.93	0.9989	0.0855	150.20	11
Tetrachloroethylene	2.51E+02	± 5.17	0.9941	0.0595	191.88	14
Indole	3.16E+00	± 0.08	0.9927	0.1100	166.78	12

Freundlich Model fit								
Sample	**K_F**	**SE**	**n**	**SE**	**R^2**	**MWSE**	**AIC**	**N**
Benzene	3.34E+01	± 2.94E+01	0.94	± 0.11	0.9627	0.1532	160.72	9
Di-n-butyl ether	6.21E+02	± 1.10E+02	0.86	± 0.02	0.9981	0.0268	246.48	12
n-Hexane	4.66E+01	± 6.67E+00	1.11	± 0.03	0.9976	0.0188	85.34	8
Chlorobenzene	1.35E+02	± 1.00E+01	0.94	± 0.01	0.9990	0.4073	140.88	11
Tetrachloroethylene	2.99E+02	± 5.04E+01	0.96	± 0.04	0.9918	0.0645	194.01	14
Indole	9.46E+00	± 2.73E+00	0.88	± 0.03	0.9955	0.1263	161.32	12

a: slope of linear fit with standard error (SE); K_F: Freundlich coefficient $[(\mu g\ kg^{-1})/(\mu g\ L^{-1})]^{1/n}$; n: Freundlich exponent; R^2: regression coefficient; N: number of data points; AIC: Akaikes Information criterion; MWSE= $1/v\sum[(C_{s,exp.} - C_{s,\ predicted})^2/C^2_{s,exp.}]$ mean weighted square error with v = N-p the degrees of freedom.

Table A3-3 - Fitting results of sorption isotherms to the Freundlich model.

Sorbate	log K_f		n		R^2	N	log $K_{p/a}$ 10^3 $C_{i,sat}$	log $K_{p/w}$ 10^{-2} $C_{i,sat}$	log $K_{p/w}$ 10^{-3} $C_{i,sat}$	log $K_{p/w}$ 10^{-4} $C_{i,sat}$
	value	SE	value	SE						
cHept	2.61	0.03	0.92	0.03	0.99	12	1.66	2.41	2.49	2.57
cHex	2.58	0.01	1.00	0.01	0.99	10	1.67	2.57	2.57	2.58
cOct	2.97	0.06	1.03	0.06	0.97	10	2.58	3.03	3.00	2.96
nHept	2.68	0.05	0.92	0.03	0.99	11	0.51	2.56	2.64	2.72
nHex	1.84	0.03	1.00	0.02	0.99	8	1.85	1.85	1.85	1.84
nOct	3.19	0.05	0.75	0.05	0.96	10	0.24	2.98	3.23	3.48
1Oct	3.13	0.10	0.85	0.08	0.95	8	1.12	2.89	3.04	3.19
cHexe	0.58	0.26	1.25	0.10	0.94	11	1.54	1.40	1.15	0.90
cPente	1.45	0.13	1.03	0.06	0.97	12	2.16	1.57	1.54	1.50
TetCe	2.29	0.03	1.07	0.03	0.99	14	2.82	2.50	2.43	2.37
TriCe	1.99	0.09	0.87	0.04	0.99	10	1.97	1.48	1.61	1.74
TCM	1.83	0.03	1.00	0.02	0.99	14	2.68	1.84	1.84	1.84
Oct2on	0.95	0.06	1.06	0.03	0.99	12	3.15	1.17	1.12	1.06
DNBE	2.69	0.03	0.89	0.01	0.99	12	2.91	2.11	2.23	2.34
DNPE	1.34	0.22	0.95	0.08	0.94	10	2.10	1.09	1.16	1.20
MTBE	1.55	0.17	0.91	0.05	0.97	10	3.11	1.04	1.14	1.23
12DCB	2.36	0.04	1.09	0.03	0.99	12	3.77	2.66	2.56	2.47
Benz	1.79	0.15	0.84	0.06	0.96	9	1.79	1.12	1.28	1.43
BbF	2.28	0.04	0.81	0.02	0.99	11	-	1.55	1.75	1.93
ClB	1.87	0.04	1.06	0.02	0.99	11	2.91	2.09	2.04	1.97
nPB	2.48	0.02	1.06	0.03	0.99	12	3.13	2.65	2.59	2.53
pXy	2.11	0.09	1.15	0.05	0.98	11	3.21	2.59	2.44	2.29
Tol	1.72	0.08	1.08	0.05	0.99	8	2.62	2.00	1.92	1.85
AP	1.93	0.55	0.82	0.17	0.75	9	4.57	1.09	1.26	1.44
MPE	1.47	0.28	0.95	0.10	0.90	10	2.98	1.28	1.33	1.38
Ind	0.80	0.05	0.93	0.02	0.99	12	-	0.49	0.56	0.63

log K_F: logarithmic Freundlich coefficient [(µg kg^{-1}) (µg L^{-1}) $^{1/n}$]; n: Freundlich exponent [-]; N: number of data points log $K_{p/a}$; logarithmic polymer-air distribution coefficient [L Kg^{-1}]; log $K_{p/w}$ logarithmic polymer-water distribution coefficient [L Kg^{-1}]; $C_{i,sat}$: saturated aqueous concentration [mg L^{-1}]; SE: standard Error of the calculated value.

A3-S5 Sorption mode

For the analysis of the dominant sorption mode, Endo *et al.* proposed an approach based on the ratio of the distribution coefficients for linear (K_n) and cyclic (K_c) alkanes in order to differentiate between adsorption and absorption [2–4]. The procedure is described in detail in section 1.2.5 of this work.

The ratios for the *n*-alkanes and cycloalkanes were calculated at an aqueous concentration of C_w 10^{-2} and resulted in K_n/K_c values for C6, C7 and C8 of 0.83, 0.56 and 0.45, respectively, suggesting that *ab*sorption is the dominant sorption mode for HDPE. The data are consistent with data from Hüffer & Hofmann and from Endo *et al.* Both studies compared K_n/K_c ratios for low-density polyethylene (LDPE), polypropylene (PP) and hexadecane. LDPE showed $K_n/K_c < 0.33$ whereas PP and hexadecane for example showed K_n/K_c ratios of < 0.60 for C6, C7 and C8 [3, 4]. The decrease of the K_n/K_c value with increasing number of carbon atoms in the molecule is consistent with data from other polymers determined in literature [3, 4].

A3-S6 Leave-Many-out cross validation analysis using assorted compounds

For validation of the derived ppLFER model, a leave-many-out approach was chosen. The compound set was sorted with decreasing log $K_{p/w}$ values and a selection pattern was chosen, as suggested by Gramatica [7]. Seven compounds were selected for the internal cross-validation (33 %) following the pattern: V-T-T-T-V-T-T-T-V-T-T-T-V-T-T-T-V-T-T-T-V-T-T-T-V. With these compounds, a cross-validated correlation coefficient ($Q^2_{LMO\text{-}CV}$) and a cross-validated root mean square error ($RMSE_{LMO\text{-}CV}$) were calculated using the following equations:

$$Q^2_{LMO\text{-}CV} = 1 - \frac{\sum_n^{i=1} (y_i^{exp} - y_i^{predCV})^2}{\sum_n^{i=1} (y_i^{exp} - y^{exp})^2} \qquad \text{(Eq. A3-2)}$$

$$RMSE_{LMO\text{-}CV} = \sqrt{\frac{\sum_n^{i=1} (y_i^{exp} - y_i^{predCV})^2}{n}} \qquad \text{(Eq. A3-3)}$$

where y_i^{exp} denotes the experimental log $K_{p/w}$ value for a compound i, y_i^{predCV} denotes calculated log $K_{p/w}$ values for a compound i and n represents the number of compounds. The results of the cross-validation are shown in the following Table.

Table A3-4 - Validation set for the leave-many-out cross validation.

	Concentration level		
	10^{-2} $C_{i,sat}$	**10^{-3} $C_{i,sat}$**	**10^{-4} $C_{i,sat}$**
	cOct	nOct	nOct
	nPB	nPB	cHex
	TetCe	pXy	TetCe
	Tol	Tol	BbF
	TriCe	cPente	cPente
	Benz	cHexe	MTBE
	Ind	Ind	Ind
$Q^2_{LMO\text{-}CV}$	0,918	0,857	0,933
$RMSE_{LMO\text{-}CV}$	0,058	0,103	0,051

$Q^2_{LMO\text{-}CV}$: The cross-validated correlation coefficient; $RMSE_{LMO\text{-}CV}$: The cross-validated root mean square error.

A3-S7 Akaike's Information Criterion

The model that shows the smallest Akaike's Information Criterion (AIC) will most likely be the better fitting model. The AIC values for each model were calculated following Motulsky and Christopoulos in Gramatica [7]:

$$AIC = N \cdot \left(\frac{WSS_{res}}{N}\right) + 2p + \frac{2p \cdot (p+1)}{N-p-1} \quad \text{(Eq. A3-4)}$$

where N is the number of data points, p are the number of fitting parameters and WSS_{res} is the weighted sum of squares residual:

$$WSS_{res} = \sum \frac{(C_{s,\ measured} - C_{s,\ predicted})^2}{C_{s,\ measured}} \quad \text{(Eq. A3-5)}$$

All parameters were calculated using OriginLab 9.1.

Table A3-5 – Substance set used for multi linear regression analyses for direct sorbate interactions.

Compound	E	S	A	B	L	log $K_{p/a}$
cHept	0.35	0.10	0.00	0.00	3.70	1.66
cHex	0.31	0.10	0.00	0.00	2.96	1.67
cOct	0.41	0.10	0.00	0.00	4.33	2.58
nHept	0.00	0.00	0.00	0.00	3.17	0.51
nOct	0.00	0.00	0.00	0.00	3.68	0.24
1Oct	0.09	0.08	0.00	0.07	3.57	1.12
cHexe	0.40	0.20	0.00	0.10	3.02	1.54
cPente	0.34	0.20	0.00	0.10	2.40	2.16
TetCe	0.64	0.44	0.00	0.00	3.58	2.82
TriCe	0.52	0.37	0.08	0.03	3.00	1.97
TCM	0.43	0.49	0.15	0.02	2.48	2.68
Oct2on	0.11	0.68	0.00	0.51	4.26	3.15
DNBE	0.00	0.25	0.00	0.45	3.92	2.91
DNPE	0.01	0.22	0.00	0.44	2.80	2.10
MTBE	0.02	0.28	0.00	0.54	2.27	3.11
12DCB	0.87	0.78	0.00	0.04	4.52	3.77
Benz	0.61	0.52	0.00	0.14	2.79	1.79
ClB	0.72	0.65	0.00	0.07	3.66	2.91
nPB	0.60	0.50	0.00	0.15	4.23	3.13
pXy	0.61	0.52	0.00	0.16	3.84	3.21
Tol	0.60	0.52	0.00	0.14	3.33	2.62
AP	0.82	1.01	0.00	0.48	4.50	4.57
MPE	0.71	0.75	0.00	0.29	3.89	2.98

log $K_{p/a}$; logarithmic polymer-air distribution coefficient [L Kg^{-1}]

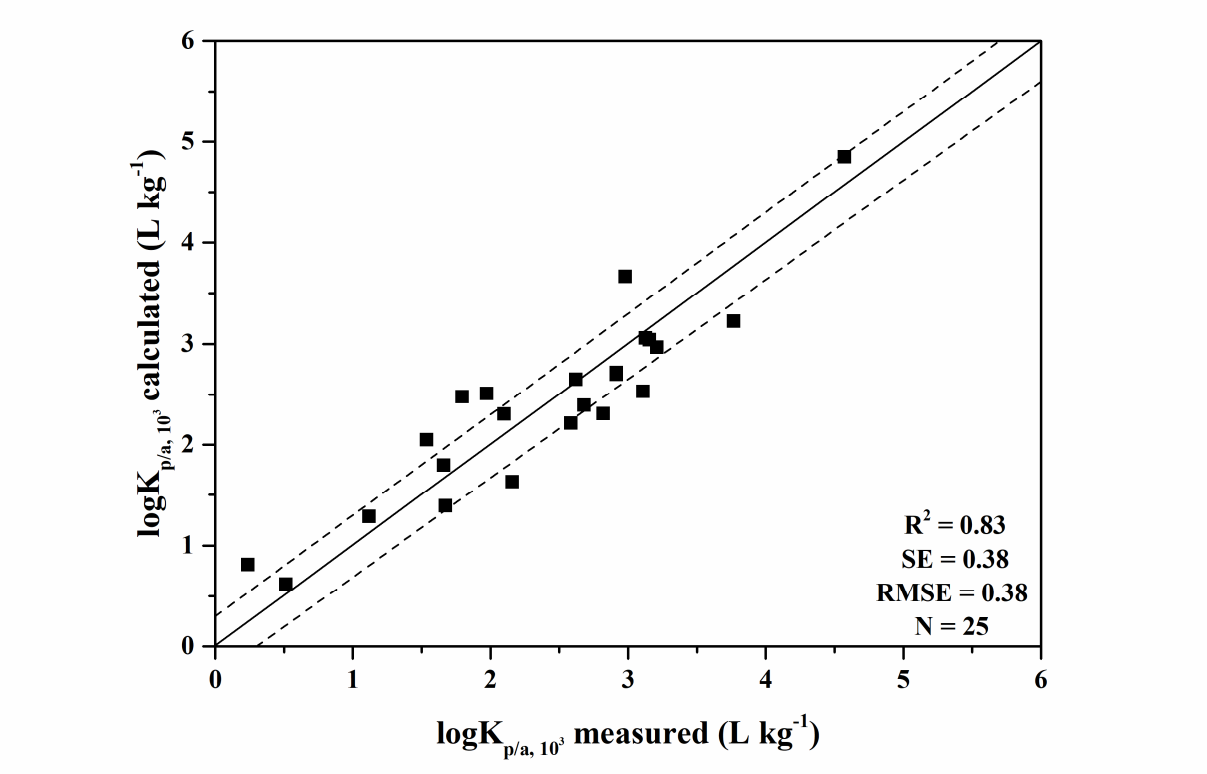

Figure A3-4 – Concentration dependence for the derived ppLFER model with descriptors representing direct interactions only (E, S, V). The solid line represents 1:1 prediction, dashed lines represent 0.3 log units' deviation. R^2: regression coefficient; SE: standard Error; RMSE: root mean square error; N: number of data points.

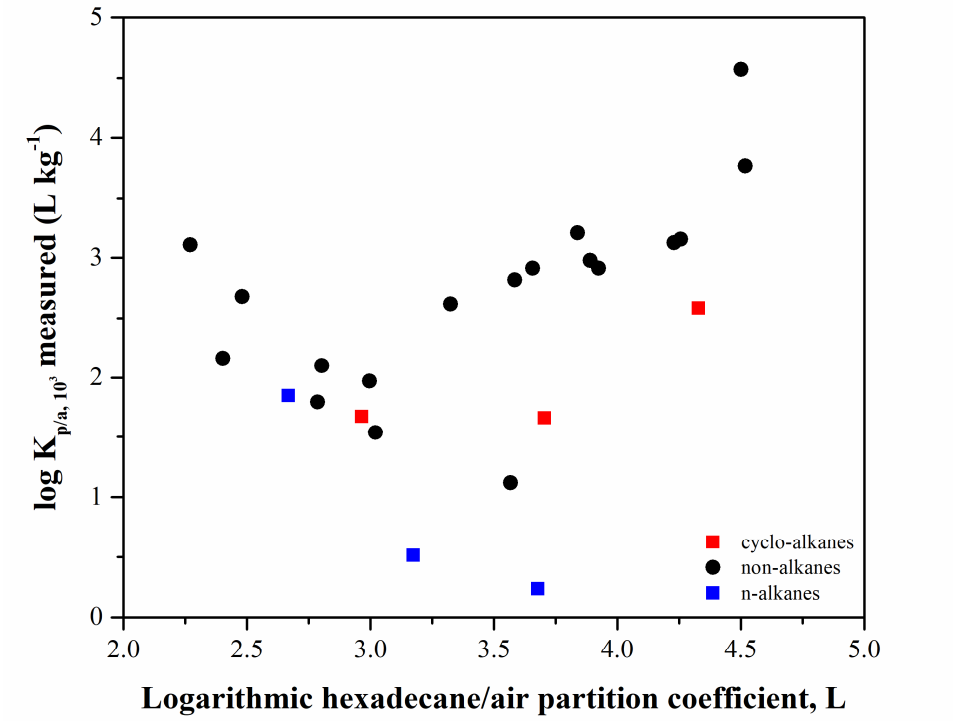

Figure A3-5 – Correlation of log $K_{p/a}$ and the L descriptor of non-alkanes (black), cyclo-alkanes (red) and n-alkanes (blue).

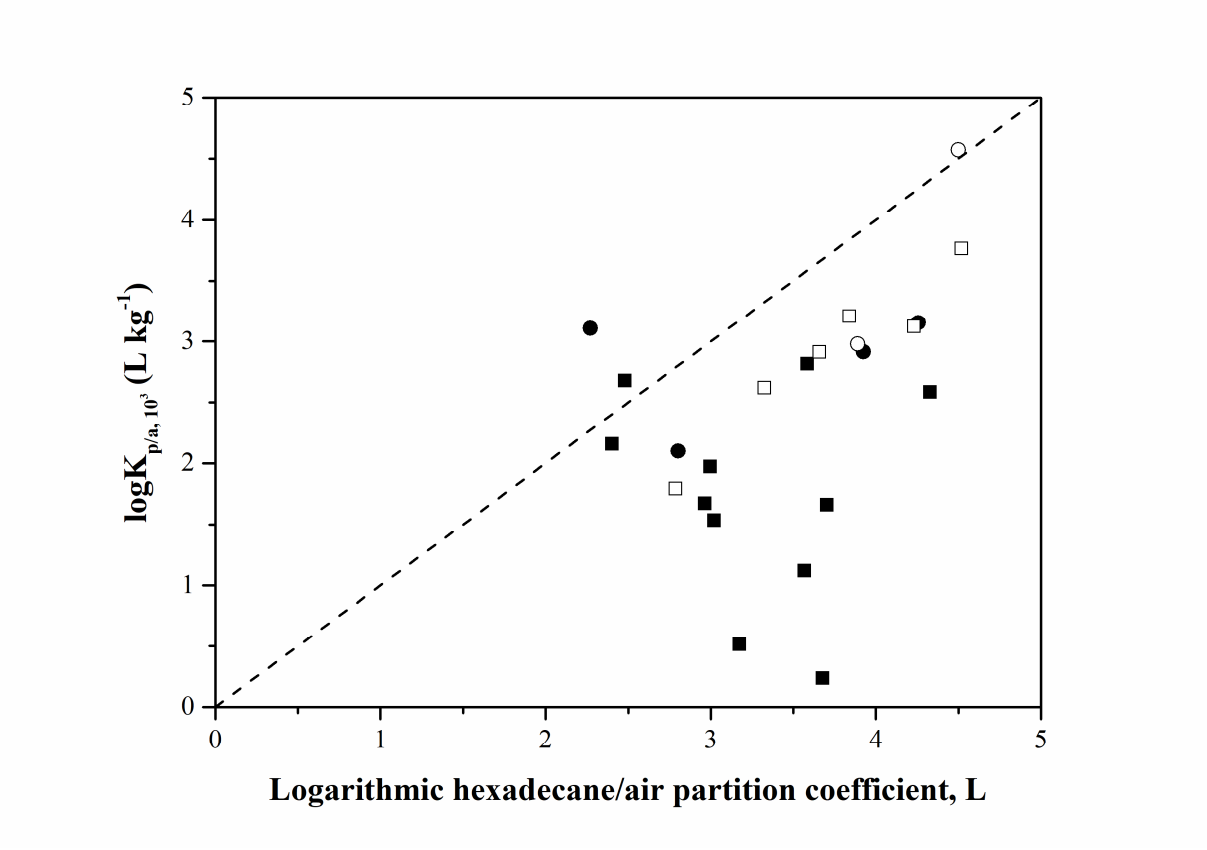

Figure A3-6 – Correlation of log $K_{p/a}$ and the logarithmic hexadecane-air coefficients, L. Squares denote nonpolar compounds and circles denote polar compounds. Filled points are aliphatic and hollow data points are aromatic compounds.

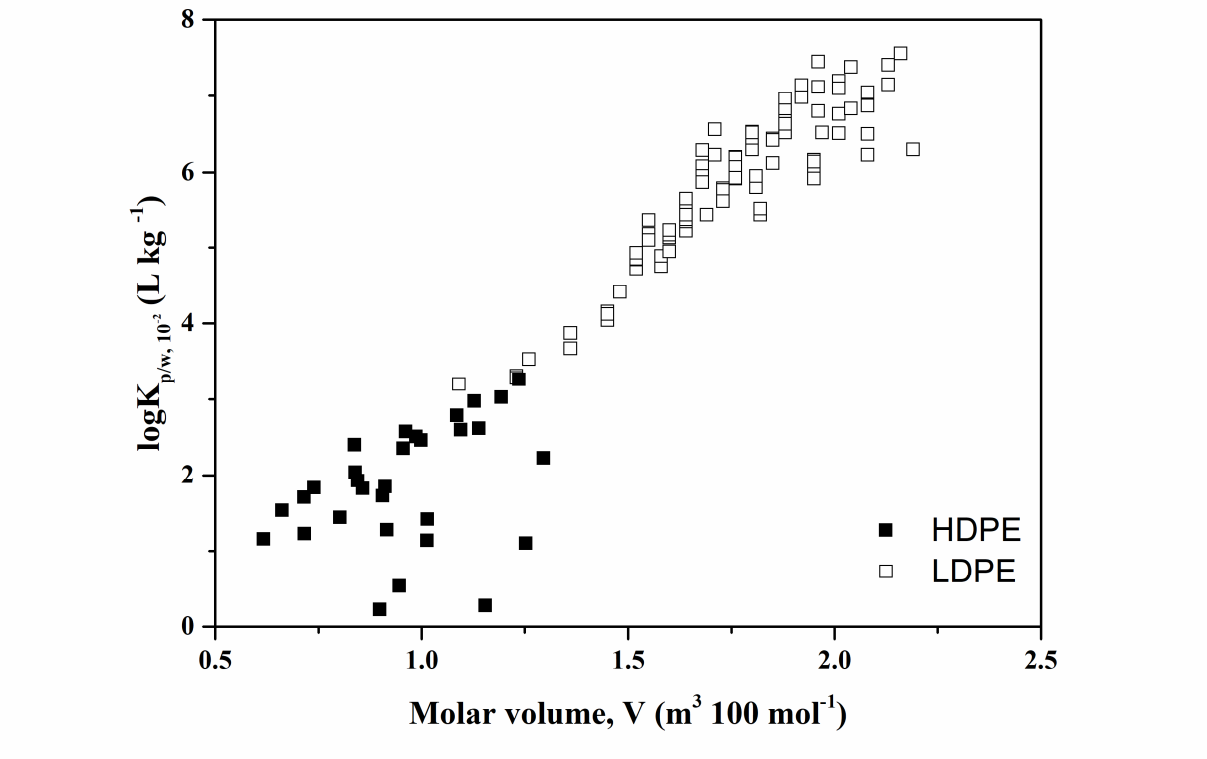

Figure A3-7 - Distribution coefficients log $K_{p/w}$ vs. the molar volume coefficient (V).

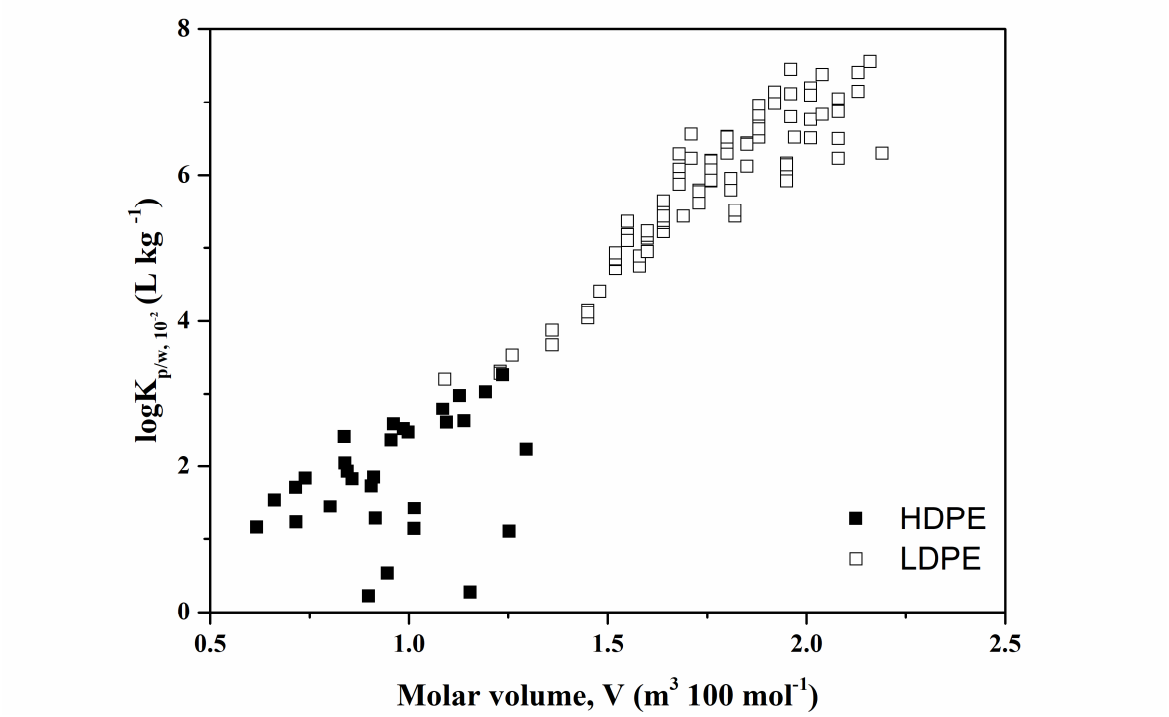

Figure A3-8 – log $K_{p/a}$ vs excess molar refraction E. Squares denote nonpolar compounds and circles denote polar compounds. Filled points are aliphatics and hollow data points are aromatic compounds.

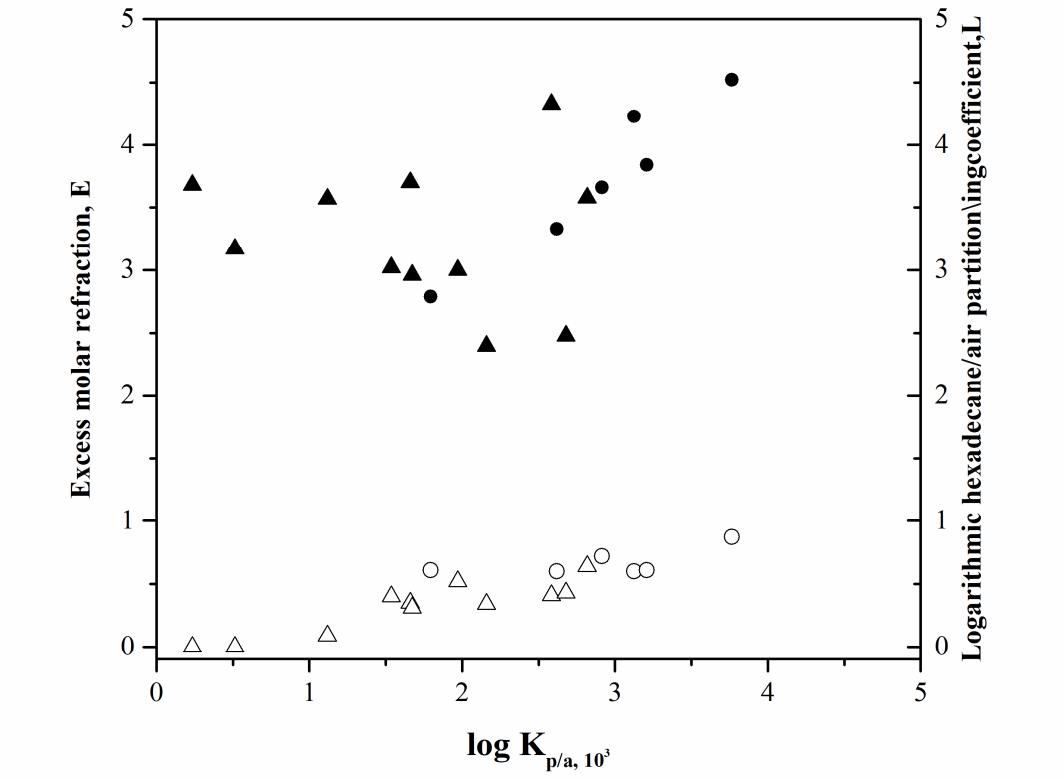

Figure A3-9 - Sorption behaviour of nonpolar aliphatics and nonpolar aromatics compared to different sorbate descriptors. The ○ and ● represent nonpolar aromatics and ▲and Δ represent nonpolar aliphatics. Hollow data points correspond to the left Y-axis (E descriptor) and filled data points correspond to the right Y-axis (L descriptor).

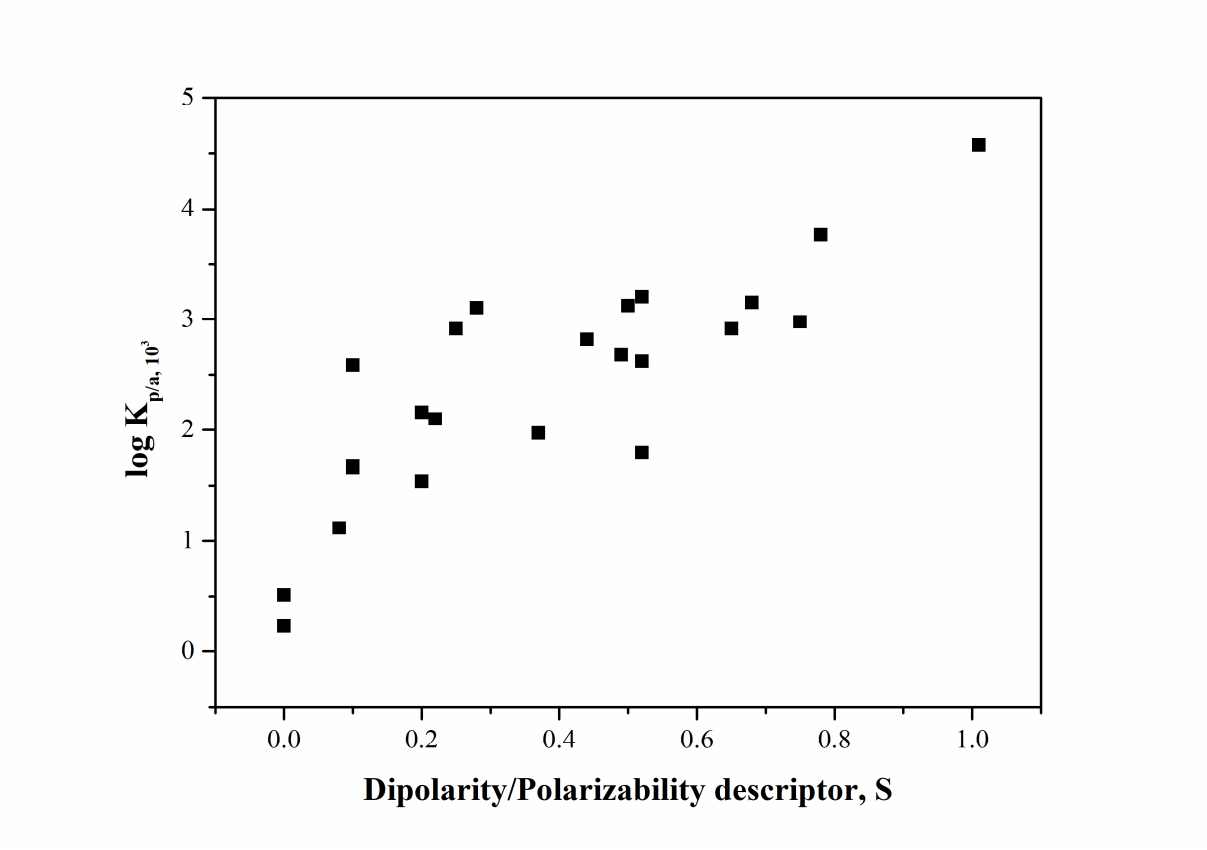

Figure A3-10 - Comparison of log $K_{p/a}$ and the S descriptor representing dipolarity and polarizability.

A3-S9 Statistical analysis of ppLFER models

Table A3-6 - Calculated parameters for the ppLFER at 10^{-2} aqueous solubility.

	Coefficient	SE	p-value
c	0.53	0.44	0.2406
e	0.06	0.64	0.9296
s	-0.15	0.71	0.8292
a	-2.56	0.82	0.0056
b	-3.10	0.70	0.0003
v	2.11	0.40	< 0.0001

Table A3-7 - ANOVA Results for the ppLFER at 10^{-2} aqueous solubility.

	DF	Sum of Squares	Mean Square	F-Value	Prob>F
Model	5	10.8491	2.16982	20.63576	4.4273E-7
Error	19	1.99782	0.10515		
Total	24	12.84692			

Table A3-8 - Calculated parameters for the ppLFER at 10^{-3} aqueous solubility.

	Coefficient	SE	p-value
c	0.50	0.43	0.2636
e	-0.10	0.63	0.8808
s	-0.05	0.69	0.9453
a	-2.33	0.80	0.0089
b	-3.14	0.69	0.0002
v	2.20	0.39	< 0.0001

Table A3-9 - ANOVA Results for the ppLFER at 10^{-3} aqueous solubility.

	DF	Sum of Squares	Mean Square	F-Value	Prob>F
Model	5	10.75449	2.1509	21.48827	3.22281E-7
Error	19	1.90183	0.1001		
Total	24	12.65632			

Table A3-10 - Calculated parameters for the ppLFER at 10^{-4} aqueous solubility.

	Coefficient	SE	p-value
c	0.46	0.48	0.3496
e	-0.25	0.71	0.7286
s	0.06	0.78	0.9405
a	-2.10	0.90	0.0305
b	-3.18	0.77	0.0006
v	2.29	0.44	< 0.0001

Table A3-11 - ANOVA Results for the ppLFER at 10^{-4} aqueous solubility.

	DF	Sum of Squares	Mean Square	F-Value	Prob>F
Model	5	10.72617	2.14523	16.97081	1.9838E-6
Error	19	2.40174	0.12641		
Total	24	13.12791			

Table A3-12 - Calculated parameters for the ppLFER at 10^{4} sorbate loading.

	Coefficient	SE	p-value
c	-0.58	0.69	0.2605
e	3.05	1.00	0.8808
s	-0.95	1.19	0.9453
a	7.32	3.75	0.0089
b	4.55	1.19	0.0002
v	0.38	0.19	< 0.0001

Table A3-13 - ANOVA Results for the ppLFER at 10^{4} sorbate loading.

	DF	Sum of Squares	Mean Square	F-Value	Prob>F
Model	5	18.80654	3.76131	17.66152	3.35622E-6
Error	17	3.62043	0.21297		
Total	22	22.42697			

Table A3-14 - Calculated parameters for the ppLFER of low-density polyethylene.

	Coefficient	SE	p-value
c	-0.32	0.28	0.2615
e	0.69	0.13	< 0.0001
s	-0.15	0.31	0.6188
a	0.00	0.00	-
b	-4.07	0.42	< 0.0001
v	2.95	0.45	< 0.0001

Table A3-15 - ANOVA Results for the ppLFER low-density polyethylene.

	DF	Sum of Squares	Mean Square	F-Value	Prob>F
Model	4	93.83061	23.45765	481.85407	0
Error	93	4.52743	0.04868		
Total	97	98.35804			

Table A3-16 - Calculated parameters for the independent ppLFER fit.

		Coefficient	SE	Prob>F
e	Intercept	0.36	6.8E-17	< 0.0001
	Slope	0.15	2.23E-17	< 0.0001
s	Intercept	-0.37	1.29E-7	< 0.0001
	Slope	-0.11	4.21E-8	< 0.0001
a	Intercept	-3.01	1.23E-7	< 0.0001
	Slope	-0.23	4.02E-8	< 0.0001
b	Intercept	-3.03	4.06E-7	< 0.0001
	Slope	0.04	1.33E-7	< 0.0001
v	Intercept	1.93	2.87E-16	< 0.0001
	Slope	-0.09	9.39E-17	< 0.0001
c	Intercept	0.60	5.08E-17	< 0.0001
	Slope	0.04	1.66E-17	< 0.0001

Table A3-17 - ANOVA Results for the independent ppLFER.

		DF	Sum of Squares	Mean Square	F-Value	Prob>F
	Model	1	7.84	7.84	4.72E31	< 0.0001
e	Error	998	1.66E-28	1.66E-31		
	Total	999	7.83			
	Model	1	3.78	3.80	6.40E12	< 0.0001
s	Error	998	5.92E-10	5.92E-13		
	Total	999	3.80			
	Model	1	17.54	17.54	3.25E13	< 0.0001
a	Error	998	5.38E-10	5.389E-13		
	Total	999	17.54			
	Model	1	0.42	0.42	7.101E10	< 0.0001
b	Error	998	5.89E-9	5.90E-12		
	Total	999	0.42			
	Model	1	2.77	2.77	9.42E29	< 0.0001
v	Error	998	2.94E-27	2.94E-30		
	Total	999	2.77			
	Model	1	0.41	0.41	4.48E30	< 0.0001
c	Error	998	9.21E-29	9.23E-32		
	Total	999	0.41			

Abbreviations and comments:

DF: degrees of freedom

SE: standard error of estimates

All parameters above were calculated at 95% confidence level using OriginLab 9.1.

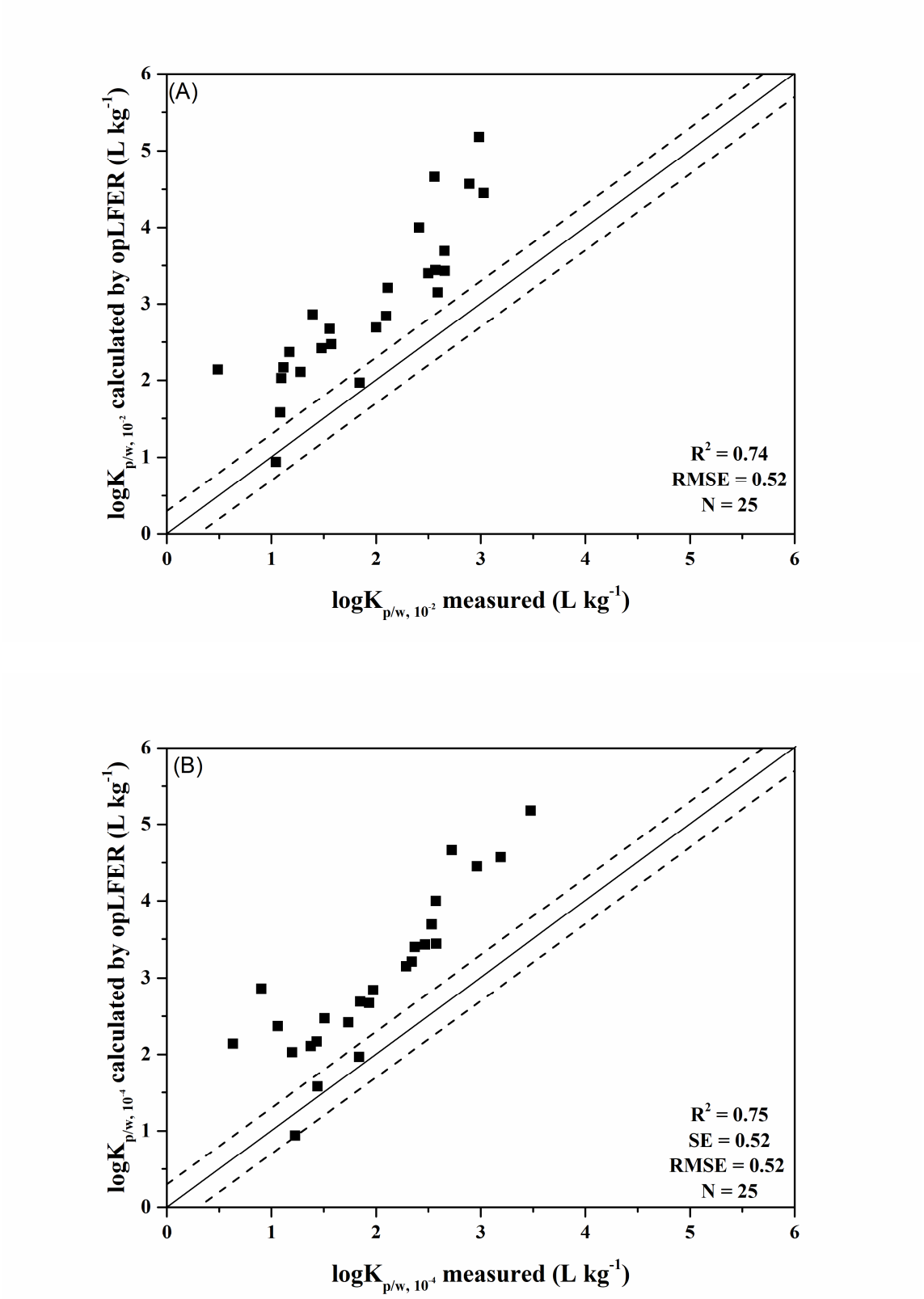

Figure A3-11 - Comparison of the opLFER-Model (log $K_{o/w}$) with experimental data at two different concentration levels; log $K_{p/w}$ 10^{-2} (A) $C_{i,sat}$ and 10^{-4} $C_{i,sat}$ (B). For both concentration levels, the predicted distribution coefficients are plotted vs. the experimental distribution coefficients. The solid line represents 1:1 prediction; the dashed lines represent 0.3 log units deviation. R^2: regression coefficient; RMSE: root mean squared error; N: number of data points.

Table A3-18 - Minimum and Maximum sorbed concentration µg kg^{-1} of the sorption isotherms.

Compound	min.	max.
12DCB	2.88E+02	8.38E+04
1Oct	3.92E+02	8.52E+04
AP	1.65E+03	2.63E+05
Benz	3.42E+02	6.82E+04
BbF	2.42E+02	6.29E+04
ClB	9.10E+00	6.26E+04
cHept	6.68E+00	7.87E+03
cHex	5.59E-01	5.00E+03
cHexe	4.86E+01	2.27E+05
cOct	9.58E+00	1.65E+03
cPente	1.13E+02	1.13E+05
DNBE	1.89E+03	1.53E+06
DNPE	1.03E+02	1.13E+05
Ind	2.05E+01	3.18E+04
MPE	4.07E+02	1.73E+05
MTBE	1.10E+03	1.65E+06
nHept	2.62E+01	1.24E+05
nHex	1.03E+01	6.44E+03
nOct	4.49E+02	3.77E+04
nPB	1.88E+01	7.10E+03
Oct2on	1.91E+02	3.18E+04
pXy	3.02E+01	1.88E+05
TetCe	1.40E+02	3.02E+04
TCM	1.04E+02	3.61E+05
Tol	3.30E+01	5.02E+04
TriCe	1.84E+03	7.99E+04

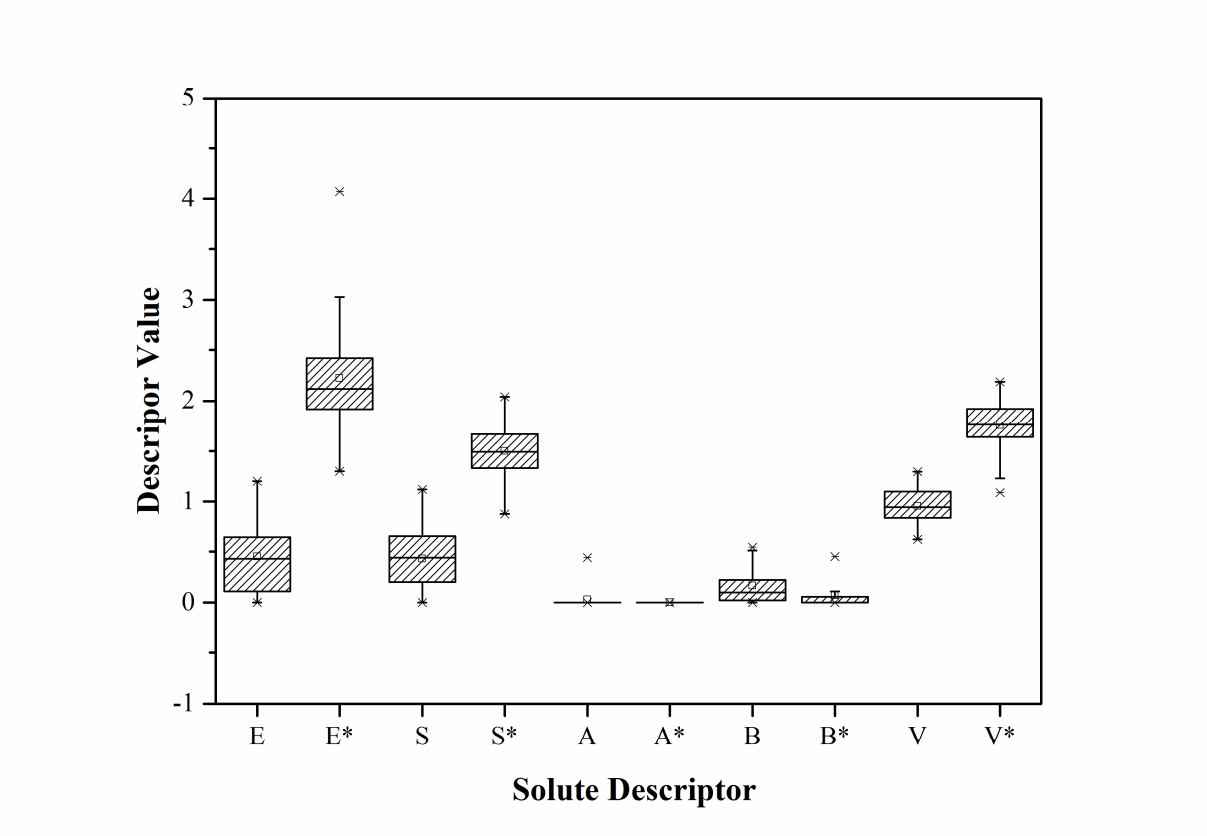

Figure A3-12 - Distribution of solute Descriptors used for the development of the ppLFER for HDPE (E, S, A, B & V) and LDPE (E*, S*, A*, B* & V*). The error bars denote the maximum and minimum value of each descriptor from the data set.

References

[1] R. P. Schwarzenbach, P. M. Gschwend, and D. M. Imboden, *Environmental Organic Chemistry*, 2nd ed., no. 2. John Wiley & Sons Inc., Hoboken, New Jersey, 2003.

[2] T. Hüffer, S. Endo, F. Metzelder, S. Schroth, and T. C. Schmidt, "Prediction of sorption of aromatic and aliphatic organic compounds by carbon nanotubes using poly-parameter linear free-energy relationships.," *Water Res.*, vol. 59, no. 1, pp. 295–303, 2014.

[3] S. Endo, P. Grathwohl, and T. C. Schmidt, "Absorption or Adsorption ? Insights from Molecular Probes n -Alkanes and Cycloalkanes into Modes of Sorption by Environmental Solid Matrices," *Environ. Sci. Technol.*, vol. 42, no. 11, pp. 3989–3995, 2008.

[4] T. Hüffer and T. Hofmann, "Sorption of non-polar organic compounds by micro-sized plastic particles in aqueous solution.," *Environ. Pollut.*, vol. 214, no. 1, pp. 194–201, Apr. 2016.

[5] K.-U. Goss, "The Air/Surface Adsorption Equilibrium of Organic Compounds Under Ambient Conditions," *Crit. Rev. Environ. Sci. Technol.*, vol. 34, no. 4, pp. 339–389, Jul. 2004.

[6] S. Endo, P. Grathwohl, S. B. Haderlein, and T. C. Schmidt, "Characterization of sorbent properties of soil organic matter and carbonaceous geosorbents using n-alkanes and cycloalkanes as molecular probes.," *Environ. Sci. Technol.*, vol. 43, no. 2, pp. 393–400, 2009.

[7] P. Gramatica, "Principles of QSAR models validation: internal and external," *QSAR Comb. Sci.*, vol. 26, no. 5, pp. 694–701, 2007.

Chapter 4 Sorption of non-ionic organic compounds by polystyrene in water

Adapted with permission from : Uber, T. H.; Hüffer, T.; Planitz, S.; Schmidt, T. C. Sorption of non-ionic organic compounds by polystyrene in water. *Submitted manuscript.*

4.1 Abstract

Plastic materials exist in many different chemical configurations with a large number of different properties. Polystyrene (PS) is a plastic material that is well known for its use as insulating material in construction, as heat resistant material for beakers and cutlery or as a packaging material for shock sensitive goods in its expanded form (EPS). With its wide range of application and the prevalence across the society, PS contributes significantly to the overall plastic load in aqueous systems. Sorption of organic compounds by plastic waste, especially micrometre sized particles, in the environment has become a hot topic and a concern in the past years.

The aim of this study was to improve the understanding of sorption properties of PS, one of the major plastic pollutants in the aqueous environment. Batch experiments with PS film (29 μm thickness) were performed for 4 days using a diverse set of 24 sorbates to account for varying molecular properties like polarity or molecular volume. Isotherms were evaluated using different sorption models to elucidate the sorption process of PS. Sorption to PS film was non-linear and absorption into the bulk material was the dominant sorption mode. The non-linear sorption to PS was shown to be controlled by the molar volume but also by the polarizability/dipolarity parameter (S) of the ppLFER model. The latter is influenced by the aromatic π-π-interactions of PS with the sorbate. Similar to other plastics like polyethylene, sorption to PS is driven by hydrophobic interactions but phase descriptors of pristine PS were significantly different than descriptors for other environmental relevant plastics.

4.2 Abstract Art

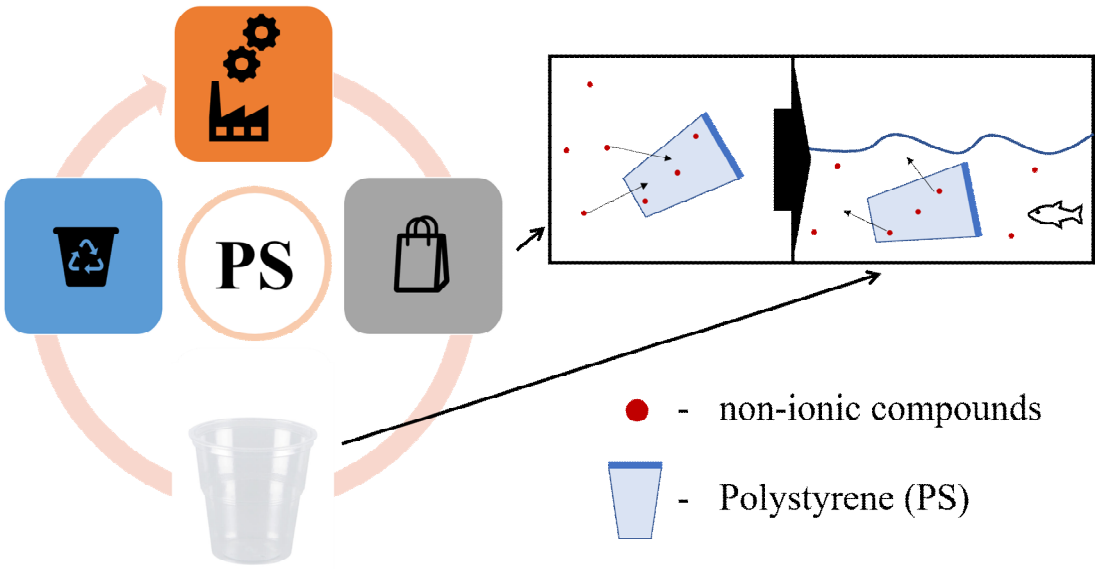

Figure 4-1 - Graphical Abstract of the studies described in this chapter.

4.3 Introduction

Polystyrene (PS) is an aromatic polymer made from the petrochemical monomer styrene. It is produced as either general-purpose grade PS or high-impact grade PS, which is a version with modified polybutadiene. General-purpose PS is a linear homo-polymer with the base unit -CH_2-$CH(C_6H_5)$. All commercially available polystyrenes are atactic and amorphous and do not crystallize when stretched [1]. PS can be expanded by use of gases to a light foam with excellent insulating properties. Expanded PS (EPS) is used as an insulating material and as a packaging material, often for electronic goods [2].

PS and plastics in general have the advantage of a high strength-to-weight ratio, allowing minimal material consumption for packaging. PS plastic packaging amounts only to 1 – 3 % of the total product weight, making it an extremely cost-efficient packaging material that also saves energy during transport due to its low weight [3]. On the other hand, plastic packaging increases the amount of plastic litter [4]. PS has been identified as one of the main components of microplastics in different water bodies [5–7]. After entering the waterbodies plastics are degraded into micrometer size particles which are nearly impossible to remove [8–10]. The ingestion, digestion and adherence of PS beads was shown to negatively impact function and health for several zooplankton taxa from the Northeast Atlantic [11]. A study of marine debris in 2013 found very high levels of persistent organic pollutants (POPs) like polycyclic aromatic hydrocarbons (PAHs) on PS foam packaging material as well as PS in marine debris [12]. The impact on the transport of POPs through plastic particles is minor with regard to the amount of plastic in the world's oceans [13] but is still an ongoing discussion [14–16]. Recently, many review articles were published, regarding the interactions of microplastics and POPs in the environment [14, 15, 17]. Sorption by PS has been discussed in different contexts [18–20], e.g. as a packaging material in the pharmaceutical industry [21]. For this case, studies were undertaken to investigate the sorption behaviour of the PS containers used for drugs [21].

Knowledge on the dominant sorption mode of a given sorbent (i.e. PS) is of importance for the assessment of environmental fate and behaviour of contaminants [22]. *Ad*- and *ab*sorption can be influenced by different material properties like pore sizes as shown by literature for PE and PS and surface tension [20, 23]. The mechanisms and interactions for sorption can be London-dispersion forces, dipole interactions, H-bond interactions, π-π-interactions or hole filling by dissolution [24]. In any case, sorption is described by many different postulated isotherms.

Prediction of equilibrium constants can be done by single-parameter free energy relationships for example based on the 1-octanol-water (log $K_{o/w}$) or the hexadecane-water distribution coefficient (log $K_{h/w}$). More precise predictions of sorption for a large variety of compounds are done with the help of linear solvation-energy models like the Abraham model (ppLFER) [25].

This study systematically investigates sorption behaviour of PS in water, applying different models describing sorption. These models were compared with each other and a ppLFER was created based on the best model fit. Sorption properties were then interpreted based on the descriptors of the ppLFER. A mutual comparison of the ppLFER equations for PS was done with aged PS and other polymers to demonstrate the sorption properties directing sorption to PS in water.

4.4 Materials and Methods

4.4.1 Materials

PS was ordered from GoodFellow (Hamburg, Germany) as a transparent film with a thickness of 29 µm. The PS film was cut with scissors into squares of approximately 3.5 x 3.5 cm (~ 50 mg). Every cut PS piece was then weighed on a balance and the weight was then incorporated in the mass balance, calculating the sorbed concentration [26]. 24 organic probe sorbates were ordered from VWR Germany (purity > 99 %) and stock solutions were prepared in methanol and kept at 4 °C to avoid losses due to evaporation. The concentrations of the stock solutions for batch experiments were chosen based on the sorbates' aqueous solubilities ($C_{i,sat}$) and the desired concentration range of the sorbate sorption isotherm. A list of the sorbates and assorted physicochemical properties can be found in the appendix (Table A4-1). The compound set is divided into six groups: alkanes, alkenes, halo-aliphatics, monopolar aliphatics and nonpolar aromatics and polar aromatics. Purified water was gathered from an ELGA Purelab water purifier (T = 23 °C, TOC ≤ 1 ppb and σ ≤ 0.055 µS).

4.4.2 Sorption batch experiments

For the sorption batch experiments, the PS material (~ 50 mg pieces) was placed in 10 mL purified water to investigate only the interactions between PS and water. The batch samples were spiked with a stock solution in a 20-mL glass headspace vial (BGB Germany) with a Screw cap and butyl/PTFE septa. The amount of stock solution was chosen to reach concentrations between 10^{-2} and 10^{-4} of the sorbates' $C_{i,sat}$ (controlled by GC-MS analysis). The methanol content did not exceed 0.25 % (v/v) to avoid co-solvent effects. For blank control, a

PS square was placed in a vial with a background solution containing purified water and 0.25 % methanol (v/v). The samples were then shaken in an overhead shaker (Reax 2) from Heidolph for at least 4 days at a constant temperature of 21 °C. The methodology for sorption batch experiments has been described in more detail elsewhere [26–28]. Recently, an equilibration time of 17 days was reported for polystyrene beads (169 µm) in water [27]. However, for the PS film, preliminary experiments prior to the batch experiments showed that a shaking time of 4 days was sufficient to reach equilibrium (Figure A4-1). Shorter equilibration times observed in this study can be explained by the faster diffusion into the thin, untreated, PS film compared to the bigger, UV-degraded, PS beads from the literature experiments.

Loss of analytes during the experimental measurements was monitored by preparing spiked samples with no sorbent and incorporating these results in the mass balance for calculating the sorbed concentration. Air-water partitioning (log $K_{a/w}$) constants were incorporated to calculate the according phase distribution of the probe sorbates and the results are given in Table A4-2 in the appendix.

4.4.3 PS Characterization

For a detailed discussion of the sorption mechanisms for PS, the sorbent properties were initially determined using different analytical techniques. The glass transition temperature and the crystallinity were determined using Differential Scanning Calorimetry (DSC). The DSC-curve and the procedure are described in the appendix (Figure A4-2). An Ubbelohde type viscometer was used to determine the medium molar mass of PS. The experiments were completed following DIN EN ISO 1628-1 [29] and DIN EN ISO 1628-3 [30]. A gas pycnometer was used for the determination of the density and experiments were completed according to DIN EN ISO 1183-1. The surface tension was determined through the contact angle of substances on the PS surface. The contact angle of PS was determined with 4 substances (methanol, formamide, toluene and ethylene glycol). Following the method of Owens, Wendt, Rabel and Kaelble (OWRK), the surface tension was calculated from the contact angles of each substance [31, 32]. Other information on the PS material used was extracted from the product sheet of the supplier and is also shown in detail in the appendix (Table A4-2).

4.4.4 Sorption Models and Statistics

Evaluation of the sorption isotherms is the key to interpreting the processes driving sorption. Sorption to polymers has been shown to be linear or non-linear, depending on the properties of the polymer particles [27]. Sorption by PS determined using only seven probe

compounds was shown to be non-linear [27]. In the present study, sorption of a more diverse and extended compound set was measured. The experimental isotherm data were fit to the three non-linear models Freundlich (FM), Langmuir (LM) and Polanyi-Manes (PMM). The FM has previously been applied to sorption isotherms for synthetic polymers and has been found to describe sorption to HDPE very well [26]. Additionally, the LM has been known to describe non-linear sorption in cases where there are limited sorption sites on the sorbent surface. This is the case for sorbents having a perfectly flat plane with no corrugations and equally distributed sorption sites like pristine plastics [24, 33].

The PMM has previously been used to describe sorption by several micro sized synthetic polymer particles like PS, low-density polyethylene (LDPE) and poly acrylate (PA) from water [27]. There have also been investigations using this model to describe sorption to polystyrene/divinylbenzene matrices [34]. The method to determine the fitting parameters is described in brief in the appendix (A4-S3) [35]. The fitting models were compared based on the correlation coefficient (R^2), the root-mean-square error (RMSE) based on the comparison between predictions from the sorption model and the data from the experiments, and the Akaikes information criterion (AIC) [36].

Table 4-1 - Fitting parameters of the sorption models.

Name	Abbr.	Equation	Linear Form	Fitting parameters
Freundlich	FM	$C_p = K_F C_w^{n^{-1}}$	$\log C_p = \frac{1}{n} C_w + \log K_F$	n, K_F
Langmuir	LM	$C_p = \frac{Q^0 C_w}{K_L + C_w}$	$\frac{C_{i,w}}{C_{i,s}} = \frac{1}{Q_0} C_w + \frac{1}{K_{i,L} \cdot Q_0}$	K_L, Q^0
Polanyi-Manes	PMM	$\log C_p = \log Q^0 + a(\frac{\epsilon_{SW}}{V_S})^b$	No linear form	Q^0, a, b

C_p: equilibrium adsorbed concentration [µg kg^{-1}]; log K_F: logarithmic Freundlich coefficient [(µg kg^{-1}) (µg L^{-1}) n^{-1}]; n: Freundlich exponent [-]; C_w: equilibrium aqueous concentration [µg L^{-1}]; Q_0: adsorbed capacity [µg kg^{-1}]; ε_{sw}: effective adsorption potential [kJ mol^{-1}]; a [$(mL)^{b+1}$ $(mol\ J^b)^{-1}$] and b [-] fitting parameters; V_s: molar volume of solute [mL mol^{-1}].

The characterization of sorption relevant properties from PS was done by multiple regression analysis (MRA) from distribution coefficients and sorbate descriptors.

The necessary fitting parameters of all the models are listed in Table 4-1. Statistical analysis of the validity of the sorption models was done using OriginPro Lab 8.1 software.

4.5 Results and Discussion

4.5.1 Polymer characterization

Sorption to polymer material can be prone to several properties like density, glass transition temperature (T_g), surface tension and mean molecular mass. The PS material was characterized by several methods to determine these properties and the results of the characterization are shown in Table 4-2.

With a density of 1.05 g cm^{-3}, the PS material has a higher density than other polymers like polyethylene (PE). A Tg of 109 °C and the density show that PS at room temperature is a glassy polymer demonstrating the high degree of chain branching and indicating concurrent dissolution (absorption) and hole filling (adsorption) [37]. The rubbery or glass-like state of a sorbent was shown to influence sorption, i.e. the contribution of adsorption has been suggested to increase with higher glass transition temperatures [27].

Table 4-2 - Determined properties of the used polystyrene material.

Monomeric unit	Density	Glass transition temperature	Surface tension	Mean Molecular mass
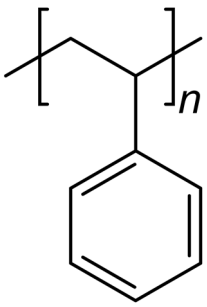	1.05 g cm^{-3}	109 °C	29 mN m^{-1}	15817 g mol^{-1}

An additional parameter influencing the sorption behaviour of a polymer is the surface tension [38]. The surface tension indicates the surface (adsorption) activity of substances [39]. Generally, due to a low surface tension, liquids will not wet polymer surfaces very well resulting in a contact angle greater than 90° and liquid molecules are then less attracted to the polymer surface [40]. The PS material from this study had a low surface tension of 29 mN m^{-1}, compared with literature surface tension data around 40 mN m^{-1} [41], hinting a low surface activity (absorption). Sometimes inorganic filler materials are used for plastic production, which can alter the surface tension. The crystallinity was also investigated using differential scanning calorimetry but did not show a point for the crystallinity. Literature shows the same

result for different PS materials [41, 42]. Crystallinity was previously shown to be an indicator for sorption potential of a sorbent [18, 26].

4.5.2 Fitting of experimental isotherms by sorption models

Sorption of the organic compounds to PS was generally strong, based on the Freundlich coefficient $K_F > 1.5$ [$(\mu g\ kg^{-1})\ (\mu g\ L^{-1})\ n^{-1}$], both for hydrophobic and hydrophilic compounds (Table A4-3). Recently, microplastic PS and aged microplastic PS were characterized with the help of several isotherms from non-ionic organic compounds with the FM [19, 27, 43]. There, sorption to PS was characterized as non-linear (n-values between 0.59 and 0.88). In this study Freundlich exponent (n) values were spread over a higher range between 0.49 and 1.18. Polymeric materials usually have n-values < 1.0 but previous studies also showed that certain materials can result in n > 1.0 for some sorbates [26, 44]. In this study, only three compounds had n-values > 1.0 with isohexan (iHex) being the only one showing a high deviation from n =1 (> 10%). Changes in sorption linearity (n) of up to 0.1 units did not show a significant impact in the phase descriptors of the ppLFER derived (ANOVA test, $p > 0.05$). The high sorption linearity deviation of iHex from n = 1 has therefore no significant impact on the model fits.

Isotherms for sorption of the probe compounds by PS are shown in Figure 4-2. The model fitting results are listed in the appendix (Table A4-3 to A4-5). All compounds showed a correlation with the fitting models with an $R^2 > 0.68$. The goodness of fit based on the mean R^2 for the investigated compounds of all isotherms generally increased in the order LM < FM < PMM. Both, the FM and PMM had similar mean R^2 values with few outliers that showed R^2 < 0.94. The PMM fit showed a major outlier for cyclohexane (cHex) with $R^2 = 0.76$. The RMSE for each model decreased from 0.638 for the LM to 0.141 for the FM and 0.123 for the PMM. The lower RMSE values for the FM and PMM indicate a better data fit, which in case of PMM results from more fitting parameters. The AIC values calculated for the FM and PMM indicate that the improvement of the fits is due to over-parameterization of the PMM, which has more degrees of freedom (2 for FM and 3 for PMM). Among AIC values for FM and PMM, the results for the FM are generally lower, which shows that the FM is likely the better fit without over-parameterization [45, 46]. The FM is actually a special case of the PMM, where b = 1 [47], which could explain why the PMM and the FM showed similarly good fitting of the data. In combination with the very good R^2 and low RMSE, the FM was used for the calculation of the distribution coefficient between PS and water ($\log K_{p/w}$) and the following ppLFER modelling.

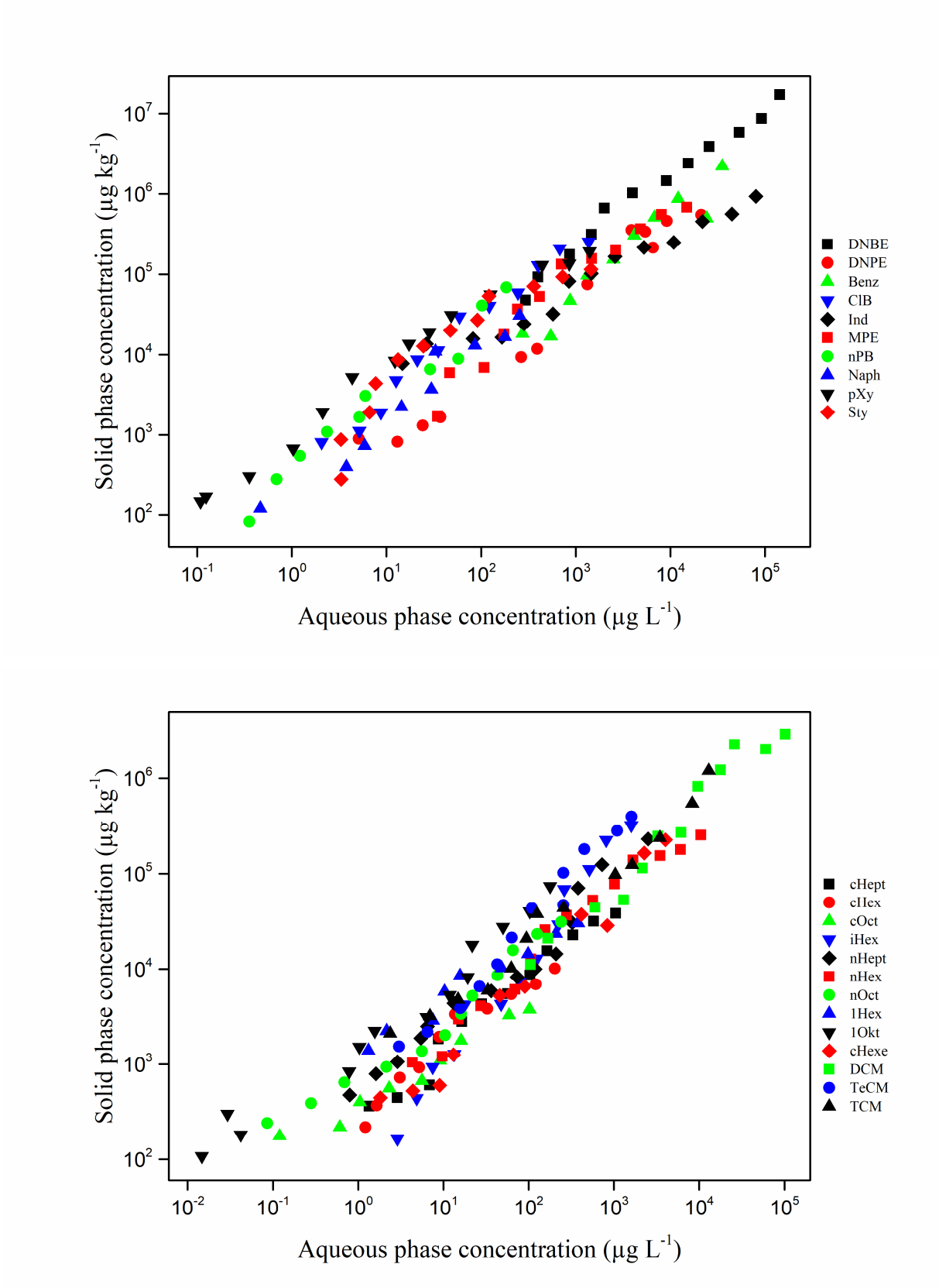

Figure 4-2 - Isotherms for the sorption of polar or aromatic (top) and aliphatic (bottom) probe compounds with PS.

4.5.3 Sorption mode and ppLFER development

Since the isotherm data for the LM resulted in the lowest goodness of fit, it indicates a heterogeneous distribution of sorption site energies of PS. It also shows that no saturation-limited monolayers are formed on the sorbent surface in the observed concentration range [27]. Non-linear sorption also suggests that adsorption onto the polymer surface could to be the dominant sorption mode. It was recently shown that polymers with low (< 25 °C) glass transition temperatures (e.g. HDPE) exhibited a combination of *ad*sorption and *ab*sorption for the sorption mode [26]. As shown by the T_g, PS is a glassy polymer. Sorption by glass-like polymers has been described by a combination of concurrent dissolution and hole filling mechanism. The first has been described as *ab*sorption and the latter as *ad*sorption like interactions of the sorbate with the sorbent surface [37]. Hole filling is considered to dominate sorption by glass-like polymers at low concentrations, meaning *ad*sorption is likely the dominant sorption mode [48].

To further differentiate Endo et. al. proposed an approach to discriminate between *ad*sorption and *ab*sorption based on different sorption energies of alkanes [49]. To determine the sorption mode for PS, the ratio of the distribution coefficients from *n*-alkanes (K_n) and cyclo-alkanes (K_c) was calculated with single point distribution coefficients of C6-, C7- and C8-alkanes using the solutes' air-water partition coefficients (K_{aw}) at an air-phase concentration of 10 μg L^{-1} [49, 50]. The K_n/K_c values were calculated using distribution coefficients obtained from the FM for C6, C7 and C8 and were 0.79, 0.64 and 0.59, respectively [49]. Values clearly below 1.0 indicate *ab*sorption [49]. Those values are lower than previously reported values (PS C6 K_n/K_c = 1.09) for PS [27]. However, the K_n/K_c ratio from the recently reported literature for PS is higher than reported values for glassy polymers (PVC C6 K_n/K_c = 0.44). The decrease of the K_n/K_c ratio with increasing carbon number (C6 > C7 > C8) also suggests that *ab*sorption is dominant. The diffusivity of the n-alkanes into the polymer decreases with increasing molar volume of the molecules since absorption requires diffusion into the bulk phase. Polymers have free volume (molar volume) within their matrix that act as sorption sites for sorbates (*ab*sorption) [51]. It was stated by Endo et al. (2008) for K_n/K_c that sorption data on glassy polymers is generally rare due to the increased experiment time. Therefore, a robust literature comparison with glassy polymers is not yet possible [49]. For PS, the dominant sorption mode from K_n/K_c can be assumed to be *ab*sorption into the bulk material. As stated above, the surface activity does also suggest *ab*sorption. Adsorption would be of importance for sorption in a short time [37].

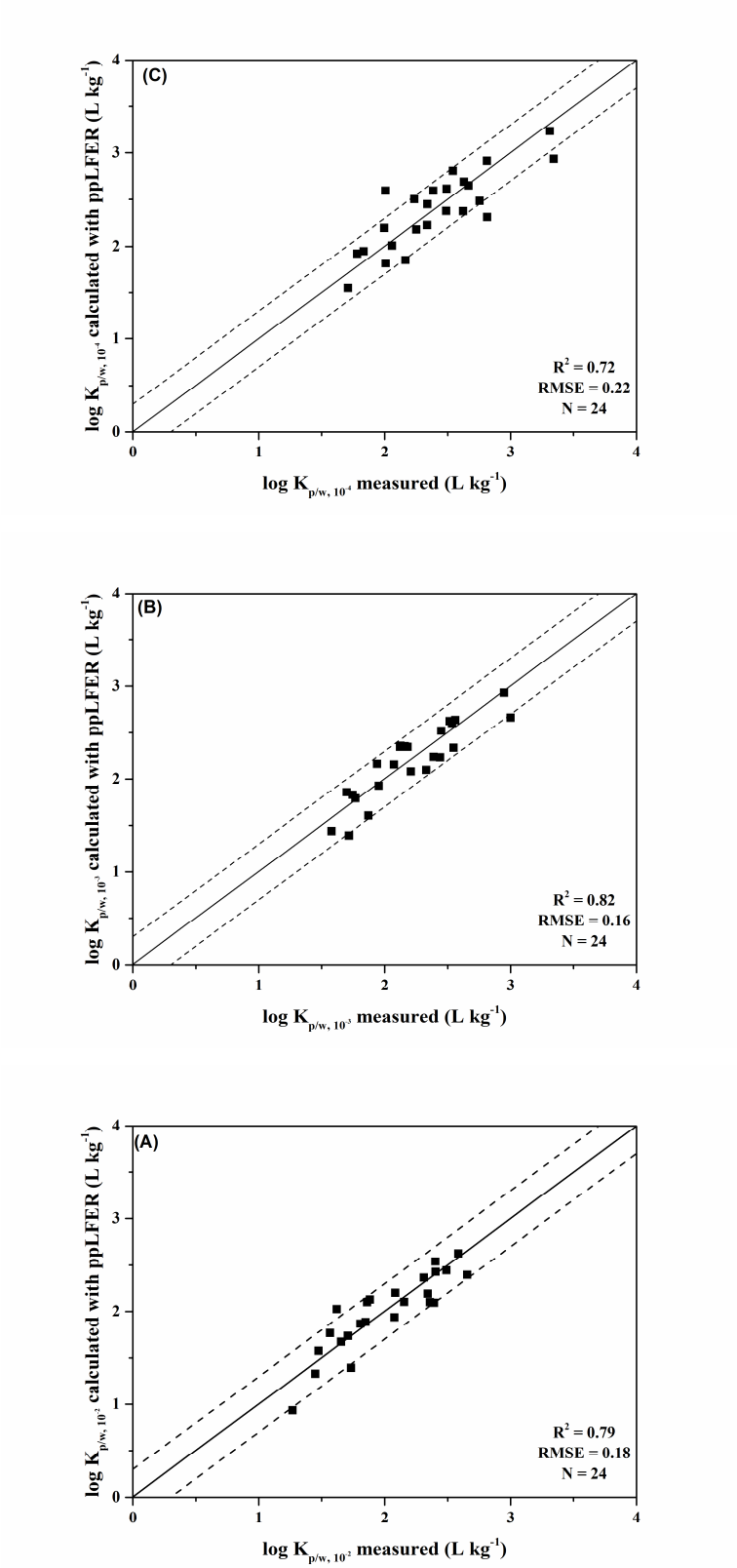

Figure 4-3 - Comparison of the calculated and measured log $K_{p/w}$ values for all compounds at concentration levels 10^{-2} (A), 10^{-3} (B) and 10^{-4} (C) of the aqueous sorbates' solubilities. The solid lines represent the 1:1 prediction and the dashed lines represent 0.3 log units deviation of the log $K_{p/w}$ values. R^2 is the regression coefficient; RMSE is the root mean squared error; N is the number of data points.

Over a longer time period, organic compounds will diffuse into the PS bulk material showing *ab*sorption [52]. For future investigations on the sorption mode of PS it would be important to consider different PS sorbents, e.g. PS pellets, expanded or not expanded PS.

Additional to the sorption mode, a comparison of different sorption relevant properties is done with the help of the ppLFER approach. The results from the MRA, being ppLFER equations, are shown in Table 4-3 for the three concentration levels. Figure 4-3 shows the comparison of the experimentally determined log $K_{p/w}$ with the calculated log $K_{p/w}$ based on the ppLFER for the three concentration levels below $C_{i,sat}$. For all concentration levels there were few data points outside a 0.3 log unit deviation from the 1:1 prediction line. This in agreement with previous studies of the ppLFER approach [26]. The standard error for the predicted values for all concentration levels is ≤ 0.3 log units and the model proved to be robust ($Q^2_{LMO\text{-}CV}$ > 0.8) [36].

Utilizing the distribution data from the PMM or LM fits rendered MRA results with R^2 < 0.77 ($p < 0.05$) while the FM showed $R^2 > 0.92$ and details are shown in the appendix (Table A4-10 to A4-20).

Therefore, the sorption data obtained from FM were further used to describe the sorption of PS with the help of the ppLFER model. With the ppLFER proving to be robust, sorption properties can be gathered from the individual phase descriptors. A comparison between the individual phase descriptors and to literature data gives additional insights into the PS sorption behaviour. High positive values indicate strong interactions in the polymer phase, whereas negative values indicate interactions mainly in the water phase [53]. Values close to zero suggest similar importance of the interactions in either the aqueous or polymer phase.

A concentration dependent ppLFER (cdppLFER) model [54] gathered from the sorption data rendered similar phase descriptors as the ppLFER phase descriptors gathered in this study. The cdppLFER can be found with additional information in the appendix (Figure A4-3) and its discussion is beyond the scope of this work.

4.5.4 Characterization of sorption by PS using ppLFER

As can be seen in Table 4-3 the phase terms for the excess molar refraction (eE), H-bond acidity (aA) and H-bond basicity (bB) indicate all strong interactions in the water phase with negative values below -1.03. Due to the lack of functional groups capable of H-bond interactions in PS, weak H-bond interactions (aA and bB) are expected for PS. It should be noted that the domain of applicability for the ppLFER from PS demonstrate robust prediction

for compounds with A values < 0.1 only [55]. The training set for the ppLFER only contained few compounds with A > 0.1.

The eE term inherits the sorbates' interactions with the sorbent that involve an induced dipole [56]. PS doesn't show dipole interactions with its aromatic monomeric unit (Table 4-2). Therefore, a significant ($p < 0.05$) negative eE term is feasible. PS aging rendered an eE term in the positive range as was demonstrated by Hüffer et al. [19]. There, the UV-induced aging influenced the surface functionality, e.g., by generating carbonyl and hydroxyl groups giving the possibility for dipole interactions. Also indicated by a higher literature *a* descriptor (-1.53) for aged PS than for the *a* descriptor from this present study (- 3.26).

Table 4-3 - Results of the multiple regression analyses utilizing the distribution data from the Freundlich fit.

Sorbent	e	s	a	b	v	c	R^2	N	RMSE
PS 10^{-2}	-1.59	2.78	-3.26	-3.0	1.82	0.36	0.79	24	0.18
SE	0.37	0.54	0.56	0.53	0.29	0.28			
PS 10^{-3}	-.134	2.29	-2.16	-3.06	2.01	0.43	0.82	24	0.16
SE	0.34	0.48	0.51	0.47	0.26	0.26			
PS 10^{-4}	-1.08	1.79	-1.03	-3.13	2.20	0.50	0.72	24	0.22
SE	0.47	0.68	0.71	0.66	0.37	0.36			
PS aged[a]	0.67	-0.75	-1.53	-3.52	2.86	0.74	0.94	21	0.17
PS aged[a,b]	0.43	-1.02	-1.43	-3.64	1.45	1.01	0.92	21	0.19
LDPE[c]	0.69	-0.15	0.00	-4.07	2.95	-0.32	0.95	98	-
SE	0.13	0.31	0.00	0.42	0.45	0.28			
HDPE[d]	-0.25	0.06	-2.10	-3.18	2.29	0.46	0.85	25	-
SE	0.71	0.78	0.90	0.77	0.44	0.48			
PA[e]	0.50	-0.16	0.16	-4.00	3.28	-0.12	0.97	79	-
SE	0.10	0.16	0.10	0.15	0.11	0.11			
POM[f]	0.39	0.28	-0.46	-3.98	2.98	-0.37	0.99	116	-
SE	0.06	0.10	0.15	0.09	0.10	0.11			

PS: polystyrene; HDPE: high-density polyethylene; SE: Standard error of the estimates; N: number of data points; RMSE: root mean square error; [a] the L descriptor was used instead of the E descriptor [b] [19] [c] distribution coefficients from literature were used to calculate the ppLFER [59]; [d,e,f] ppLFER obtained from literature [26, 44, 60].

Only the terms for the molar volume (vV) and the bipolarity/polarizability (sS) indicate strong interactions in the polymer phase (positive algebraic sign). As previously shown by other investigations on polymer materials with the ppLFER approach, the free volume within the polymer chain network exhibits possible sorption sites (non-specific interaction) [19]. Molar volume had a big impact on the sorption on LDPE over HDPE [26]. A high vV term (v > 1.8) for PS is in accordance with other studies on polymer materials indicating similar importance.

A correlation between the distribution coefficients of PS and the partitioning constant log $K_{o/w}$ for the sorbates can be an indicator for hydrophobic interactions. A significant relationship ($p < 0.05$) between the sorption coefficients for PS (Table A4-3) and log $K_{o/w}$ of the sorbates show that for PS hydrophobic interactions influence sorption [27]. Based on the monomeric unit of PS, hydrophobic interactions make sense and is also seen by other plastic materials [19, 26, 27, 43, 44].

The s values ranged from 2.78 to 1.79 from high to low concentrations indicating an impact by specific interactions. By calculating the distribution coefficient between the polymer and air (log $K_{p/a}$) to exclude interactions with water, specific interactions can be further investigated [28]. The distribution is calculated at a sorbate loading of 10, 100 and 1000 mg kg^{-1} (distribution coefficients shown in the appendix Table A4-6). Comparing log $K_{p/a}$ with the hexadecane-air partition coefficients (L) will exhibit if specific interactions are really present for sorption to PS [57]. This comparison can be seen in Figure 4-4, where the log $K_{p/a}$ values for three different concentration levels are plotted against L.

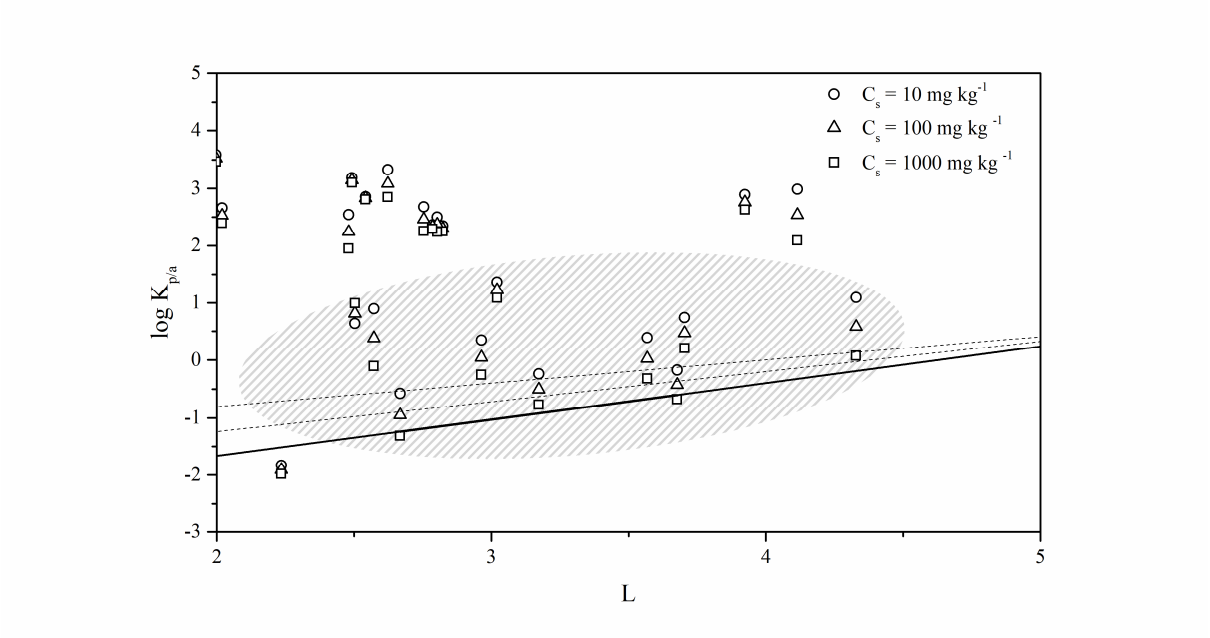

Figure 4-4 - Plots of log $K_{p/a}$ against the log hexadecane-air partitioning coefficient (L). Linear regressions for n-alkanes are shown, with the dashed lines representing the concentration levels 10 and 100 mg kg^{-1} and the solid line representing the 1000 mg kg^{-1} concentration level. The grey pattern area shows the data points of alkanes and alkenes.

Since *n*-alkanes can only undergo nonspecific interactions, their regression of log $K_{p/a}$ values with the L descriptor is meant to demonstrate non-specific interaction lines (NSILs) [49] and can be seen in the appendix (Figure A4-4) for the alkanes only.

Every compound that does show vertical deviations from the NSILs does inherit specific interactions with PS [49]. All compounds, except the cyclo-, isoalkanes, alkenes (grey pattern area) and naphthalene deviate vertically more than 1 order of magnitude from the NSILs, indicating substantial contribution of specific interactions.

To further distinguish between the specific interactions a correlation of the descriptors for specific interactions (S, A and B) with log $K_{p/a}$ was done, corrected by the subtraction of non-specific interactions (E and V) from log $K_{p/a}$ (Δlog K). The Δlog K represents the polymer/air distribution, without the non-specific interactions eE, lL and c. It showed insignificant correlations ($R^2 < 0.5$, $p > 0.05$) for the aA and bB terms. But there was a significant correlation between Δlog K and S ($R^2 > 0.74$, $p < 0.05$). As stated above, the ppLFER in Table 4-3 suggested contributions from the sS term of PS. A correlation may be a good indicator for specific interactions other than H-bonding. The interactions from the sorbates with the aromatic ring system through π-π- and π-η-interactions impact sorption to PS as shown by the phase descriptor sS. A similar finding has already been suggested for π-π-interactions by a recent study [58] and is underlined by the finding from the ppLFER model. Comparing the PS ppLFER to literature ppLFER equations of polymer materials will further underline this conclusion.

4.5.5 Comparing sorption properties of different polymers from literature

Several plastic materials like polyacrylate (PA), polyoxymethylene (POM) and HDPE have been characterized using the ppLFER approach [19, 26, 27, 43, 44]. The sorption properties of PS from this study were compared with literature sorption data of plastic materials. The methodology for HDPE was the same as for this study. Sorption coefficients by PS were generally higher than sorption coefficients for HDPE. Only *n*- and *cyclo*-alkanes had similar sorption coefficients. Higher sorption coefficients for PS indicate the contribution of specific interactions, since HDPE did only undergo non-specific interactions.

When comparing the sS terms of several polymers like HDPE, POM, PA and PDMS with PS it is obvious that the π-interactions of PS have an additional impact on the sorption, besides hydrophobic interactions. Other, similar polymers show much lower s values and even significant negative values (PA -0.16, POM 0.28 or HDPE 0.06). It does underline that the π-interactions with the aromatic ring also lead to interactions with hydrophilic sorbates. The ratio of log K_{nOct} and log K_{1Oct} (K_{nOct}/K_{1Oct}) does demonstrate the higher impact of specific interactions for PS than HDPE. For PS, K_{nOct}/K_{1Oct} is < 1.0 and for HDPE it is > 1.0 [26]. If PS

can undergo specific interactions besides the non-specific interactions, it will result in a higher K_{1Oct} compared to K_{nOct}.

For PS, the higher sorption for alkenes and the negative s descriptor underline the importance of aromatic π-electron donor-acceptor interactions for sorption behaviour in the aquatic environment. Alkenes will undergo specific interactions, due to their double bonds. The impact of specific interactions is also demonstrated by a weaker sorption of hydrophilic compounds to HDPE than PS from previous reports [26]. The comparison of the ppLFER models from both plastic materials suggest a stronger sorption to PS in the aquatic environment. The slopes in Figure 4-5 increase with concentration from 3.98 to 4.45 ($R^2 > 0.74$, $p < 0.05$) for PS and HDPE from 4.24 to 4.67 ($R^2 > 0.64$, $p < 0.05$). An increase indicates, that the contribution from specific interactions, coming only from the dipolarity/polarizability of PS, has a high impact on sorption to PS [49], especially with higher concentrations.

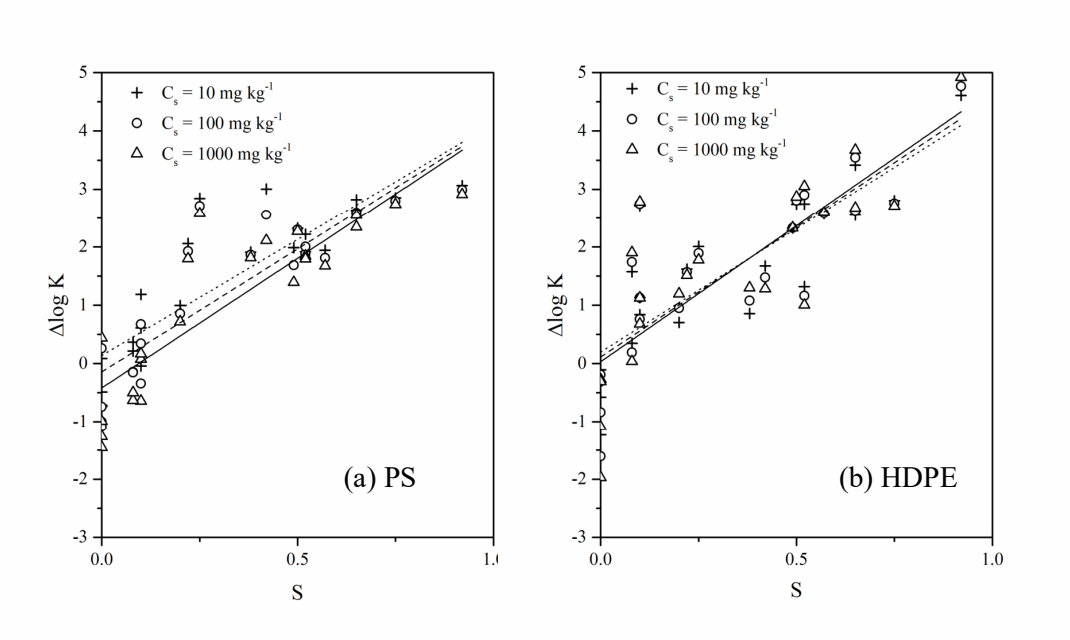

Figure 4-5 - Contributions of specific interactions (Δlog K) vs the dipolarity/polarizability (S) for PS (left) and HDPE (right). Slopes for concentration levels 10 and 100 mg kg^{-1} are dashed and the solid line represents the 1000 mg kg^{-1} concentration level.

4.6 References

[1] H.-G. Elias, *An introduction to Plastics*, 2nd ed. Wiley-VCH, 2003.

[2] A. L. Andrady and M. a Neal, "Applications and societal benefits of plastics.," *Philos. Trans. R. Soc. Lond. B. Biol. Sci.*, vol. 364, no. 1526, pp. 1977–84, Jul. 2009.

[3] PlasticsEurope, "Plastic - the Facts 2016," p. 38, 2016.

[4] M. Eriksen *et al.*, "Plastic Pollution in the World's Oceans: More than 5 Trillion Plastic Pieces Weighing over 250,000 Tons Afloat at Sea," *PLoS One*, vol. 9, no. 12, 2014.

[5] S. L. Moore, D. Gregoria, M. Carreon, S. B. Weisberg, and M. K. Leecaster, "Composition and distribution of beach debirs in orange county, California," *Mar. Pollut. Bull.*, vol. 42, no. 3, pp. 241–245, 2001.

[6] T. Mani, P. Blarer, F. R. Storck, M. Pittroff, T. Wernicke, and P. Burkhardt-Holm, "Repeated detection of polystyrene microbeads in the Lower Rhine River," *Environ. Pollut.*, vol. 245, pp. 634–641, Feb. 2019.

[7] R. E. Engler, "The complex interaction between marine debris and toxic chemicals in the ocean," *Environ. Sci. Technol.*, vol. 46, no. 22, pp. 12302–12315, 2012.

[8] V. Hidalgo-ruz, L. Gutow, R. C. Thompson, and M. Thiel, "Microplastics in the Marine Environment: A Review of the Methods Used for Identification and Quantification," *Environ. Sci. Technol.*, vol. 46, p. 3060−3075, 2012.

[9] M. C. Fossi *et al.*, "Large filter feeding marine organisms as indicators of microplastic in the pelagic environment: The case studies of the Mediterranean basking shark (Cetorhinus maximus) and fin whale (Balaenoptera physalus)," *Mar. Environ. Res.*, vol. 100, 2014.

[10] S. L. Wright, R. C. Thompson, and T. S. Galloway, "The physical impacts of microplastics on marine organisms: A review," *Environ. Pollut.*, vol. 178, pp. 483–492, 2013.

[11] M. Cole *et al.*, "Microplastic Ingestion by Zooplankton," *Environ. Sci. Technol.*, vol. 47, no. 12, pp. 6646–6655, Jun. 2013.

[12] C. M. Rochman, C. Manzano, B. T. Hentschel, S. L. M. Simonich, and E. Hoh, "Polystyrene Plastic: A Source and Sink for Polycyclic Aromatic Hydrocarbons in the Marine Environment," *Environ. Sci. Technol.*, vol. 47, no. 24, pp. 13976–13984, Dec. 2013.

[13] A. A. Koelmans, A. Bakir, G. A. Burton, and C. R. Janssen, "Microplastic as a Vector for Chemicals in the Aquatic Environment . Critical Review and Model-Supported Re-interpretation of Empirical Studies . Microplastic as a Vector for Chemicals in the Aquatic Environment . Critical Review and Model-Supported Re- in," 2016.

[14] S. Zhang *et al.*, "Microplastics in the environment: A review of analytical methods, distribution, and biological effects," *TrAC Trends Anal. Chem.*, vol. 111, pp. 62–72, Feb. 2019.

[15] J. P. Rodrigues, A. C. Duarte, J. Santos-Echeandía, and T. Rocha-Santos, "Significance of interactions between microplastics and POPs in the marine environment: A critical overview," *TrAC Trends Anal. Chem.*, vol. 111, pp. 252–260, Feb. 2019.

[16] F. Ribeiro, J. W. O'Brien, T. Galloway, and K. V. Thomas, "Accumulation and fate of nano- and micro-plastics and associated contaminants in organisms," *TrAC Trends Anal. Chem.*, vol. 111, pp. 139–147, Feb. 2019.

[17] R. Triebskorn *et al.*, "Relevance of nano- and microplastics for freshwater ecosystems: A critical review," *TrAC Trends Anal. Chem.*, vol. 110, pp. 375–392, Jan. 2019.

[18] X. Guo, X. Wang, X. Zhou, X. Kong, S. Tao, and B. Xing, "Sorption of four hydrophobic organic compounds by three chemically distinct polymers: role of chemical and physical composition.," *Environ. Sci. Technol.*, vol. 46, no. 13, pp. 7252–9, Jul. 2012.

[19] T. Hüffer, A. K. Weniger, and T. Hofmann, "Sorption of organic compounds by aged polystyrene microplastic particles," *Environ. Pollut.*, vol. 236, pp. 474-4218–225, 2018.

[20] S. Seidensticker, P. Grathwohl, J. Lamprecht, and C. Zarfl, "A combined experimental and modeling study to evaluate pH-dependent sorption of polar and non-polar compounds to polyethylene and polystyrene microplastics," *Environ. Sci. Eur.*, vol. 30, no. 1, pp. 1–12, 2018.

[21] J. J. Palmgrén, J. Mönkkönen, T. Korjamo, A. Hassinen, and S. Auriola, "Drug adsorption to plastic containers and retention of drugs in cultured cells under in vitro conditions," *Eur. J. Pharm. Biopharm.*, vol. 64, no. 3, pp. 369–378, 2006.

[22] K. Yang, L. Zhu, and B. Xing, "Adsorption of Polycyclic Aromatic Hydrocarbons by Carbon Nanomaterials," *Environ. Sci. Technol.*, vol. 40, no. 6, pp. 1855–1861, 2006.

[23] K.-U. Goss, "The Air/Surface Adsorption Equilibrium of Organic Compounds Under Ambient Conditions," *Crit. Rev. Environ. Sci. Technol.*, vol. 34, no. 4, pp. 339–389, Jul. 2004.

[24] R. P. Schwarzenbach, P. M. Gschwend, and D. M. Imboden, *Environmental Organic Chemistry*, 2nd ed., no. 2. John Wiley & Sons Inc., Hoboken, New Jersey, 2003.

[25] T. H. Nguyen, K.-U. Goss, and W. P. Ball, "Polyparameter linear free energy relationships for estimating the equilibrium partition of organic compounds between water and the natural organic matter in soils and sediments.," *Environ. Sci. Technol.*, vol. 39, no. 4, pp. 913–924, 2005.

[26] T. H. Uber, T. Hüffer, S. Planitz, and T. C. Schmidt, "Characterization of sorption properties of high- density Polyethylene sheets using the poly-parameter linear-free energy relationships," *Environ. Pollut.*, vol. 248, no. C, pp. 312–319, 2019.

[27] T. Hüffer and T. Hofmann, "Sorption of non-polar organic compounds by micro-sized plastic particles in aqueous solution.," *Environ. Pollut.*, vol. 214, no. 1, pp. 194–201, Apr. 2016.

[28] T. Hüffer, S. Endo, F. Metzelder, S. Schroth, and T. C. Schmidt, "Prediction of sorption of aromatic and aliphatic organic compounds by carbon nanotubes using poly-parameter linear free-energy relationships.," *Water Res.*, vol. 59, no. 1, pp. 295–303, 2014.

[29] D. E. Norm, "Determination of the viscosity of polymers in dilute solution using capillary viscometer - Part 1: General principles (ISO 1628-1:2009 + Amd 1:2012)," 2012.

[30] Norm. D, "Determination of the viscosity of polymers in dilute solution using capillary viscometers - Part 3: Polyethylenes and polypropylenes (ISO 1628-3:2010)," 2010.

[31] D. K. Owens and R. C. Wendt, "Estimation of the surface free energy of polymers," *J. Appl. Polym. Sci.*, vol. 13, no. 8, pp. 1741–1747, Aug. 1969.

[32] D. H. Kaelble and E. H. Cirlin, "Dispersion and polar contributions to surface tension of poly(methylene oxide) and Na-treated polytetrafluoroethylene," *J. Polym. Sci. Part A-2 Polym. Phys.*, vol. 9, no. 2, pp. 363–368, Feb. 1971.

[33] X. Chen, "Modeling of experimental adsorption isotherm data," *Inf. - Open Access Inf. Sci. J.*, vol. 6, no. 1, pp. 14–22, 2015.

[34] G. Xia and W. P. Ball, "Polanyi-based models for the competitive sorption of low-polarity organic contaminants on a natural sorbent," *Environ. Sci. Technol.*, vol. 34, no. 7, pp. 1246–1253, 2000.

[35] L. Li, P. A. Quinlivan, and D. R. U. Knappe, "Predicting Adsorption Isotherms for Aqueous Organic Micropollutants from Activated Carbon and Pollutant Properties," *Environ. Sci. Technol.*, vol. 39, no. 9, pp. 3393–3400, May 2005.

[36] P. Gramatica, "Principles of QSAR models validation: internal and external," *QSAR Comb. Sci.*, vol. 26, no. 5, pp. 694–701, 2007.

[37] B. Xing and J. J. Pignatello, "Dual-Mode Sorption of Low-Polarity Compounds in Glassy Poly(Vinyl Chloride) and Soil Organic Matter," *Environ. Sci. Technol.*, vol. 31, no. 3, pp. 792–799, Mar. 1997.

[38] K. Holmberg, B. Jönssin, B. Kronberg, and B. Lindman, "Surface Tension and Adsorption at the Air–Water Interface," in *Surfactants and Polymers in Aqueous Solution*, Wiley-Blackwell, 2003, pp. 337–355.

[39] T. Kairaliyeva, E. V. Aksenenko, N. Mucic, A. V. Makievski, V. B. Fainerman, and R. Miller, "Surface Tension and Adsorption Studies by Drop Profile Analysis Tensiometry," *J. Surfactants Deterg.*, vol. 20, no. 6, pp. 1225–1241, 2017.

[40] K. S. Birdi, *Handbook of Surface and Colloid Chemistry*, 3rd ed. CRC Press, 2009.

[41] A. Franck, B. Herr, H. Ruse, and G. Schulz, *Kunststoff Kompendium*, 7th ed. Vogel Business Media, 2011.

[42] E. Baur, S. Brinkmann, T. A. Osswald, and E. Schmachtenberg, *Saechtling Kunststoff Taschenbuch*, 29th ed. Carl Hanser Verlag GmbH & Co. KG, 2004.

[43] T. Hüffer, A. K. Weniger, and T. Hofmann, "Data on sorption of organic compounds by aged polystyrene microplastic particles," *Data Br.*, vol. 18, pp. 474–479, 2018.

[44] S. Endo, S. E. Hale, K.-U. Goss, and H. P. H. Arp, "Equilibrium partition coefficients of diverse polar and nonpolar organic compounds to polyoxymethylene (POM) passive sampling devices.," *Environ. Sci. Technol.*, vol. 45, no. 23, pp. 10124–32, Dec. 2011.

[45] M. Harvey and A. Christopoulos, *Fitting Models to Biological Data using Linear and Nonlinear Regression*. Oxford University Press, 2003.

[46] T. Hüffer, M. Kah, T. Hofmann, and T. C. Schmidt, "How Redox Conditions and Irradiation A ff ect Sorption of PAHs by Dispersed Fullerenes (nC60)," *Environ. Sci. Technol.*, vol. 47, no. 13, pp. 6935–6942, 2013.

[47] J. B. Condon, "Equivalency of the Dubinin–Polanyi equations and the QM based sorption isotherm equation. B. Simulations of heterogeneous surfaces," *Microporous Mesoporous Mater.*, vol. 38, no. 2–3, pp. 377–383, 2000.

[48] J. J. Pignatello, Y. Lu, E. J. LeBoeuf, W. Huang, J. Song, and B. Xing, "Nonlinear and competitive sorption of apolar compounds in black carbon-free natural organic materials.," *J. Environ. Qual.*, vol. 35, no. 4, pp. 1049–1059, 2006.

[49] S. Endo, P. Grathwohl, and T. C. Schmidt, "Absorption or Adsorption ? Insights from Molecular Probes n -Alkanes and Cycloalkanes into Modes of Sorption by Environmental Solid Matrices," *Environ. Sci. Technol.*, vol. 42, no. 11, pp. 3989–3995, 2008.

[50] S. Endo, P. Grathwohl, S. B. Haderlein, and T. C. Schmidt, "Characterization of sorbent properties of soil organic matter and carbonaceous geosorbents using n-alkanes and cycloalkanes as molecular probes.," *Environ. Sci. Technol.*, vol. 43, no. 2, pp. 393–400, 2009.

[51] M. S. Iotov, "Chapter 5 Methods for studying diffusion in Polymers," in *Diffusion in amorphous media*, California Institute of Technology, 1998.

[52] A. Turner and L. Holmes, "Occurrence, distribution and characteristics of beached plastic production pellets on the island of Malta (central Mediterranean)," *Mar. Pollut. Bull.*, vol. 62, no. 2, pp. 377–381, 2011.

[53] M. H. Abraham, "Scales of Solute Hydrogen-bonding: Their Construction and Application t o PhysicochemicaI and BiochemicaI Processes," vol. 096, no. 5, 1992.

[54] Y. H. Shih and P. M. Gschwend, "Evaluating activated carbon-water sorption coefficients of organic compounds using a linear solvation energy relationship approach and sorbate chemical activities," *Environ. Sci. Technol.*, vol. 43, no. 3, pp. 851–857, 2009.

[55] K. Roy, S. Kar, and A. Pravin, "On a simple approach for determining applicability domain of QSAR models.," *Chemom. Intell. Lab. Syst.*, vol. 145, pp. 22–29, 2015.

[56] J. S. Arey, W. H. Green, and P. M. Gschwend, "The electrostatic origin of Abraham's solute polarity parameter," *J. Phys. Chem. B*, vol. 109, no. 15, pp. 7564–7573, 2005.

[57] S. Endo, P. Grathwohl, S. B. Haderlein, and T. C. Schmidt, "Compound-Specific Factors Influencing Sorption Nonlinearity in Natural Organic Matter," *Environ. Sci. Technol.*, vol. 42, no. 16, pp. 5897–5903, Aug. 2008.

[58] J. Wang *et al.*, "Size effect of polystyrene microplastics on sorption of phenanthrene and nitrobenzene," *Ecotoxicol. Environ. Saf.*, vol. 173, no. February, pp. 331–338, 2019.

[59] Y. Choi, Y. M. Cho, and R. G. Luthy, "Polyethylene-water partitioning coefficients for parent- and alkylated-polycyclic aromatic hydrocarbons and polychlorinated biphenyls," *Environ. Sci. Technol.*, vol. 47, pp. 6943–6950, 2013.

[60] S. Endo, S. T. J. Droge, and K.-U. Goss, "Polyparameter Linear Free Energy Models for Polyacrylate," *Anal. Chem.*, vol. 83, pp. 1394–1400, 2011.

4.7 Appendix

A4-S1 Experimental procedure for batch experiments

The samples for the batch experiments were spiked with a stock solution in a 20 mL glass Headspace Vials (BGB Germany) with a Screw cap and butyl/PTFE septa. The samples were then shaken in an overhead shaker (Reax 2) from Heidolph for at least 4 days (Figure A4-1). After shaking, the glass vials with the plastic squares were then placed in the tray of the Autosampler at least two hours prior to analysis to allow for water gas equilibrium [4, 5]. For analysing the samples, the procedure was as described in Chapter 3.4.2

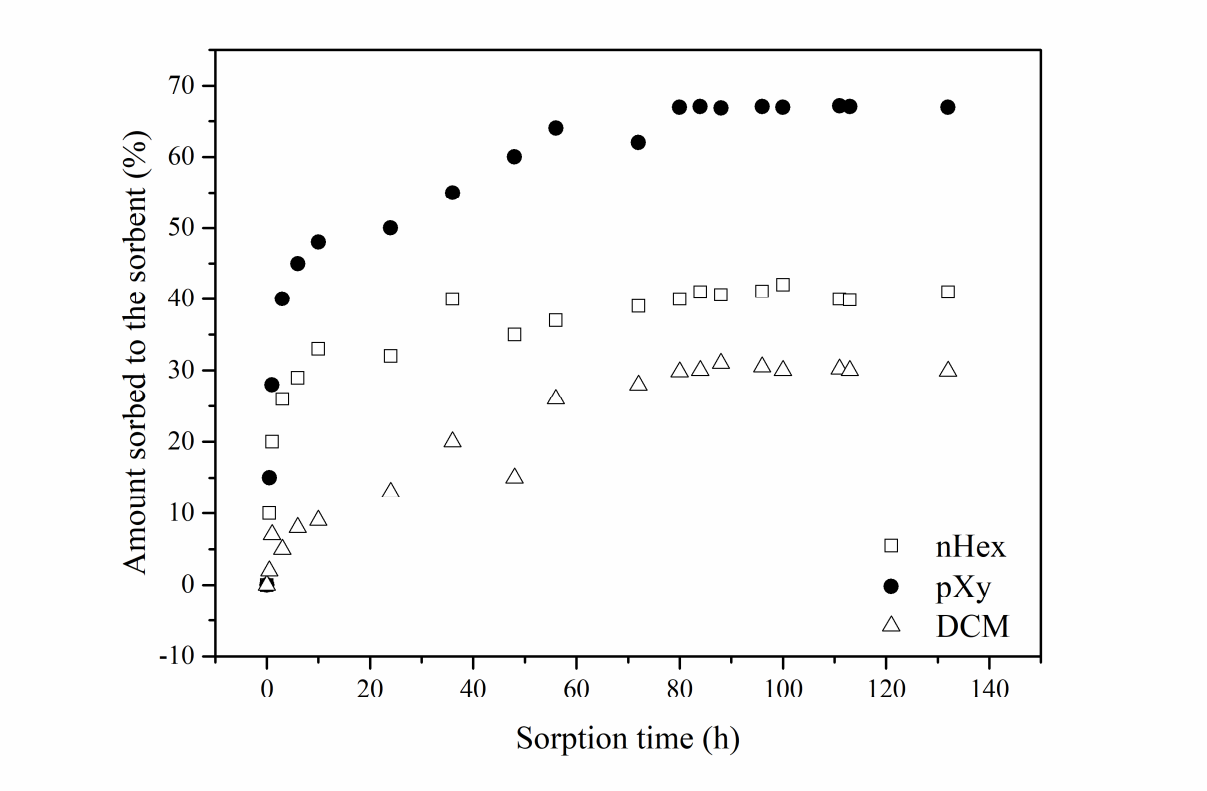

Figure A4-1 - Experimental determined equilibration times in hours for p-xylene, n-hexane and dichloromethane.

A4-S2 Experimental determination of PS properties

The glass transition temperature and the crystallinity were determined using the Differential Scanning Coulometry (DSC). An Ubbelohde type viscometer was used to determine the medium molar mass of PS. The experiments were done per DIN EN ISO 1628-1 (Norm, 2012) and DIN EN ISO 1628-3 (Norm. D, 2010). A gas pycnometer was used for the determination of the density and experiments were done according to DIN EN ISO 1183-1. The surface tension was determined through the contact angle of substances on the PS surface. The

contact angle of PS was determined with 4 substances being methanol, form amide, toluene and ethylene glycol. In brief, 10 µl of a substance were placed on the PS surface and a picture was taken of the drop on the surface. With a software (Surftense 4.5) the dimensions of the droplet were determined, and the contact angle was calculated. Then applying the Owens-Wendt-Rabel-Kaelbe-method, the surface tension was calculated from the contact angles of each substance [1, 2, 3]. Other information of the used PS was extracted from the product sheet from the supplier, which is also shown in detail in Table A4-2.

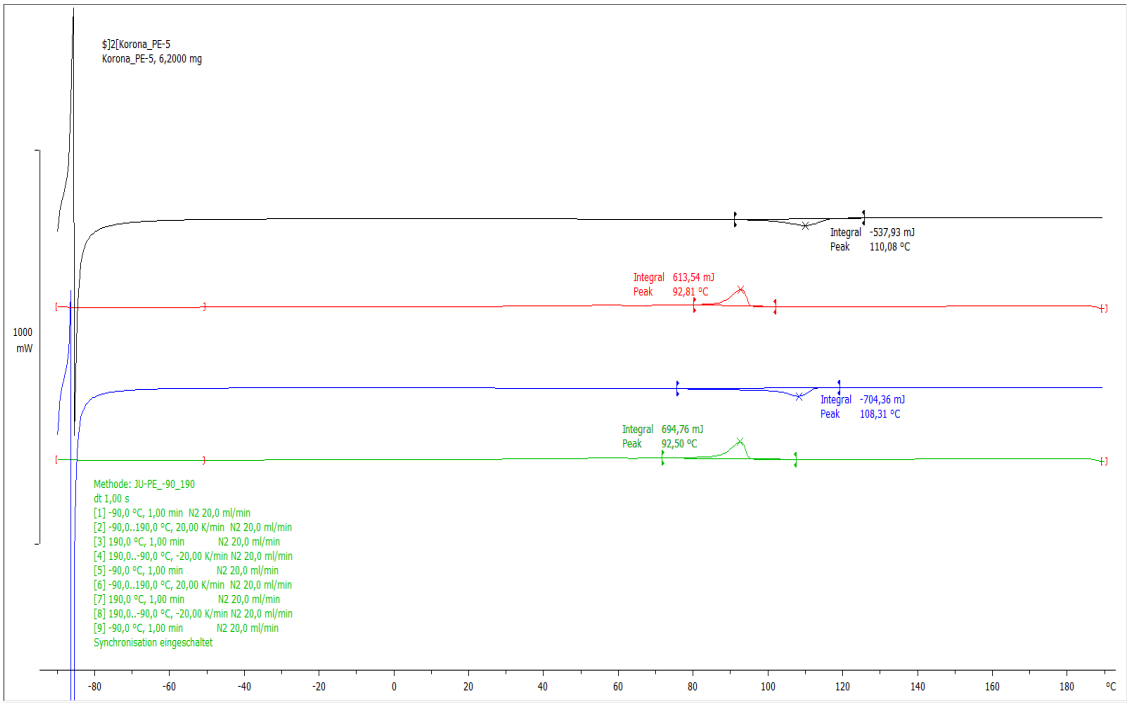

Figure A4-2 - Results of the differential scanning calorimetry measurements of the polystyrene film.

A4-S3 Polanyi-manes model

In brief, the PMM model assumes that there is a fixed space around the adsorbent surface where adsorption occurs. Every sorbate in the area around the adsorbent has a fixed adsorption potential, denoted as ε. The potential is dependent on the distance between the sorbate and the sorption surface and the property of the sorbent. Every point of the sorbent that has the same distance to the sorption surface will have the same potential ε, leading to an equipotential sorbent surface. Those sorbate areas will enclose a volume V(ε) between itself and the surface of the adsorbent [6]. These micro volumes can affect sorption to the surface.

Table A4-1 - Selected sorbate properties of the compound set used in this study.

	Abb.	log $C_{i,sat}$	log $K_{a/w}$	log $K_{o/w}$	E	S	A	B	V	L
alkanes										
Cycloheptan	cHept	1.70	0.63	4.00	0.35	0.10	0.00	0.00	0.99	3.70
Cyclohexane	cHex	1.74	0.89	3.44	0.31	0.10	0.00	0.00	0.85	2.96
Cyclooctane	cOct	0.89	-0.68	4.45	0.41	0.10	0.00	0.00	1.13	4.33
Isohexane	iHex	2.15	1.86	3.21	0.00	0.00	0.00	0.00	0.95	2.50
n-Heptan	nHept	0.53	1.84	4.66	0.00	0.00	0.00	0.00	1.10	3.17
n-Hexane	nHex	0.98	1.74	3.9	0.00	0.00	0.00	0.00	0.95	2.67
n-Octane	nOct	-0.18	1.95	5.18	0.00	0.00	0.00	0.00	1.24	3.68
alkenes										
1-Hexen	1Hex	1.70	0.22	3.39	0.08	0.08	0.00	0.07	0.91	2.57
1-Octen	1Oct	0.61	1.41	4.57	0.09	0.08	0.00	0.07	1.19	3.57
Cyclohexen	cHexe	2.33	0.27	2.86	0.40	0.20	0.00	0.10	0.80	3.02
halo-aliphatics										
Dichloromethane	DCM	4.30	-0.93	1.25	0.39	0.57	0.10	0.05	0.49	2.02
Tetrachloromethane	TeCM	2.90	0.04	2.83	0.46	0.38	0.00	0.00	0.74	2.82
Trichloromethane	TCM	3.90	-0.84	1.97	0.43	0.49	0.15	0.02	0.62	2.48
monopolar aliphatics										
Di-n-butyl ether	DNBE	2.48	-0.69	3.21	0.00	0.25	0.00	0.45	1.30	3.92
Di-n-propyl ether	DNPE	3.69	-0.97	2.03	0.01	0.22	0.00	0.44	1.01	2.80
nonpolar aromatics										
Benzene	Benz	3.25	-0.65	2.17	0.61	0.52	0.00	0.14	0.72	2.79
benzo[b]furan	BbF	2.83	-2.34	2.67	0.89	0.83	0.00	0.15	0.91	
Chlorobenzene	ClB	2.70	-0.80	2.84	0.72	0.65	0.00	0.07	0.84	3.66
n-Propylbenzene	nPB	1.78	-0.40	3.69	0.60	0.50	0.00	0.15	1.14	4.23
Naphthalene	Naph	1.49	-1.74	3.33	1.34	0.92	0.00	0.20	1.09	5.16
p-Xylene	pXy	2.21	-0.51	3.15	0.61	0.52	0.00	0.16	1.00	3.84
polar aromatics										
Methyl phenyl ether	MPE	3.02	-1.70	2.11	0.71	0.75	0.00	0.29	0.92	3.89
Styrene	Sty	2.49	-1.31	3.05	0.85	0.65	0.00	0.16	0.96	3.86
Indole	Ind	3.28	-4.40	2.14	1.20	1.12	0.44	0.22	0.95	

Abb.: Abbreviation of every compound; log $C_{i,sat}$: saturated aqueous concentration [µg L^{-1}]; log $K_{a/w}$: logarithmic air/water partitioning constant; log $K_{o/w}$: logarithmic n-octanol/water partitioning constant;

Table A4-2 - Polystyrene properties extracted from the material data sheet, provided by GoodFellow.

Chemical Resistance	
Acids – concentrated	Fair-Poor
Acids – dilute	Good-fair
Alcohols	Good-Fair
Alkalis	Good-Fair
Aromatic hydrocarbons	Poor
Greases and Oils	Good-Poor
Halogenated Hydrocarbons	Poor
Halogens	Poor
Ketones	Poor
Mechanical properties	
Elongation at break (%)	1.6
Hardness – Rockwell	M60-90
Izod impact strength (J m^{-1})	19-24
Poisson's ratio	0.35
Tensile modulus (GPa)	2.3 – 4.1
Tensile strength (MPa)	30 – 100
Physical properties	
Abbe number	30.8
Density (g cm^{-3})	1.05
Flammability	HB
Limiting oxygen index (%)	19
Radiation resistance	Good
Refractive Index	1.59 – 1.60
Resistance to Ultra-violet	Poor
Water absorption – over 24 hours (%)	< 0.4 %
Thermal properties	
Coefficient of thermal expansion (x10^{-6} K^{-1})	30 – 210
Heat-deflection temperature – 0.45MPa (C)	90
Heat-deflection temperature – 1.8MPa (C)	80
Specific heat (J K^{-1} kg^{-1})	1200
Thermal conductivity @23C (W m^{-1} K^{-1})	0.1 – 0.13
Upper working temperature (C)	50 - 95

Table A4-3 - Fitting data for the Freundlich Model.

Sorbate	log K_f	n	R^2	RMSE	AIC	N	log $K_{p/w}$ 10^{-2} $C_{i,sat}$	log $K_{p/w}$ 10^{-3} $C_{i,sat}$	log $K_{p/w}$ 10^{-4} $C_{i,sat}$
cHept	2.466	0.733	0.982	0.092	20.86	12	1.807	2.073	2.339
cHex	2.473	0.707	0.943	0.135	18.28	10	1.670	1.963	2.256
cOct	2.578	0.495	0.964	0.091	15.60	9	1.620	2.125	2.630
iHex	1.805	1.176	0.974	0.170	23.04	13	1.533	1.831	2.130
nHept	2.694	0.750	0.957	0.171	24.12	14	2.296	2.526	2.756
nHex	2.568	0.738	0.965	0.151	25.55	14	1.860	2.122	2.384
nOct	2.883	0.637	0.954	0.150	20.22	12	2.586	2.949	3.311
1Hex	3.151	0.517	0.956	0.095	18.13	9	1.848	2.331	2.814
1Oct	3.210	0.657	0.964	0.172	21.50	13	2.656	2.999	3.342
cHexe	2.192	0.862	0.973	0.168	19.16	10	1.451	1.698	1.946
DCM	2.272	0.867	0.960	0.168	25.56	12	1.566	1.699	1.832
TeCM	1.838	1.022	0.920	0.230	21.37	11	2.392	2.440	2.488
TCM	2.906	0.708	0.971	0.147	24.86	13	1.474	1.767	2.059
DNBE	2.729	0.870	0.989	0.116	26.89	12	2.077	2.207	2.338
DNPE	2.058	0.870	0.959	0.198	23.12	12	1.449	1.579	1.709
Benz	1.545	1.069	0.974	0.118	22.39	9	1.708	1.745	1.781
BbF	2.910	0.870	0.982	0.103	20.76	10	2.402	2.534	2.666
ClB	2.568	0.956	0.976	0.135	22.62	12	2.404	2.448	2.493
nPB	2.562	0.974	0.972	0.155	18.02	10	2.490	2.516	2.542
Naph	2.272	0.924	0.951	0.182	17.22	9	2.142	2.108	2.073
pXy	3.000	0.794	0.981	0.152	23.96	14	2.342	2.548	2.754
MPE	2.110	0.940	0.946	0.196	24.03	12	1.882	1.939	1.997
Sty	2.927	0.766	0.987	0.106	22.48	14	2.155	2.389	2.623
Ind	3.186	0.552	0.950	0.148	27.30	14	1.269	1.717	2.165

log K_f: logarithmic Freundlich coefficient [(μg kg^{-1}) (μg L^{-1}) n^{-1}]; n: Freundlich exponent [-]; N: number of data points; log $K_{p/w}$ logarithmic polymer-water distribution; coefficient [L Kg^{-1}]; $C_{i,sat}$: saturated aqueous concentration [μg L^{-1}].

Table A4-4 - Fitting results from the data to the Polanyi-Manes model.

Sorbate	$logQ_0$	a	b	R^2	RMSE	AIC	N	log $K_{p/w}$ 10^{-2} $C_{i,sat}$	log $K_{p/w}$ 10^{-3} $C_{i,sat}$	log $K_{p/w}$ 10^{-4} $C_{i,sat}$
cHept	5.340	-25.751	1.423	0.975	0.107	24.50	12	1.969	2.272	2.467
cHex	15.666	-19.149	0.255	0.757	0.394	21.76	11	2.119	1.944	2.033
cOct	5.480	-8.723	0.609	0.975	0.071	20.39	9	1.641	2.097	2.621
iHex	8.126	-25.510	0.931	0.978	0.152	26.54	13	2.380	2.187	2.022
nHept	5.699	-12.869	0.747	0.970	0.138	27.44	14	2.253	2.577	2.956
nHex	5.389	-30.980	1.309	0.983	0.096	27.48	14	1.415	1.523	1.531
nOct	5.743	-9.355	0.507	0.982	0.090	23.87	12	2.492	2.937	3.467
1Hex	5.084	-19.329	1.478	0.968	0.078	22.94	9	1.823	2.362	2.820
1Oct	8.413	-12.329	0.416	0.981	0.120	24.96	13	2.654	2.893	3.269
cHexe	8.613	-12.878	0.594	0.979	0.141	23.45	10	1.767	1.808	1.973
DCM	8.338	-9.796	1.090	0.966	0.147	29.23	12	1.538	1.704	1.845
TeCM	8.900	-15.145	0.836	0.979	0.114	26.81	12	2.462	2.438	2.470
TCM	12.571	-12.735	0.406	0.984	0.108	28.35	13	1.900	1.866	2.023
DNBE	7.232	-51.547	1.332	0.987	0.087	30.55	12	0.812	0.795	0.657
DNPE	9.380	-18.339	0.726	0.972	0.186	26.81	12	1.655	1.617	1.672
Benz	6.789	-34.480	1.811	0.939	0.167	26.58	10	1.708	1.805	1.618
BbF	6.664	-29.164	1.686	0.992	0.064	25.04	10	2.177	2.534	2.723
ClB	6.610	-26.760	1.600	0.983	0.110	26.27	12	2.101	2.359	2.451
nPB	6.478	-29.602	1.239	0.969	0.154	22.26	10	2.366	2.496	2.552
Naph	6.519	-17.780	0.969	0.958	0.159	22.03	9	2.090	2.158	2.235
pXy	5.948	-31.026	1.662	0.993	0.090	27.25	14	2.145	2.573	2.858
MPE	6.125	-104.645	2.507	0.979	0.118	27.73	12	1.740	2.090	2.015
Sty	5.050	-1904.334	4.812	0.970	0.140	25.81	12	1.529	2.355	2.748
Ind	7.136	-8.787	0.798	0.970	0.113	30.65	14	1.305	1.711	2.157

Log Q_0: adsorbed capacity; a and b: fitting parameters of the Polanyi-Manes model fit; N: number of data points; log $K_{p/w}$ logarithmic polymer-water distribution; coefficient [L Kg^{-1}]; $C_{i,sat}$: saturated aqueous concentration [µg L^{-1}].

Table A4-5 - Fitting data for the Langmuir Model.

Sorbate	K_L	Q_0	R^2	RMSE	AIC	N	log $K_{p/w}$ 10^{-2} $C_{i,sat}$	log $K_{p/w}$ 10^{-3} $C_{i,sat}$	log $K_{p/w}$ 10^{-4} $C_{i,sat}$
cHept	246.524	5452.855	0.852	0.438	19.938	12	1.229	2.020	2.337
cHex	198.056	68221.459	0.979	1.190	18.553	11	1.882	2.232	2.290
cOct	1673.128	817.997	0.702	0.348	15.168	9	1.012	1.989	2.806
iHex	123.156	918814.240	0.934	1.525	22.872	13	2.016	2.082	2.090
nHept	586.063	10199.817	0.971	0.543	23.156	14	2.298	2.690	2.760
nHex	218.559	25859.672	0.894	0.507	24.544	14	1.621	2.186	2.322
nOct	2852.576	2345.276	0.874	0.550	19.226	12	2.500	3.199	3.422
1Hex	1180.248	12446.169	0.931	0.191	17.978	9	1.387	2.313	2.903
1Oct	1284.572	19449.795	0.932	1.150	20.556	13	2.540	3.005	3.097
cHexe	225.458	3914.541	0.753	0.886	17.692	10	0.261	1.230	2.005
DCM	112.942	405690.150	0.973	0.465	24.986	12	0.299	1.235	1.861
TeCM	481.283	31951.458	0.934	0.539	22.254	12	0.598	1.567	2.339
TCM	872.742	22586.056	0.845	0.753	22.573	13	-0.547	0.452	1.440
DNBE	229.467	19930052.758	0.991	0.795	26.933	12	2.028	2.313	2.356
DNPE	148.182	7662.273	0.689	1.139	20.879	12	-0.806	0.190	1.151
Benz	56.993	717361.751	0.821	0.281	21.974	10	1.374	1.699	1.750
BbF	644.325	174199.090	0.958	0.733	20.570	10	1.393	2.264	2.712
ClB	359.427	28619.852	0.909	0.493	21.651	12	0.753	1.695	2.345
nPB	420.355	84812.619	0.994	1.018	18.073	10	2.024	2.511	2.611
Naph	262.447	3281.268	0.966	0.534	16.341	9	1.008	1.878	2.323
pXy	1344.278	6385.097	0.977	0.747	22.020	14	0.594	1.583	2.484
MPE	114.665	284671.730	0.878	0.717	23.745	12	1.344	1.907	2.042
Sty	619.726	101789.597	0.988	1.239	22.492	12	1.494	2.332	2.717
Ind	575.923	66745.877	0.811	0.537	25.301	14	0.543	1.520	2.339

K_L: Langmuir affinity coefficient [µg L^{-1}]; Q_0: maximum sorption capacity [µg kg^{-1}]; RMSE: root mean square error; N: number of data points; $C_{i,sat}$: saturated aqueous concentration [µg L^{-1}]; log $K_{p/w}$ logarithmic polymer-water distribution; coefficient [L Kg^{-1}].

Table A4-6 - Calculated distribution coefficients between the polymer and air at different sorbate loadings.

Sorbate	log $K_{p/a,10}$	log $K_{p/a,100}$	log $K_{p/a,1000}$
cHept	0.739	0.469	0.203
cHex	0.346	0.044	-0.254
cOct	1.093	0.581	0.075
iHex	0.636	0.812	0.989
nHept	-0.172	-0.427	-0.677
nHex	-0.241	-0.507	-0.769
nOct	-0.577	-0.951	-1.315
1Hex	0.893	0.381	-0.105
1Oct	0.391	0.024	-0.321
cHexe	1.362	1.223	1.085
DCM	2.662	2.528	2.395
TeCM	2.347	2.299	2.251
TCM	2.544	2.243	1.949
DNBE	2.892	2.759	2.628
DNPE	2.502	2.371	2.241
Benz	2.367	2.331	2.295
ClB	3.190	3.146	3.101
nPB	2.858	2.831	2.805
Naph	-1.832	-1.909	-1.984
pXy	2.678	2.463	2.256
MPE	3.582	3.524	3.466
Sty	3.328	3.085	2.850

Log $K_{p/a}$: logarithmic distribution between the polymer and air at a sorbate loading in mg kg^{-1}.

A4-S4 Leave-Many-out cross validation analysis using assorted compounds

The Leave-Many-out cross validation was done, following literature [7].

Table A4-7 - Validation set for the leave-many-out cross validation.

	Concentration level		
	10^{-2} $C_{i,sat}$	10^{-3} $C_{i,sat}$	10^{-4} $C_{i,sat}$
	1Oct	1Oct	1Oct
	BbF	BbF	pXy
	nHept	Sty	nPB
	MPE	Naph	cHept
	cHexe	cHex	Ind
	DCM	Benz	MPE
	Ind	DNPE	DNPE
Q^2_{LMO-CV}	0.837	0.885	0.817
$RMSE_{LMO-CV}$	0.035	0.024	0.041

Q^2_{LMO-CV} : The cross-validated correlation coefficient; $RMSE_{LMO-CV}$: The cross-validated root mean square error.

A4-S5 Statistical analysis of ppLFER models

Table A4-8 - Calculated parameters for the ppLFER at 10^4 sorbent loading using FM log $K_{p/w}$ values for PS.

	Coefficient	SE	p-value
c	-1.20427	2.07853	0.57938
e	-5.95521	2.72147	2.18824
s	10.19292	4.2196	2.41561
a	-4.07825	9.82874	0.41493
b	-1.34614	3.32643	0.40468
v	0.65934	0.64244	1.0263

Table A4-9 - ANOVA results for the ppLFER at 10^4 sorbent loading using the FM for PS.

	DF	Sum of Squares	Mean Square	F-Value	Prob>F
Model	5	22.51759	4.50352	3.03143	0.04111
Error	16	23.76973	1.48561		
Total	21	46.28732			

Table A4-10 - Calculated parameters for the ppLFER at 10^{-2} sorbent loading using FM log $K_{p/w}$ values for PS.

	Coefficient	SE	p-value
c	0.36299	0.28321	0.21621
e	-1.59057	0.3734	0.0004
s	2.7751	0.53503	< 0.0001
a	-3.28501	0.56168	< 0.0001
b	-2.99745	0.52488	< 0.0001
v	1.82218	0.29201	< 0.0001

Table A4-11 - ANOVA results for the ppLFER at 10^{-2} sorbent loading using the FM for PS.

	DF	Sum of Squares	Mean Square	F-Value	Prob>F
Model	5	2.93167	0.58633	13.9447	1.17117E-5
Error	18	0.75685	0.04205		
Total	23	3.68851			

Table A4-12 - Calculated parameters for the ppLFER at 10^{-3} sorbent loading using FM log $K_{p/w}$ values for PS.

	Coefficient	SE	p-value
c	0.43032	0.25521	0.10903
e	-1.33626	0.33649	0.0009
s	2.28459	0.48214	0.0001
a	-2.15786	0.50616	0.0004
b	-3.06405	0.473	< 0.0001
v	2.01039	0.26314	< 0.0001

Table A4-13 - ANOVA results for the ppLFER at 10^{-3} sorbent loading using the FM for PS.

	DF	Sum of Squares	Mean Square	F-Value	Prob>F
Model	5	2.75292	0.55058	16.125	4.23514E-6
Error	18	0.6146	0.03414		
Total	23	3.36752			

Table A4-14 - Calculated parameters for the ppLFER at 10^{-4} sorbent loading using FM log $K_{p/w}$ values for PS.

	Coefficient	SE	p-value
c	0.43906	0.39056	0.27494
e	-1.25852	0.50866	0.02295
s	2.23174	0.70618	0.00515
a	-2.01035	0.59903	0.00332
b	-3.7644	0.6516	< 0.0001
v	2.25798	0.40273	< 0.0001

Table A4-15 - ANOVA results for the ppLFER at 10^{-4} sorbent loading using the FM for PS.

	DF	Sum of Squares	Mean Square	F-Value	Prob>F
Model	5	5.18887	1.03777	12.90397	1.45987E-5
Error	19	1.52803	0.08042		
Total	24	6.7169			

Table A4-16 - Calculated parameters for the ppLFER at 10^{-2} aqueous solubility using PMM log $K_{p/w}$ values for PS.

	Coefficient	SE	p-value
c	1.76901	0.31582	< 0.0001
e	-1.10112	0.46054	0.02732
s	1.39499	0.58607	0.02793
a	-5.01317	0.76628	< 0.0001
b	-2.02383	0.47819	< 0.0001
v	0.54244	0.32583	0.11236

Table A4-17 - ANOVA results for the ppLFER at 10^{-2} aqueous solubility using the PMM for PS.

	DF	Sum of Squares	Mean Square	F-Value	Prob>F
Model	5	5.65919	1.13184	16.16214	2.85816E-6
Error	19	1.33057	0.07003		
Total	24	6.98977			

Table A4-18 - Calculated parameters for the ppLFER at 10^{-2} aqueous solubility using LM log $K_{p/w}$ values for PS.

	Coefficient	SE	p-value
c	-1.95264	0.89163	0.04121
e	-1.71769	1.16125	0.15548
s	2.60626	1.61218	0.12245
a	-2.60348	1.36755	0.0722
b	-4.51331	1.48758	0.00683
v	3.72268	0.91941	< 0.0001

Table A4-19 - ANOVA results for the ppLFER at 10^{-2} aqueous solubility using the LM for PS.

	DF	Sum of Squares	Mean Square	F-Value	Prob>F
Model	5	11.47268	2.29454	5.47423	0.00276
Error	19	7.96389	0.41915		
Total	24	19.43657			

Table A4-20 - Statistical results of the MRA for the three isotherm model fits.

	FM 10^{-2}	**FM 10^{-3}**	**FM 10^{-4}**	**FM 10^{4}**	**PMM 10^{-2}**	**LM 10^{-2}**
N	25	25	25	23	25	25
DF	19	19	19	17	19	19
RSS	0.979	0.882	1.528	23.804	1.331	7.964
R^2	0.843	0.832	0.713	0.363	0.760	0.482
RMSE	0.227	0.215	0.284	1.183	0.265	0.647

Abbreviations and comments:

DF: degrees of freedom

SE: standard error of estimates

RSS: Residual sum of squares

RMSE: Root-mean square error

All parameters above were calculated at 95% confidence level using OriginLab 9.1.

A4-S6 Concentration dependent ppLFER

The calculation of the concentration dependent ppLFER followed the approach by Gschwend et al. [8] with α being the equilibrium concentration/$C_{i,sat}$.

$$\text{Log } K_{p/w} = [-0.07 \log\alpha + 0.23] + [-0.19 \log\alpha + 1.45]V_i + [[0.01 \log\alpha - 2.86]B_i \quad \text{(Eq. A4-1)}$$
$$+ [-1.13 \log\alpha - 5.54]A_i + [0.49 \log\alpha + 3.76]S_i + [-0.25 \log\alpha - 2.10]E_i$$

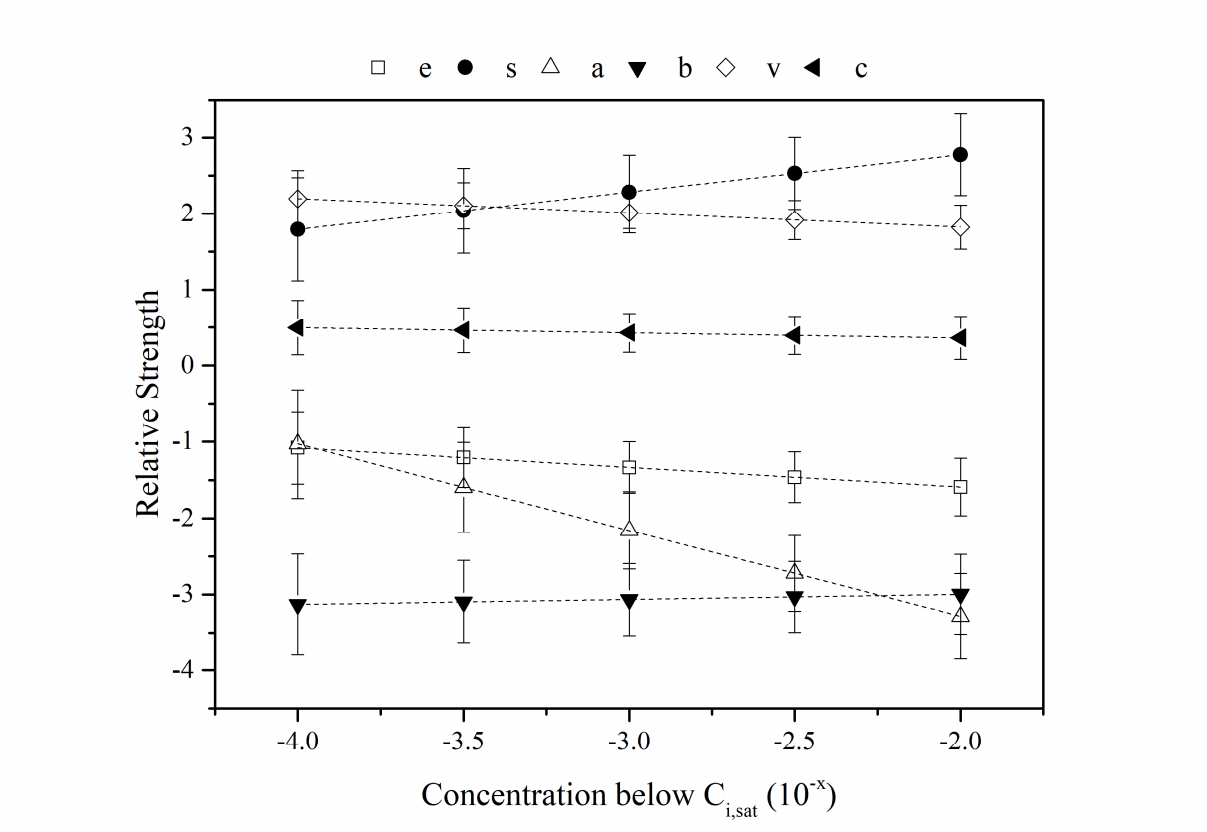

Figure A4-3 - Relative molecular interactions strengths on PS varied with different aqueous concentration levels.

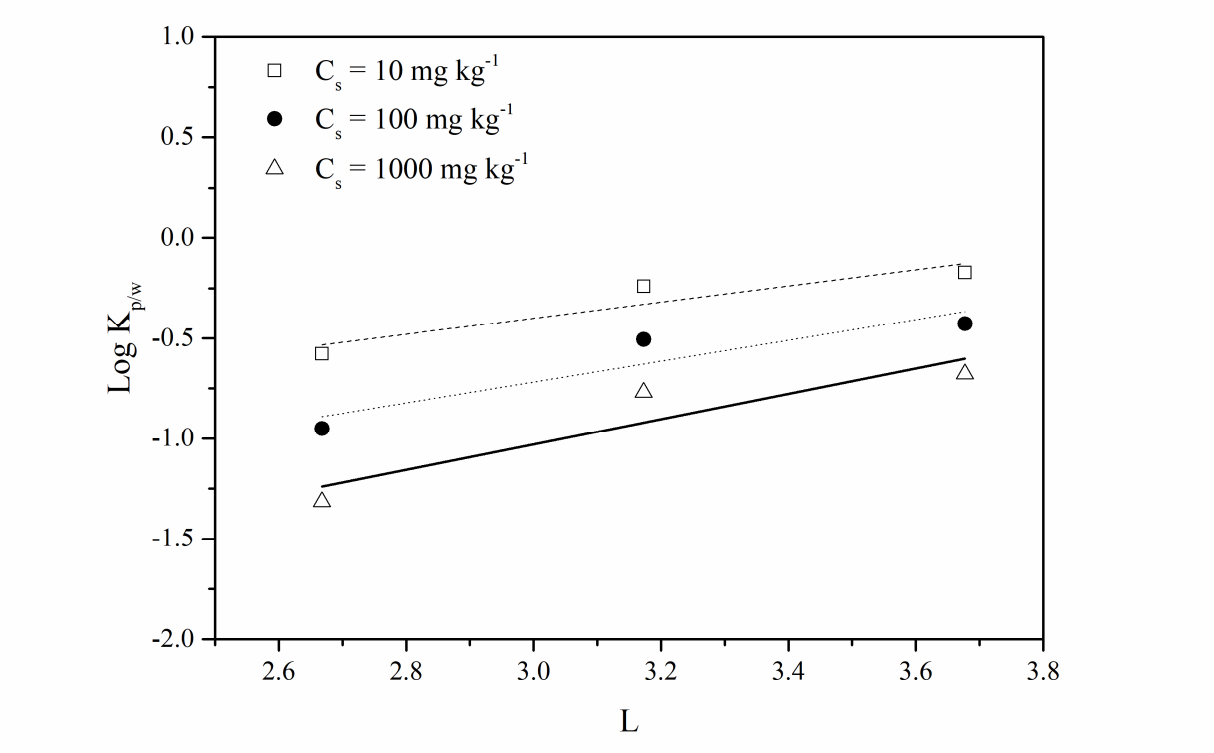

Figure A4-4 - Non-specific interaction lines for PS foil using n-hexane (left), n-heptane (middle) and n-octane (right) at four different concentration levels.

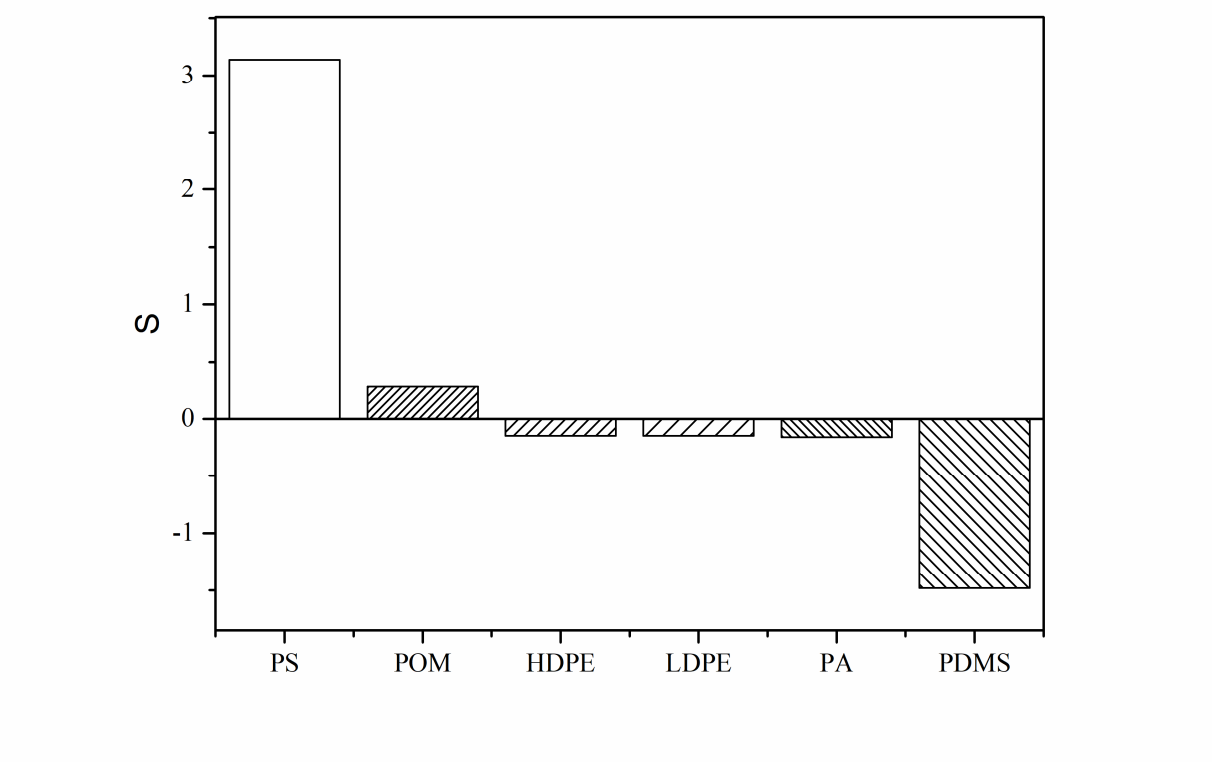

Figure A4-5 - Comparison of the polarizability/dipolarity (S) of assorted polymers with PS from this study.

References

[1] D. H. Kaelbe, "Dispersion-Polar Surface Tension Properties of Organic Solids", *J. Adh.* Vol. 2, pp. 66-81, 1970.

[2] D. Owens; R. Wendt, „Estimation of Surface Free Energy of Polymers", *J. Appl. Polym. Sci.*, vol 13, pp. 1741-1747, 1969.

[3] W. Rabel, "Einige Aspekte der Benetzungstheorie und ihre Anwendung auf die Untersuchung und Veränderung der Oberflächeneigenschaften von Polymeren", *Farbe und Lack*, vol. 70, no. 10, pp. 997-1005, 1971.

[4] T. Hüffer and T. Hofmann, "Sorption of non-polar organic compounds by micro-sized plastic particles in aqueous solution.," *Environ. Pollut.*, vol. 214, no. 1, pp. 194–201, Apr. 2016.

[5] T. Hüffer, S. Endo, F. Metzelder, S. Schroth, and T. C. Schmidt, "Prediction of sorption of aromatic and aliphatic organic compounds by carbon nanotubes using poly-parameter linear free-energy relationships.," *Water Res.*, vol. 59, no. 1, pp. 295–303, 2014.

[6] L. Li, P. A. Quinlivan, and D. R. U. Knappe, "Predicting Adsorption Isotherms for Aqueous Organic Micropollutants from Activated Carbon and Pollutant Properties," *Environ. Sci. Technol.*, vol. 39, no. 9, pp. 3393–3400, May 2005.

[7] P. Gramatica, "Principles of QSAR models validation: internal and external," *QSAR Comb. Sci.*, vol. 26, no. 5, pp. 694–701, 2007.

[8] Y. H. Shih and P. M. Gschwend, "Evaluating activated carbon-water sorption coefficients of organic compounds using a linear solvation energy relationship approach and sorbate chemical activities," *Environ. Sci. Technol.*, vol. 43, no. 3, pp. 851–857, 2009.

Chapter 5 Using inverse liquid chromatography to determine sorption properties of high-density polyethylene in water

5.1 Abstract

Sorption to environmentally relevant sorbents, like plastic materials, is typically studied in batch experiments. There, the required amount of material and time consumed are major disadvantages. A complimentary experimental procedure is inverse liquid chromatography (ILC) where the sorbent is the packing material inside an analytical column. Sorbates are injected into these ILC columns and the sorption isotherms or directly distribution coefficients (log K_d) are derived from the sorbate elution profile. In order to test the feasibility of this approach for sorption to polymers, high-density polyethylene (HDPE) was used as sorbent applying the ILC approach with a large compound set. LC columns were packed with HDPE material and a sorbate set was measured with these columns under different conditions, e.g. temperature, flow rate and column length. The chromatographic parameters of all columns were initially determined with the help of a non-retarded tracer (deuterium oxide). As additional sorbent, UV-B aged HDPE material was also packed in an ILC column and distribution coefficients were determined. Lastly, the distribution coefficients from the aged HDPE material were investigated at high ionic strength. The sorption strength for nonpolar compounds did not change for aged HDPE in comparison to fresh HDPE but sorption for polar compounds did decrease significantly. The achieved results demonstrate that the ILC approach used to investigate sorption properties under environmentally relevant conditions is promising.

5.2 Introduction

The sorption of organic compounds to plastic waste in aquatic systems could be a major process determining the impact from the presence of organic compounds on aquatic ecosystems [1, 2]. To characterize sorption properties and study the influence of environmental conditions on sorption a wide range of data on sorption behaviour within a plastic-water system is required.

The determination of the sorption behaviour of plastics in water systems is especially gaining interest in the food industry [3], in pharmaceutical industry [4], in the field of analytical chemistry [5–7] and in environmental pollution discussions [8–11]. For example, improving the methodology to determine the sorption behaviour of certain substances in a plastic-water system will lead towards enhanced development of passive-sampling-devices (PSD) including a wider range of specific phases for PSD [12, 13]. With PSD, the substance of interest (analyte / sorbate) will ad- or absorb to the bulk material, coming from the surrounding aqueous media, and will then be desorbed either with a solvent or through thermal desorption [5].

One of the major plastics that is used for technical applications is polyethylene, especially high-density polyethylene (HDPE). It has a density equivalent to water, which makes it a good carrier for hydrophobic organic compounds (HOCs) in aquatic systems. With its excellent properties in terms of robustness and durability, it is one of the most used polymers as a packaging material in Europe [14]. Due to this application, a lot of the used plastic will potentially end up in the environment as waste.

The ecological effects of plastic waste on the environment are widely discussed [2, 15–21]. An improved understanding of sorption mechanisms for polymers in water will render a better understanding of the ecological effects of plastic waste in the oceans.

A common method to determine sorption data is the batch approach. In this approach, sorption isotherms are measured, and the distribution coefficient is derived from a fitting model. This approach to determine sorption isotherms requires many experiments and analyses per compound for obtaining a distribution coefficient [22–24]. A potentially more efficient method is offered by inverse chromatography (IC) which has already been used to determine sorption data for several systems such as stationary phases for gas chromatography [25–29], soils [30–33], mineral surfaces [34] or carbon nanotubes [35, 36]. Inverse liquid chromatography (ILC) is a method which analyses the interactions of an analyte between a liquid and a solid phase based upon the chromatographic principle. The stationary phase is the phase of interest for which the sorption behaviour should be determined. The mobile phase in case of water-related

distribution coefficients is water that transports organic substances through the stationary phase. From the elution profiles distribution coefficients can be derived.

Compared to batch experiments, ILC offers significant advantages [37]. It uses less resources like sorbent material and sorbates than batch experiments and has a high sorbent-to-sorbate ratio. The latter will allow to investigate sorption of weakly interacting sorbates [36]. Once the system is set up and calibrated, many compounds may be investigated in a small amount of time, which allows to more systematically study the effect of environmental conditions on sorption.

The research on sorption to plastic materials in water systems can greatly benefit from an improved methodology to determine the sorption processes [38]. For some sorption prediction systems, among which the octanol-water system is of interest here, there is already a wide range of distribution coefficients available [25 , 39]. This study aims to demonstrate the benefit of ILC use to generate distribution data for plastic-water systems. In the experiments, several organic compounds have been chosen, including nonpolar and polar aliphatic and aromatic compounds. With a calibrated ILC set up, environmental conditions like aging or ionic strength of the surrounding media can be varied. With the help of a linear solvation-energy relationship model, sorption properties of HDPE could then be derived.

5.3 Material and Methods

5.3.1 Chemicals and Packing Materials

HDPE tubing (Hostalen CRP 100 blue) was provided by Lyondel Basell Industries with characteristic parameters given in Table 3-1. Chemicals used in this study were simple organic compounds and more complex organic compounds (Table A5-1). All probe compounds used were purchased from Sigma Aldrich as listed in the appendix (Table A5-1) with abbreviations and selected properties added. Additional chemicals incorporated in this study were deuterium oxide (D_2O) (≥ 99.5 %, AppliChem Panreac) and sodium bromide (NaBr) (≥ 99 %, Fluka). The water used as the eluent was purified (T = 23 °C, TOC ≤ 1 ppb and σ ≤ 0.055 µS) and provided by a PURELAB Flex instrument from ELGA. Quartz sand with a particle size < 63 µm was purchased from Fluka (purity ≥ 99.7 %). The bulk HDPE material for the manually packed columns was ground with the help of a Cryomill (Retsch, Germany) and sieved to different particle size batches with < 128 µm, < 85 µm and < 48 µm.

5.3.2 Instrumentation

Empty stainless-steel LC columns were bought from Bischoff Chromatography, Germany with dimensions of 5.3, 3.0 and 1.4 cm in length and with 3 mm inner diameter. Additionally, precolumns, connecting nuts, metal sieves and glass fibre filters were also bought from Bischoff.

The experiments were run on an Ultimate 3000 UHPLC System from Dionex. It contained a binary pump (UltiMate 3000 RS Pump and degasser), an autosampler with a 130-µL sample loop (UltiMate 3000 RS Autosampler), a column oven (UltiMate 3000 RS column heater) and a diode array detector (UltiMate 3000 RS diode array detector). Additionally, an RI detector was connected to the UV detector (see Figure 1-10 for a schematic set up).

For aging of HDPE, ground HDPE powder (< 48 µm) was placed 3 cm under a UV-B light (wave length 280 - 315 nm, UV-B 3.0 W) for 30 days. The changes of the plastic material due to aging were monitored with the help of the medium molar mass (MMW) analysis. The procedure for measuring the MMW is described in more detail in literature [22, 40] and the appendix from this study (Section A5-S1). Usually gel permeation measurements are done to determine the MMW, but in this study the MMW was determined with the help of a viscometer by Ubbelohde and then following the Mark-Kuhn-Houwink-Sakurada equation [41].

5.3.3 Chromatographic procedure

The packing procedure of the ILC columns was mainly based on literature for reference soil or multi-walled carbon nanotubes [27, 35, 42]. To avoid excess backpressure in the columns, as seen in initial experiments, the HDPE material was mixed with an inert material (Quartz sand) at various mass ratios (see below). This approach has also been suggested in literature [35] and led to a stable packing of the material without clogging.

The columns were filled with a premixed packing material using a stainless-steel spatula. The column was tapped on the lab bench between the filling steps to ensure a homogeneous and dense column packing without dead volume. After each filling step, the packing material was compressed using a stamp, as opposed to literature procedures. Then the column was closed with a nut, and a precolumn was connected with additional filling material. The columns were then installed in the column oven and were filled with purified water. A flow rate ramp from 0.01 mL min^{-1} up to 3.5 mL min^{-1} over a period of 4 hours was used for packing (Figure A5-2). The pH of the water was checked regularly and was between 6.8 and 7.1. Once the 3.5 mL min^{-1} flow rate was reached, the system was left at that flow rate to check for changes in the column head pressure. This would hint at leaks, large voids or a bad column packing. Once the column head pressure was stable for at least six hours, the packed column was ready for ILC experiments.

5.3.4 Data analysis

The packed columns served as the stationary phase in the ILC setup, in accordance to previously reported methodology [27, 42]. Single compound injections of sorbates were done for the ILC experiments. Determining the retention time (t_R) in ILC experiments can be a critical task, as different approaches render different t_R. The three common approaches to determine the t_R in ILC experiments are the first moment approach, the apex point approach or the half-mass point approach [43–45]. In this work, the half-mass point determination was applied, which is described in detail in literature [27]. In short, the half-mass point is the time point when half of the solute mass has eluted (i.e., where the peak area can be divided in two equal parts). The benefit of this approach is the low influence of bad peak integration or peak shapes, i.e. peak tailing, or baseline noise on the resulting t_R. In LC experiments, peaks of solutes can exhibit strong interactions with the packing material, giving a pronounced peak tailing. Additionally, the half-mass point has previously been proven to deliver robust data for multiwalled carbon nanotubes [35, 36] and soils [30, 46].

As the organic compounds move through the column, they distribute between the HDPE stationary phase and the aqueous mobile phase. When linear sorption is assumed, the distribution between the two phases can be calculated following the approach used by Bi et. al. [27]. This approach uses the retention factor Rf for determination of the distribution coefficient $K_{p/w}$ [L kg^{-1}] (Eq. 5-1). The Rf is calculated (Eq. 5-2) using t_R [min] and the travel time of a non-retarded tracer compound t_0 [min] but also requires the dead time of the system t´ [min] to take extra-column dead volumes into account. The dead time was determined by a 1 µL injection of D_2O (undiluted) without the column installed in the system. In the present study, D_2O was used as non-retarded tracer. The t_R of the tracer renders the travel time of the system, without any interactions.

$$Rf = 1 + (\rho_b \cdot K_{p/w}) \cdot \theta^{-1} \quad \text{(Eq. 5-1)}$$

$$Rf = (t_R - t') \cdot (t_0 - t')^{-1} \quad \text{(Eq. 5-2)}$$

Where ρ_b is the bulk density [kg L^{-1}] and θ the porosity [-]. Both are determined using repeated measurements of the non-retarded tracer D_2O with and without the column installed and calculated following literature. Control injections of D_2O rendered no shifts in the t_R and showed stable results for > 300 injections. The determined column characteristics are summarized in Table 5-1.

All computational calculations were done using the OriginPro Software 9.1 from OriginLab.

5.3.5 Experimental conditions

For all ILC experiments a 1.4 cm column with purified water (pH) was used as the eluent, if not stated otherwise. Sorbate injections (1 µL) were done into a 130-µL sample loop and the following parameters were varied:

(1) *HDPE/sand ratio*: MTBE injections at a flow rate of 1 mL min^{-1} and at 30 °C, with HDPE/sand ratios of 95/5 w/w %, 50/50 w/w % and 5/95 w/w %. HDPE particles < 83 µm were used for these experiments.

(2) *Flow rate*: nPb and Benz injections at 30 °C with HDPE/sand ratios of 95/5 w/w % and flow rates of 0.5, 1.0 and 2.0 mL min^{-1}. HDPE particles < 83 µm were used for these experiments.

(3) *Particle Sizes*: Injections of nPb, Benz, Tol and pXy with HDPE particle sizes of < 128 µm, < 83 µm and < 48 µm at 30 °C.

(4) *Temperature*: Injections of nPb, Benz and Sty at a flow rate of 1 mL min^{-1} at 30, 40, 50 or 60 °C column oven temperature with HDPE particle sizes < 48 µm.

(5) *Column length*: Injections of organic compounds at 30 °C, a flow rate of 1 mL min^{-1} and a 5 %/95 % HDPE/sand ratio packing material were done onto columns with a length of 1.4 cm (Column SI), 3.0 cm (Column SII) and 5.3 cm (Column SIII) and with HDPE particle sizes < 48 µm. Substance set can be seen in Table A5-5.

(6) *Aged HDPE*: aHDPE column: Packed with 5 % aged HDPE (< 48 µm) and 95 % quartz sand. Duplicate Injections of 2Octon, Benz, 1,4DMB, nPb, Sty, 2ClP, Benza, MTBE and Atrp.

(7) *Eluent salt content*: NaHDPE column: The aHDPE packed column (as in 6) with an eluent of purified water, containing 7 % NaCl. D_2O injections at 30 °C, a flow rate of 1 mL min^{-1} and a 5 %/95 % HDPE/sand ratio packing material and with aHDPE particle sizes < 48 µm. Duplicate injections of substance set from (6).

5.4 Results and Discussion

5.4.1 Method development

The determined system t_0 by D_2O injections for all columns used in this study are summarized in Table 5-1. When considering different column length (Columns SI, SII and SIII in the appendix), the RSDs of the Rf from all columns are below 8 %. The t_R for all columns and each compound are stable with an RSD below 10 % and t_R increase from column SI to column SIII (Table 5-3 and Table A5-5). Increased column length will lead to longer t_R when all other parameters are kept constant. Following Eq. 5-1 and 5-2, the increased column length is accounted for by incorporating the Rf for calculating log $K_{p/w}$ values. The experiments with longer columns than 1.4 cm did not show an improvement over the 1.4 cm column, and the results are shown in the appendix (Table A5-5). Therefore, the following studies were taken by incorporating the 1.4 cm column (Column SI).

Table 5-1 - Determined relevant parameters of the packed columns by D_2O injections.

Column abbreviation	Length (cm)	Diameter (cm)	Travel Time (min)	Pore volume (mL)	Porosity (-)	Bulk density (kg L^{-1})
Column SI	1.4	0.3	0.16	0.07	0.73	1.33
aHDPE	1.4	0.3	0.16	0.07	0.71	1.35
NaHDPE	1.4	0.3	0.16	0.07	0.71	1.35

In water, polyethylene is known to swell [47] which can lead to a higher backpressure and eventually column clogging at a higher PE content. Previous ILC investigations overcame clogging problems by adding inert material like quartz sand into the column [35, 36], which was also done here. Initial experiments with the quartz sand showed negligible interactions with the chemical probes (data not shown). The HDPE-to-quartz sand ratio was determined by incorporating different mixtures and monitoring the t_R of MTBE and the column head pressure. Subsequent injections of MTBE showed the best results in terms of reproducible t_R (< 10 %) and peak width with the 5 % (w/w) HDPE/sand ratio. A HDPE content > 5 % (w/w) in the columns rendered too high column head pressures (> 30 MPa) and strong peak tailing of MTBE.

The stability of the columns was continuously monitored with intermediate D_2O injections over the course of the experiments.

The optimum flow rate would render robust and reproducible Rf at equilibrium-like conditions, while at the same time providing a short experimental time. The experiments with varying flow rates gave good results (RSD of Rf < 2.5 %) at 1 mL min^{-1} in terms of reproducibility for the solutes nPb, Benz and pXy. The compound nPb showed a strong tailing of the peak, which is due to the very strong sorption of nPb to HDPE [22] and would indicate non-linear sorption under equilibrium conditions. Non-linear sorption to HDPE has previously been reported with the conventional batch approach [22].

To further investigate the required time for the experiments, different HDPE particle sizes were measured. Smaller particles allow for faster equilibration, since the influence of the pore diffusion and diffusion into the polymer is decreased, compared to bigger particles. The smallest possible particle sizes were < 48 µm and LC experiments rendered similar results (RSD < 10 %) as the ones with < 128 µm and < 83 µm particles, although at a shorter experiment time (Figure A5-2). Particles < 48 µm were further on used for the ILC experiments.

Table 5-2 - Results of the temperature study.

Temperature °C	Compound	t_R	Rf
30	nPb	21.8	325
	Benz	0.8	10
	Sty	3.8	55
40	nPb	20.9	311
	Benz	0.8	10
	Sty	3.8	55
50	nPb	17.5	261
	Benz	0.8	10
	Sty	3.3	48
60	nPb	15.7	234
	Benz	0.8	10
	Sty	3.4	50

t_R: retention time in minutes; (min); Rf: Retention factor.

The data for the temperature studies are presented in Table 5-2. As the temperature of the column oven is increased from 30 to 60 °C in steps of 10 °C, the Rf decreases significantly for nPb by about 30 % ($p < 0.05$), whereas for Sty it only decreases insignificantly by 8 % ($p > 0.05$). Following the van't Hoff equation, nPb showed a phase transfer enthalpy (ΔH) of – 9.68 kJ mol^{-1} ($p < 0.05$). The van't Hoff plot is presented in the appendix (Figure A5-4) with additional information. The van't Hoff plot indicates that sorption is an exothermic process for

nPb [36], which is in accordance with previous studies [48]. In the case of benzene, which has no side chains, the Rf is deviating insignificantly (RSD < 5 %, $p > 0.05$). Incorporating other compounds with a t_R below 1 minute showed that the ability to reliably integrate those peaks decreases at T > 30 °C. Further on, 30 °C was used as the experimental temperature as it represents stable conditions close to ambient, while also rendering robust results. Stable temperature below 30 °C could not be achieved with the experimental set up.

5.4.2 Method robustness

To analyse the robustness of the ILC experiments, it is necessary to test how close the conditions represent the sorption at equilibrium. The equilibrium state with ILC experiments can be determined by measurements at multiple flow rates. If Rf increases significantly while decreasing the flow rate (increased contact time), sorption is not at equilibrium [27]. An alternative would be stopped-flow experiments, but this requires much more experiment time and is less convenient than measuring at multiple flow rates [49]. The longitudinal diffusion during the stopped-flow experiment would increase the peak width, the longer the column flow rate would be 0 mL min^{-1} and therefore reduce the sensitivity. Figure 5-1 compares the Rf with different flow rates for a hardly retarded compound (Benz), an intermediately retarded compound (pXy) and a stronger retarded compound (nPb). The results from the linear fits of the data between 0.5 and 2 mL min^{-1} are represented in the appendix (Table A5-2). As can be seen in Figure 5-1, the Rf values for the duplicates of Benz at 0.5 mL min^{-1} deviate significantly ($p < 0.05$) from each other, where both have a significant impact on the fitting. Without the higher data point, the y-intercept (b) is 0.293 ± 0.006 ($p < 0.05$), compared to 0.385 ± 0.071 ($p < 0.05$) with the higher data point, and represents very well the flow rate at 1 mL min^{-1}. For nPb, the high flow rate of 2 mL min^{-1} has a significant impact ($p < 0.05$) on the fit and the Rf does deviate strongly from the other two flow rates.

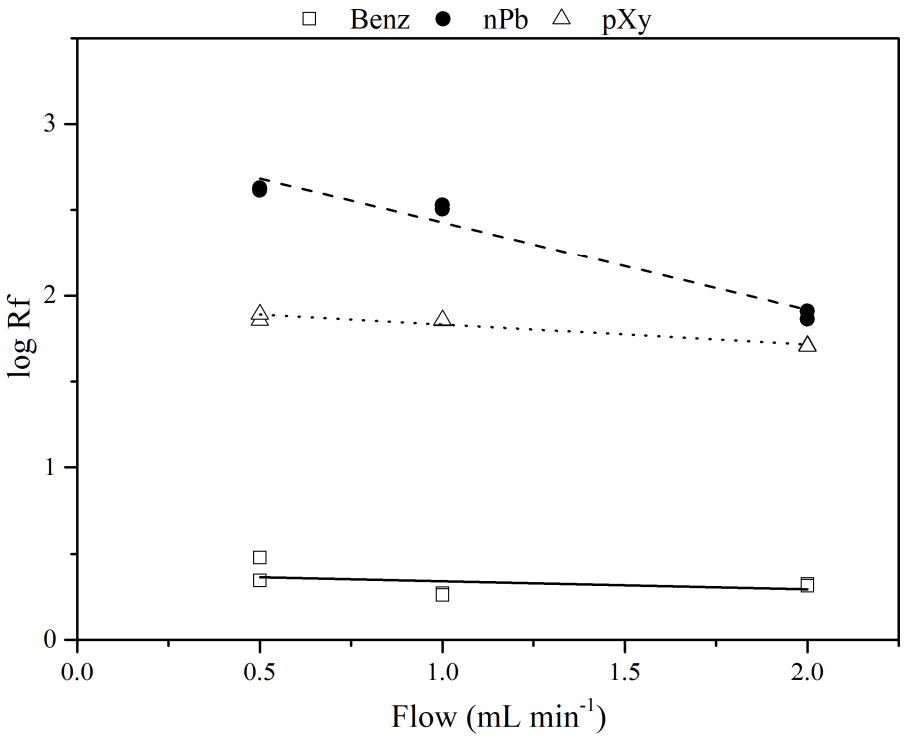

Figure 5-1 - Comparison of the retention factor with the flow rate between 0.5 and 2 mL min $^{-1}$ with an injection volume of 1 µL. The regression lines represent a linear fit with the data between 0.5 and 2 mL min^{-1}.

If only using the flow rates of 0.5 and 1 mL min^{-1} for nPb, a flow rate of 1 mL min^{-1} does very well represent the Rf values with a deviation < 15 % from the extrapolated flow rate at 0 mL min^{-1}. The low deviation of Rf (< 15 %) at 1 mL min^{-1} from the y-intercept is suggesting near-equilibrium conditions for all three compounds using this flow rate.

To further validate the experimental ILC set up, column SI was used for a larger substance set. The results are listed in Table 5-3 and in the appendix (Table A5-5), where hydrophobic compounds (log $K_{o/w}$ > 1.0) do show in general high sorption coefficients (log $K_{p/w}$ > 1.5). Strong sorption for hydrophobic compounds is expected since sorption to PE is mainly driven by non-specific van-der Waals interactions [8, 22]. Interestingly, the compounds ACN, Glu and Aa showed very strong sorption (log $K_{p/w}$ > 3.0) while having low log $K_{o/w}$ values (< 1.0). Low log $K_{o/w}$ values would suggest weak sorption. The reasons for a higher sorption strength of the hydrophilic substances ACN, Glu and Aa are unclear at this point.

Table 5-3 - Experimental results for the complete dataset using different column lengths and chromatographic conditions.

	Column I	Column II	Column III

Substance	t_R	Rf	log $K_{p/w}$	t_R	Rf	log $K_{p/w}$	t_R	Rf	log $K_{p/w}$
Oct2on	0.3	3.5	1.8	0.5	4.9	1.9	0.7	6.6	1.9
Benz	0.3	3.5	1.8	0.5	5.1	1.9	0.7	6.8	1.9
pXy	4.7	63.8	3.1	4.9	54.2	2.9	5.0	54.5	2.8
nPb	19.1	264.6	3.7	23.1	260.6	3.6	24.2	267.9	3.5
cOcte	0.4	4.5	1.9	0.5	5.1	1.9	0.7	6.6	1.9
1Hex	0.4	4.8	2.0	0.6	5.3	1.9	0.7	6.2	1.9
Styr	2.0	25.9	2.7	2.1	23.0	2.6	2.3	24.2	2.5
Atz [a]	4.7	63.6	3.1	4.9	54.0	2.9	5.0	54.4	2.8
12DCB	0.2	2.1	1.6	0.4	3.6	1.8	0.5	4.8	1.8
MPE	0.7	8.3	2.2	0.9	9.0	2.1	1.0	10.3	2.1
Ppl [b]	0.6	6.5	2.1	0.8	7.6	2.1	0.9	8.7	2.0
AP	0.4	3.5	1.8	0.5	5.1	1.9	0.7	6.4	1.9
2CP	0.2	2.1	1.6	0.4	3.8	1.8	0.6	5.2	1.8
BbF	0.2	2.0	1.6	0.5	4.2	1.8	0.5	5.0	1.8
Tea	1.3	17.4	2.5	1.5	16.4	2.4	1.7	17.4	2.3
Benzal	13.5	186.8	3.5	13.7	153.9	3.4	13.8	152.4	3.8
oXy	0.2	1.8	1.5	0.4	3.7	1.8	0.5	4.9	1.8
ACN	18.5	256.0	3.7	20.4	229.9	3.6	20.5	227.2	3.5
MTBE	2.2	28.9	2.7	2.4	25.7	2.6	2.5	26.6	2.5
Atp [c]	6.6	90.2	3.2	6.8	75.7	3.1	6.9	75.6	3.0
Caf	0.7	8.2	2.2	0.9	8.9	2.1	1.0	10.2	2.1
Cph	58.2	807.7	4.2	58.3	658.5	4.0	58.5	649.1	3.9
Ba	3.0	40.9	2.9	3.2	35.5	2.7	3.4	36.2	2.7
Bzi	8.6	118.2	3.3	8.7	97.4	3.2	8.8	97.0	3.1
Flu	0.9	11.3	2.3	1.1	11.2	2.2	2.0	12.3	2.2
Glu	57.4	796.9	4.2	57.7	651.4	4.0	57.8	641.1	3.9
Aa	52.1	722.8	4.1	52.3	590.3	4.0	52.4	581.1	3.9
Ma	0.2	2.0	1.6	0.4	3.8	1.8	0.6	5.1	1.8
Non2on	0.3	3.9	1.9	0.6	5.5	1.9	0.7	6.3	1.9
Lin	9.2	127.2	3.4	9.4	105.8	3.2	9.6	105.2	3.1
Ner	19.4	267.9	3.7	19.7	222.1	3.5	20.3	224.1	3.5
Glut	2.1	28.3	2.7	2.4	26.2	2.6	2.4	26.1	2.5

t_R: Retention time in minutes; Rf: Retention factor; log $K_{p/w}$: Logarithmic HDPE-water distribution coefficient; [a] 100 µg mL^{-1} in acetone; [b] 1% solution in ethanol; [c] 50 mg L^{-1} solution.

5.4.3 Sorption experiments with aged polyethylene

Any plastic compound exposed to environmental processes will degrade. The main drivers for degradation would be UV light, mechanical impact, or biological effects. The results

from the characterization of the ILC column packed with UV-B aged HDPE (aHDPE), are shown in Table 5-1. The column length for the ILC experiments with aHDPE was chosen based on the previous experiments. Degradation of polymers through UV-B-light leads to breaking of the polymer chains, resulting in a different morphology than non-aged polymers [50–53], which is reflected in the different MMW of HDPE and aHDPE. For the aHDPE an MMW of 3002 g mol^{-1} was found whereas the HDPE resulted in 5526 g mol^{-1}. With a shorter average chain length of the polymer, inhibited rearranging of the chains leads to a higher crystallinity [54]. An increase of crystallinity through degradation was already observed for HDPE and similar polymers, like polypropylene [55, 56]. A higher crystallinity exhibits a smaller number of amorphous segments (sorption sites) as was shown previously [22].

Log $K_{p/w}$ values from the substance set from the aHDPE column are compared to log $K_{p/w}$ values from Column SI in Figure 5-2 where the figure is separated in nonpolar compounds (left) and polar compounds (right). Sorption coefficients for nonpolar compounds show an insignificant ($p > 0.05$) increase in the distribution coefficient for all compounds. Hüffer et. al. have shown that there is a microcrack formation during the aging process of plastics [57]. These cracks would leave the plastic material prone to liquid permeation [58] acting as pores (sorption sites). This is in direct contrast to the section above, where aging leads to less sorption sites due to increased crystallinity. One approach would be that the effect of the micro crack formation would need several aging cycles to expand their effect on sorption, whereas the increased crystallinity shows a significant effect after just one cycle. As both effects will occur during aging [55, 57] a prediction with the current data is not feasible. Additional investigations on the individual impact from either micro crack formation or increased crystallinity on the sorption sites would be necessary but is beyond the scope of this study.

For most of the polar compounds (log $K_{o/w} < 2.0$) a significant decrease in sorption coefficients ($p < 0.05$) for aHDPE can be observed, except for 2ClP. The decrease in sorption coefficients for the aged HDPE can be a result of the presence of oxygen-containing surface groups due to aging [57, 59]. Those oxygen-containing groups can allow the formation of hydrogen bonds, especially with the surrounding water molecules, similar to the influence of surface oxidation on sorption as shown previously [57, 60]. The replacement of the water molecules by the sorbates would then be less favoured and the formation of three-dimensional water clusters can block sorption sites [61–63]. The impact on sorption from plastic aging has previously been shown for aged PS [57]. The effect of surface-oxidation has already been discussed previously where the increased oxygen-containing functional groups decreased the adsorption of molecules which can form H-bonds [61]. There have even been molecular

simulations, showing three-dimensional clustering of water molecules around H-bonding sites (oxygen-containing groups) [62, 63]. The decreased sorption strength of the polar compounds represents this effect also for HDPE. The accessibility of the nonpolar compounds to the polymer due to the water clusters might not be affected due to the increase of sorption sites from the chain breaking process and lack of H-bond interactions. The mechanism of sorption to aged HDPE is rather complex and will need further investigations of possible changes in the molecular interactions from HDPE aging. A comparison between pristine and aged HDPE with a large data set would give additional insights but is not done here.

5.4.4 Sorption experiments using environmentally relevant conditions

To investigate the sorption behaviour under saline conditions as in marine environments or some lakes, the aHDPE column from above (Table 5-1) was used with a mobile phase, containing about 7 % sodium chloride (NaCl). Seawater usually has a salinity of 3.5 % (35.16 g kg^{-1}) [64] but several lakes worldwide have salinities up to 400 g kg^{-1} [65]. To enhance the experimental effect and to render possible changes more drastic, a higher salt concentration was chosen.

When directly comparing the probe sorbate results from the purified water experiments HDPE & aHDPE with the salt water experiments NaHDPE (Figure 5-2), the difference in log $K_{p/w}$ for the nonpolar compounds is again lower than for the polar compounds as seen before. But in comparison to the aHDPE experiments, the difference between aHDPE and NaHDPE is not significant ($p > 0.05$). As was investigated previously for aqueous sorption, the salt content has only a low effect on sorption of neutral organic compounds [66]. Even at very high concentrations, the sorption strength did only deviate within a small range.

The experimental data and the literature data suggest that a major impact on sorption of non-ionic organic compounds to HDPE in aqueous media results from the UV-B aging of the HDPE material itself, i.e. decrease of sorption strength for polar compounds. Additional salt content, i.e. the salinity in water bodies like oceans or lakes, has little to no effect on the sorption from the compounds investigated here. Salting out effects for organic compounds in seawater were shown to be as low as 0 – 0.3 log units of deviation [66].

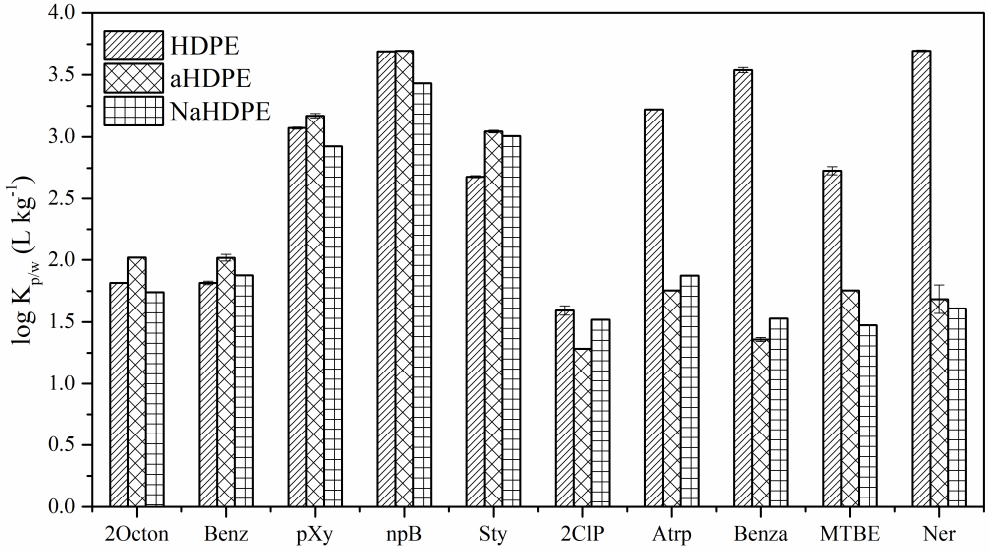

Figure 5-2 - Comparing results from the triplicate measurements of the normal HDPE ILC experiments with aged HDPE experiments and experiments with sea water and aged HDPE (NaHDPE). The compounds are represented from left to right with increasing log $K_{o/w}$ values and error bars given.

5.4.5 Sorption properties from inverse liquid chromatography

To further investigate the impact on sorption due to degradation, the sorption properties were compared with the ppLFER approach following literature procedures [22, 23]. A multiple regression analysis (MRA) was done with the experimental log $K_{p/w}$ data and literature sorbate descriptors [22–24, 67]. It should be noted that the comparison based on the ppLFER can only indicate changes of individual molecular interactions (phase descriptors) due to the small training set used for the MRA. When comparing the ppLFER descriptors e, s, a, b and v for the three columns (Column SI, aHDPE and NaHDPE), the impact of degradation through UV-B can be seen (Figure 5-3). The aged HDPE and NaHDPE columns show different capacities for certain intermolecular interactions than fresh HDPE. According to literature, a positive value of a descriptor suggests that this type of interaction is more favourable for the stationary phase compared to the liquid phase in case of $K_{p/w} = C_p\ C_w^{-1}$ [68, 69]. When an interaction is dominant in the mobile phase, the descriptor would be negative. None of the interactions changed in terms of algebraic sign, showing no complete switch in interactions after aging. For the H-bond interaction bB, a significant decrease for the aged PE can be observed compared to the original PE.

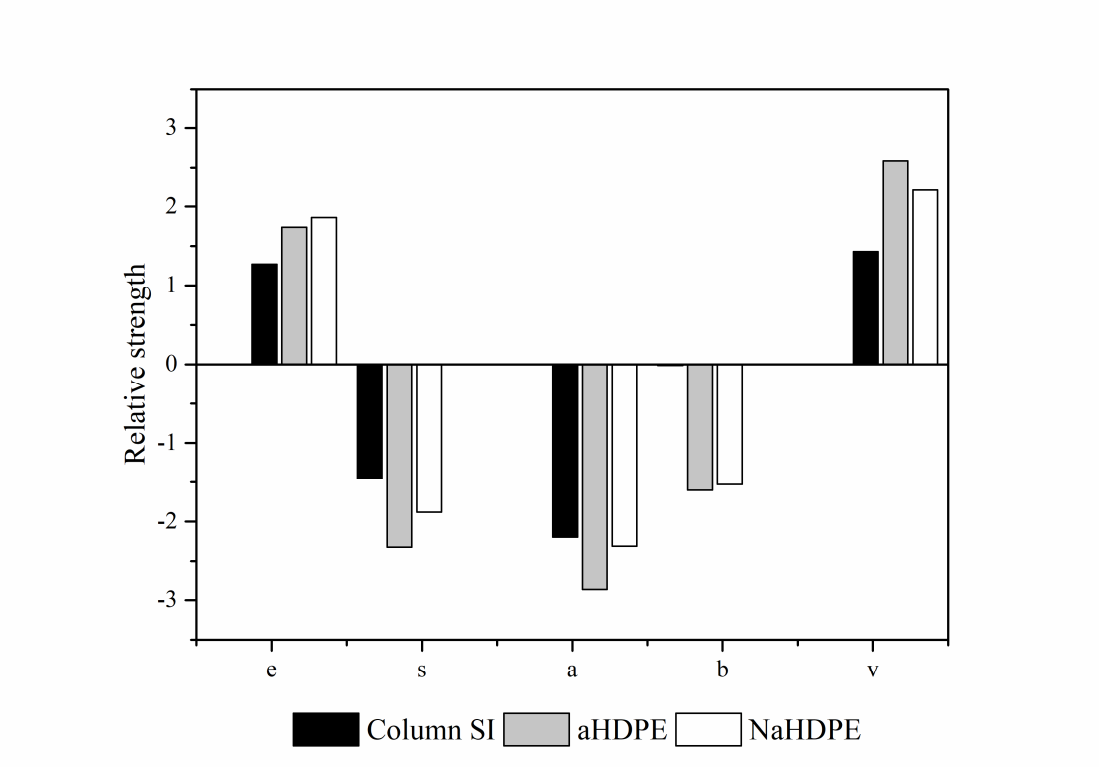

Figure 5-3 - Influence of the HDPE degradation and variation of the mobile phase for e, s, a, b and v.

Interestingly the major difference can only be seen for the H-bond basicity (b) and not the H-bond acidity (a). As previous studies have shown, this difference can be an indicator for the compensation of inaccurate vV terms [24]. To clearly determine the reason for the higher HDPE bB term than the aHDPE bB term, multiple experiments would be necessary and would be beyond the scope of this study. The other big difference in intermolecular interactions can be observed for the v descriptor, representing open volume in either phase. As mentioned above, aging increases the surface area which does counteract for at least the nonpolar compounds the accessibility for sorption sites. In previous studies [22] the molar volume was shown to have a big impact on sorption.

The investigation of the change in molecular interactions from aging affecting sorption will need further investigations with a larger data set, in particular comprising more compounds with a larger variety of functional groups. The data suggest that the UV-B induced aging reduces the amount of sorption sites for certain compounds.

5.5 References

[1] D. Lithner, Å. Larsson, and G. Dave, "Environmental and health hazard ranking and assessment of plastic polymers based on chemical composition," *Sci. Total Environ.*, vol. 409, no. 18, pp. 3309–3324, 2011.

[2] C. G. Avio, S. Gorbi, and F. Regoli, "Plastics and microplastics in the oceans: From emerging pollutants to emerged threat," *Mar. Environ. Res.*, vol. 128, pp. 2–11, 2017.

[3] A. A. Kadam, T. Karbowiak, A. Voilley, and F. Debeaufort, "Techniques to measure sorption and migration between small molecules and packaging. A critical review," *J. Sci. Food Agric.*, vol. 95, no. 7, pp. 1395–1407, 2015.

[4] C. Wu, K. Zhang, X. Huang, and J. Liu, "Sorption of pharmaceuticals and personal care products to polyethylene debris," *Environ. Sci. Pollut. Res.*, vol. 23, no. 9, pp. 8819–8826, 2016.

[5] S. Endo, S. E. Hale, K.-U. Goss, and H. P. H. Arp, "Equilibrium partition coefficients of diverse polar and nonpolar organic compounds to polyoxymethylene (POM) passive sampling devices.," *Environ. Sci. Technol.*, vol. 45, no. 23, pp. 10124–32, Dec. 2011.

[6] S. J. Hayward, Y. D. Lei, and F. Wania, "Sorption of a diverse set of organic chemical vapors onto XAD-2 resin: Measurement, prediction and implications for air sampling," *Atmos. Environ.*, vol. 45, no. 2, pp. 296–302, 2011.

[7] A. D. Redman, J. D. Butler, D. J. Letinski, D. M. Di Toro, M. Leon Paumen, and T. F. Parkerton, "Technical basis for using passive sampling as a biomimetic extraction procedure to assess bioavailability and predict toxicity of petroleum substances," *Chemosphere*, vol. 199, pp. 585–594, 2018.

[8] T. Hüffer and T. Hofmann, "Sorption of non-polar organic compounds by micro-sized plastic particles in aqueous solution.," *Environ. Pollut.*, vol. 214, no. 1, pp. 194–201, Apr. 2016.

[9] A. a Koelmans, E. Besseling, A. Wegner, and E. M. Foekema, "Plastic as a carrier of POPs to aquatic organisms: a model analysis.," *Environ. Sci. Technol.*, vol. 47, no. 14, pp. 7812–20, Jul. 2013.

[10] O. Setälä, V. Fleming-Lehtinen, and M. Lehtiniemi, "Ingestion and transfer of microplastics in the planktonic food web," *Environ. Pollut.*, vol. 185, pp. 77–83, 2014.

[11] H. Lee, W. J. Shim, and J.-H. Kwon, "Sorption capacity of plastic debris for hydrophobic organic chemicals.," *Sci. Total Environ.*, vol. 470–471, pp. 1545–52, Feb. 2014.

[12] R. Borrelli *et al.*, "Performance of passive sampling with low-density polyethylene membranes for the estimation of freely dissolved DDx concentrations in lake environments," *Chemosphere*, vol. 200, pp. 227–236, 2018.

[13] I. J. Allan, A. Ruus, M. T. Schaanning, K. J. Macrae, and K. Næs, "Measuring nonpolar organic contaminant partitioning in three Norwegian sediments using polyethylene passive samplers," *Sci. Total Environ.*, vol. 423, pp. 125–131, 2012.

[14] PlasticsEurope, "Plastic - the Facts 2016," p. 38, 2016.

[15] J. G. B. Derraik, H. Sciences, and N. Zealand, "The pollution of the marine environment by plastic debris: A review," *Mar. Pollut. Bull.*, vol. 44, no. 9, pp. 842–852, 2002.

[16] O. M. Lönnstedt and P. Eklöv, "Environmentally relevant concentrations of microplastic particles influence larval fish ecology," *Science (80-.).*, vol. 352, no. 6290, p. 1213 LP-1216, Jun. 2016.

[17] W. C. Li, H. F. Tse, and L. Fok, "Plastic waste in the marine environment: A review of sources, occurrence and effects," *Sci. Total Environ.*, vol. 566–567, pp. 333–349, 2016.

[18] J. R. Jambeck *et al.*, "Plastic waste inputs from land into the ocean," *Science (80-.).*, vol. 347, no. 6223, p. 768 LP-771, Feb. 2015.

[19] C. M. Rochman, M. A. Browne, A. J. Underwood, J. A. van Franeker, R. C. Thompson, and L. A. Amaral-Zettler, "The ecological impacts of marine debris: unraveling the demonstrated evidence from what is perceived," *Ecology*, vol. 97, no. 2, pp. 302–312, 2016.

[20] C. M. Rochman, B. T. Hentschel, and S. J. The, "Long-term sorption of metals is similar among plastic types: Implications for plastic debris in aquatic environments," *PLoS One*, vol. 9, no. 1, 2014.

[21] A. L. Andrady and M. a Neal, "Applications and societal benefits of plastics.," *Philos. Trans. R. Soc. Lond. B. Biol. Sci.*, vol. 364, no. 1526, pp. 1977–84, Jul. 2009.

[22] T. H. Uber, T. Hüffer, S. Planitz, and T. C. Schmidt, "Characterization of sorption properties of high- density Polyethylene sheets using the poly-parameter linear-free energy relationships," *Environ. Pollut.*, vol. 248, no. C, pp. 312–319, 2019.

[23] T. Hüffer, S. Endo, F. Metzelder, S. Schroth, and T. C. Schmidt, "Prediction of sorption of aromatic and aliphatic organic compounds by carbon nanotubes using poly-parameter linear free-energy relationships.," *Water Res.*, vol. 59, no. 1, pp. 295–303, 2014.

[24] A. Stenzel, K. Goss, and S. Endo, "Determination of Polyparameter Linear Free Energy Relationship (pp-LFER) Substance Descriptors for Established and Alternative Flame Retardants," *Environ. Sci. Technol.*, vol. 47, pp. 1399–1406, 2013.

[25] R. P. Schwarzenbach, P. M. Gschwend, and D. M. Imboden, *Environmental Organic Chemistry*, 2nd ed., no. 2. John Wiley & Sons Inc., Hoboken, New Jersey, 2003.

[26] P. Yla-Maihaniemi and D. R. Williams, "Novel inverse liquid chromatography detector configuration for studying solid-liquid adsorption.," *J. Chromatogr. A*, vol. 1138, no. 1–2, pp. 95–100, Jan. 2007.

[27] E. Bi, T. C. Schmidt, and S. B. Haderlein, "Practical issues relating to soil column chromatography for sorption parameter determination.," *Chemosphere*, vol. 80, no. 7, pp. 787–93, Aug. 2010.

[28] M. H. Abraham, C. F. Poole, and S. K. Poole, "Classification of stationary phases and other materials by gas chromatography," *J. Chromatogr. A*, vol. 842, no. 1–2, pp. 79–114, May 1999.

[29] R. I. Hadj and D. R. P., "Polymer-solvent diffusion and equilibrium parameters by inverse gas-liquid chromatography," *AIChE J.*, vol. 39, no. 4, pp. 625–635, Jul. 2018.

[30] E. Bi, T. C. Schmidt, and S. B. Haderlein, "Sorption of Heterocyclic Organic Compounds to Reference Soils: Column Studies for Process Identification," *Environ. Sci. Technol.*, vol. 40, no. 19, pp. 5962–5970, Oct. 2006.

[31] S. Altfelder, T. Streck, M. A. Maraqac, and T. C. Voiced, "Nonequilibrium Sorption of Dimethylphthalate—Compatibility of Batch and Column Techniques," *Soil Sci. Soc. Am. J.*, vol. 65, no. 1, pp. 102–111, 2001.

[32] E. Bi, T. C. Schmidt, and S. B. Haderlein, "Environmental factors influencing sorption of heterocyclic aromatic compounds to soil," *Env. Sci Technol*, vol. 41, no. 9, pp. 3172–3178, 2007.

[33] T. Hüffer, F. Metzelder, G. Sigmund, S. Slawek, T. C. Schmidt, and T. Hofmann, "Polyethylene microplastics influence the transport of organic contaminants in soil," *Sci. Total Environ.*, vol. 20, no. 657, pp. 242–247, 2019.

[34] B. T. Mader, K. Uwe-Goss, and S. J. Eisenreich, "Sorption of nonionic, hydrophobic organic chemicals to mineral surfaces," *Environ. Sci. Technol.*, vol. 31, no. 4, pp. 1079–1086, 1997.

[35] F. Metzelder and T. C. Schmidt, "Environmental Conditions Influencing Sorption of Inorganic Anions to Multiwalled Carbon Nanotubes Studied by Column Chromatography," *Environ. Sci. Technol.*, vol. 51, no. 9, pp. 4928–4935, 2017.

[36] F. Metzelder, M. Funck, and T. C. Schmidt, "Sorption of Heterocyclic Organic Compounds to Multiwalled Carbon Nanotubes," *Environ. Sci. Technol.*, vol. 52, no. 2, pp. 628–637, Jan. 2018.

[37] A. Voelkel, B. Strzemiecka, K. Adamska, and K. Milczewska, "Inverse gas chromatography as a source of physiochemical data," *J. Chromatogr. A*, vol. 1216, no. 10, pp. 1551–1566, 2009.

[38] D. Eerkes-Medrano, R. C. Thompson, and D. C. Aldridge, "Microplastics in freshwater systems: A review of the emerging threats, identification of knowledge gaps and prioritisation of research needs," *Water Res.*, vol. 75, pp. 63–82, 2015.

[39] J. Sangster, *Octanol-water partition coefficients : fundamentals and physical chemistry*. Chichester: Wiley, 1997.

[40] R. J. Young and P. A. Lovell, *Introduction to Polymers*, 3rd ed. CRC Press, 2011.

[41] A. Bhattarai, "Determination of the medium molar mass of sodium polystyrenesulphonate from viscosity measurement," *Sci. World*, vol. 10, no. 10, pp. 17–19, 2012.

[42] C. Fesch, W. Simon, S. B. Haderlein, P. Reichert*, and R. P. Schwarzenbach, "Nonlinear sorption and nonequilibrium solute transport in aggregated porous media: Experiments, process identification and modeling," *J. Contam. Hydrol.*, vol. 31, no. 3, pp. 373–407, 1998.

[43] N. Dyson, *Chromatographic Integration Methods*. The Royal Society of Chemistry, 1998.

[44] S. Droge and K. U. Goss, "Effect of sodium and calcium cations on the ion-exchange affinity of organic cations for soil organic matter," *Environ. Sci. Technol.*, vol. 46, no. 11, pp. 5894–5901, 2012.

[45] J. Schenzel, K. U. Goss, R. P. Schwarzenbach, T. D. Bucheli, and S. T. J. Droge, "Experimentally determined soil organic matter-water sorption coefficients for different classes of natural toxins and comparison with estimated numbers," *Environ. Sci. Technol.*, vol. 46, no. 11, pp. 6118–6126, 2012.

[46] B. Li, Y. Qian, E. Bi, H. Chen, and T. C. Schmidt, "Sorption behavior of phthalic acid esters on reference soils evaluated by soil column chromatography," *Clean - Soil, Air, Water*, vol. 38, no. 5–6, pp. 425–429, 2010.

[47] E. Baur, S. Brinkmann, T. A. Osswald, and E. Schmachtenberg, *Saechtling Kunststoff Taschenbuch*, 29th ed. Carl Hanser Verlag GmbH & Co. KG, 2004.

[48] J. Chmelař, K. Haškovcová, M. Podivinská, and J. Kosek, "Equilibrium Sorption of Propane and 1-Hexene in Polyethylene: Experiments and Perturbed-Chain Statistical Associating Fluid Theory Simulations," *Ind. Eng. Chem. Res.*, vol. 56, no. 23, pp. 6820–

6826, 2017.

[49] M. L. Brusseau, P. S. C. Rao, R. E. Jessup, and J. M. Davidson, "Flow interruption: A method for investigating sorption nonequilibrium," *J. Contam. Hydrol.*, vol. 4, no. 3, pp. 223–240, 1989.

[50] J. Sohma, "Mechanochemical Degradation," *Compr. Polym. Sci. Suppl.*, pp. 621–644, Jan. 1989.

[51] J. R. MacCallum, "Photodegradation," *Compr. Polym. Sci. Suppl.*, pp. 529–537, Jan. 1989.

[52] E. Yousif and R. Haddad, "Photodegradation and photostabilization of polymers, especially polystyrene: Review," *Springerplus*, vol. 2, no. 1, pp. 1–32, 2013.

[53] A. Martínez-Romo, R. González-Mota, J. J. Soto-Bernal, and I. Rosales-Candelas, "Investigating the Degradability of HDPE, LDPE, PE-BIO, and PE-OXO Films under UV-B Radiation," *J. Spectrosc.*, vol. 2015, no. November, 2015.

[54] J. M. Fischer and J. M. Fischer, "Causes of Molded Part Variation: Processing," *Handb. Molded Part Shrinkage Warpage*, pp. 81–98, Jan. 2013.

[55] J. S. Fabiyi and A. G. McDonald, "Degradation of polypropylene in naturally and artificially weathered plastic matrix composites," *Maderas. Cienc. y Tecnol.*, vol. 16, no. ahead, pp. 0–0, 2014.

[56] J. S. Fabiyi, A. G. McDonald, and D. McIlroy, "Wood Modification Effects on Weathering of HDPE-Based Wood Plastic Composites," *J. Polym. Environ.*, vol. 17, no. 1, pp. 34–48, 2009.

[57] T. Hüffer, A. K. Weniger, and T. Hofmann, "Sorption of organic compounds by aged polystyrene microplastic particles," *Environ. Pollut.*, vol. 236, pp. 474-4218–225, 2018.

[58] A. S. Maxwell, W. R. Broughton, G. D. Dean, and G. D. Sims, *Review of Accelerated Ageing Methods and Lifetime Prediction Techniques for Polymeric Materials*. National Physical Laboratory, 2005.

[59] T. Hüffer, A. K. Weniger, and T. Hofmann, "Data on sorption of organic compounds by aged polystyrene microplastic particles," *Data Br.*, vol. 18, pp. 474–479, 2018.

[60] T. Hüffer, M. Kah, T. Hofmann, and T. C. Schmidt, "How Redox Conditions and Irradiation A ff ect Sorption of PAHs by Dispersed Fullerenes (nC60)," *Environ. Sci. Technol.*, vol. 47, no. 13, pp. 6935–6942, 2013.

[61] B. Pan and B. Xing, "Adsorption mechanisms of organic chemicals on carbon nanotubes," *Environ. Sci. Technol.*, vol. 42, no. 24, pp. 9005–9013, 2008.

[62] D. Zhu, S. Kwon, and J. J. Pignatello, "Adsorption of single-ring organic compounds to wood charcoals prepared under different thermochemical conditions," *Environ. Sci. Technol.*, vol. 39, no. 11, pp. 3990–3998, 2005.

[63] E. A. Müller and K. E. Gubbins, "Molecular simulation study of hydrophilic and hydrophobic behavior of activated carbon surfaces," *Carbon N. Y.*, vol. 36, no. 10, pp. 1433–1438, 1998.

[64] F. J. Millero, R. Feistel, D. G. Wright, and T. J. McDougall, "The composition of Standard Seawater and the definition of the Reference-Composition Salinity Scale," *Deep Sea Res. Part I Oceanogr. Res. Pap.*, vol. 55, no. 1, pp. 50–72, 2008.

[65] E. Pérez and Y. Chebude, "Chemical Analysis of Gaet'ale, a Hypersaline Pond in Danakil Depression (Ethiopia): New Record for the Most Saline Water Body on Earth,"

Aquat. Geochemistry, vol. 23, no. 2, pp. 109–117, 2017.

[66] S. Endo, A. Pfennigsdorff, and K.-U. Goss, "Salting-Out Effect in Aqueous NaCl Solutions Increases with Size and Decreases with Polarities of Solute Molecule," *Environ. Sci. Technol.*, vol. 46, no. 3, pp. 1496–1503, 2012.

[67] M. H. Abraham, A. Ibrahim, and A. M. Zissimos, "Determination of sets of solute descriptors from chromatographic measurements," *J. Chromatogr. A*, vol. 1037, no. 1–2, pp. 29–47, May 2004.

[68] K. Adamska, K. Kadlec, and A. Voelkel, "Application of Inverse Liquid Chromatography for Surface Characterization of Biomaterials," *Chromatographia*, vol. 79, no. 7–8, pp. 473–480, 2016.

[69] C. F. Poole and S. K. Poole, "Column selectivity from the perspective of the solvation parameter model," *J. Chromatogr. A*, vol. 965, no. 1–2, pp. 263–299, Aug. 2002.

5.6 Appendix

A5-S1 Experimental procedures

Experimental procedures were mainly adapted from literature.[1–3] The experiments were run on a Dionex UltiMate 3000 UHPLC System. It contained an UltiMate 3000 RS Pump with a degasser, an UltiMate 3000 RS Autosampler, an UltiMate 3000 RS column heater and an UltiMate 3000 RS diode array detector.

A5-S2 Procedure to determine the medium molar mass of a polymer

The medium molecular weight (MMW) was determined with the help of a viscometer by Ubbelohde as seen in Figure A5-1 and the Staudinger approach [4].

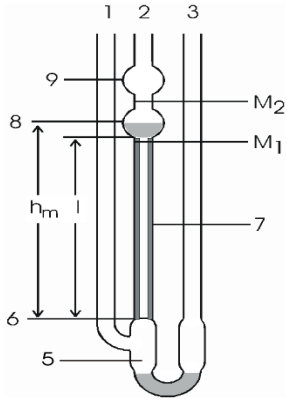

Figure A5-1- A schematic drawing of a Ubbelohde viscometer.

The viscometer consists of three glass pipes (1,2 and 3), a level container (5), a capillary (7) and a measuring bowl (8) with a pre-bowl (9). The bowl has two marks (M_1 and M_2) and the distance between 6 and 8 is h_m. The procedure to determine the viscosity (η) followed the one described in the literature [5]. In short, the pressure drop during a constant laminar flow is monitored within a capillary.

Having the viscosity of a polymer, the MMW can then be calculated following the Mark-Kuhn-Houwink-Sakurada equation [6].

$$\eta = K * M^a \quad \eta = K \cdot M^a$$

(Eq. A5-1)

There, M is the medium molar mass, K and *a* are empirical parameters.

Table A5-1 - Probe compounds used in this study and their corresponding ppLFER descriptors*.

Compound	Abb.	log $K_{o/w}$	E	S	A	B	V	L
1,2-Dichlorobenzene	12DCB	3.43	0.87	0.78	0.00	0.04	0.96	4.32
1-Hexene	1Hex	3.29	0.08	0.08	0.00	0.07	0.91	2.57
2-Chlorophenol	2CP	1.93	0.85	0.88	0.32	0.31	0.90	4.18
2-Nonanone	Non2on	3.01	0.12	0.68	0.00	0.51	1.39	4.74
2-Octanone	Oct2on	2.43	0.11	0.68	0.00	0.51	1.25	4.26
Acetonitrile	ACN	-0.35	0.24	0.90	0.07	0.32	0.40	1.74
Acetophenone	AP	1.58	0.82	1.01	0.00	0.48	1.01	4.50
Ascorbic acid	Aa	-1.66	1.40	1.60	0.58	1.48	1.11	6.48
Atrazine	Atz	1.77	1.22	1.29	0.17	1.01	1.62	7.78
Atropine	Atp	1.2	1.20	1.58	0.26	1.73	2.28	10.20
Benezoic acid	Ba	1.83	0.73	0.90	0.59	0.40	0.93	4.66
Benzaldehyde	Benzal	1.41	0.82	1.00	0.00	0.39	0.87	4.01
Benzene	Benz	2.17	0.61	0.52	0.00	0.04	0.72	2.79
Benzil	Bzi	3.18	1.45	1.59	0.00	0.62	1.64	7.61
Benzo[b]furan	BbF	2.67	0.89	0.83	0.00	0.15	0.91	-
Caffein	Caf	-0.06	1.50	1.82	0.08	1.25	1.36	7.84
Camphor	Cph	2.28	0.51	0.83	0.00	0.67	1.32	5.04
Cyclooctene	cOcte	4.04	0.46	0.24	0.00	0.10	1.08	4.12
Fluorene	Flu	4.23	1.66	1.10	0.00	0.26	1.36	6.95
Glucose	Glu	-2.59	1.34	1.70	1.14	1.80	1.20	6.97
Glutaraldehyde	Glut	-0.18	0.43	1.10	0.00	0.74	0.84	3.60
Linalool	Lin	2.87	0.39	0.48	0.24	0.75	1.49	4.80
Methyl phenyl ether	MPE	2.16	0.71	0.75	0.00	0.29	0.92	3.89
Methyl tert-butyl ether	MTBE	0.94	0.02	0.28	0.00	0.54	0.87	2.27
Methylamine	Ma	-0.78	0.25	0.35	0.16	0.58	0.35	1.30
Nerol	Ner	3.47	0.50	0.61	0.27	0.66	1.49	5.37
n-Propylbenzene	nPb	3.69	0.60	0.50	0.00	0.15	1.14	4.23
o-Xylene	oXy	3.1	0.66	0.56	0.00	0.16	1.00	3.94
Phenolphthalein	Ppl	2.41	0.61	0.52	0.00	0.16	1.00	3.84
p-Xylene	pXy	3.15	0.61	0.52	0.00	0.16	1.00	3.84
Styrene	Sty	3.05	0.85	0.65	0.00	0.16	0.96	3.86
Triethylamine	Tea	1.25	0.10	0.15	0.00	0.79	1.05	3.04

Abb.: Abbreviation of compound name; log $K_{o/w}$: logarithmic n-octanol/water partitioning constant; E: excess molar refraction; S: bipolarity/polarizability; A: solute hydrogen-bond acidity; B: solute hydrogen-bond basicity; V: characteristic McGowan volume; L: logarithmic hexadecane/air partition coefficient. * all properties were taken from literature [7].

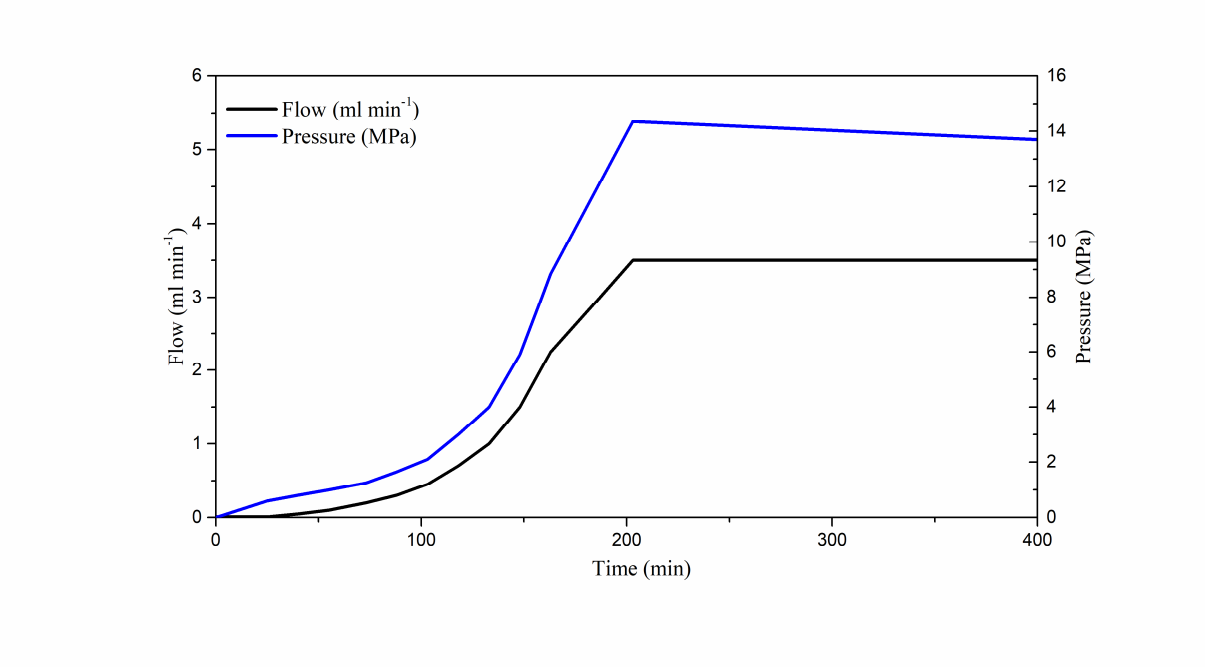

Figure A5-2 - Flow gradient for the packing procedure of the ILC columns, with the column head pressure added for column 1.

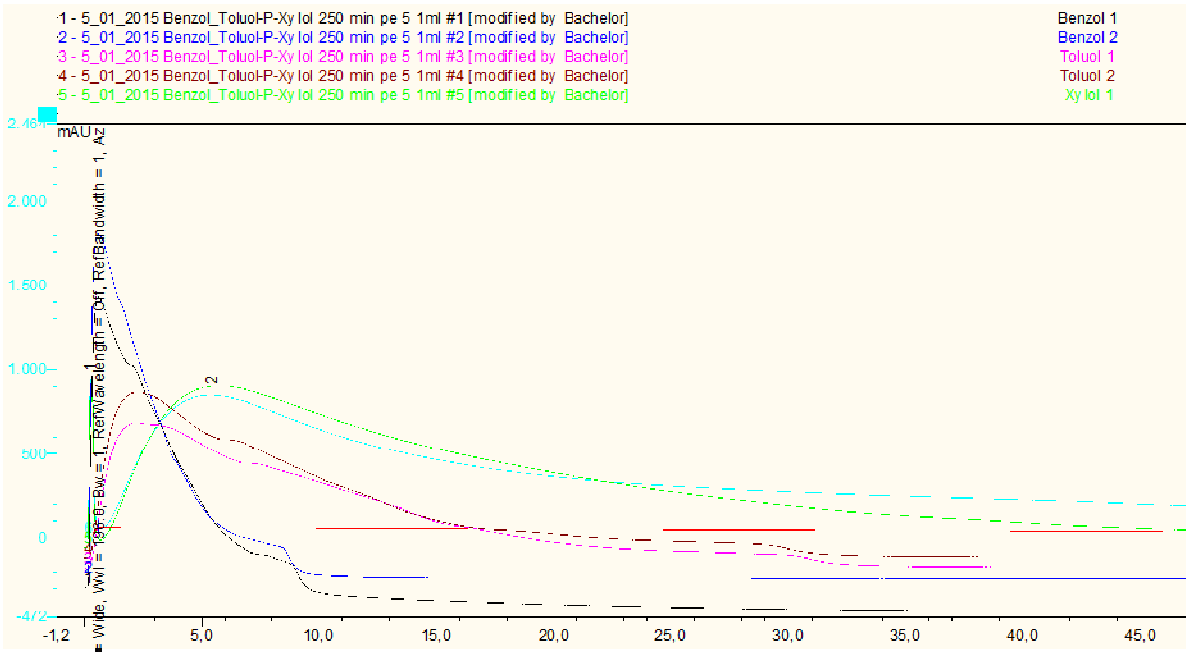

Figure A5-3 - Duplicate injections of benzene (back and blue), toluene (pink and brown) und p-xylene (green and cyan) on the column with HDPE particle sizes < 48 µm.

Table A5-2 – Linear fit results from the correlation of R_f vs flow (mL min^{-1})

Compound		Value	SE	Prob>t	log Rf_I
Benz	b	0.385	0.071	< 0.05	0.264
	m	-0.046	0.053	0.43	
pXy	b	1.949	0.022	< 0.05	1.858
	m	-0.115	0.016	< 0.05	
nPb	b	2.934	0.071	< 0.05	2.517
	m	-0.507	0.054	< 0.05	

SE: standard error of the respective fitting value; b: the intercept of the linear fit; m: the slope of the linear fit; log Rf_I:logarithmic retention factor at a flow of 1 mL min^{-1}.

Table A5-3 - Determined relevant parameters of the packed columns by D_2O injections.

Column abbreviation	Length (cm)	Diameter (cm)	Travel Time (min)	Pore volume (mL)	Porosity (-)	Bulk density (kg L^{-1})
Column SI	1.4	0.3	0.16	0.07	0.73	1.33
Column SII	3.0	0.3	0.18	0.09	0.42	1.36
Column SIII	5.5	0.3	0.18	0.09	0.23	1.12
aHDPE	1.4	0.3	0.16	0.07	0.71	1.35
NaHDPE	1.4	0.3	0.16	0.07	0.71	1.35

A5 S3 Sorption Enthalpy

The enthalpy change (ΔH) was calculated using the van't Hoff equation incorporating the slope of the regression line in Figure A5-4. The ΔH was calculated then following the following equation:

$$\ln K_{p/w} = \Delta S\ R_{const}^{-1} - \Delta H\ R_{const}^{-1}\ T^{-1} \qquad \text{(Eq. A5-2)}$$

Where ΔH is the enthalpy change (kJ mol^{-1}), R_{const}^{-1} is the gas constant (8.3145 x 10^{-3} kJ mol^{-1} K^{-1}), ΔS is the entropy change (kJ mol^{-1} K^{-1}) and T the temperature (K). The approach was previously applied to ILC data [8].

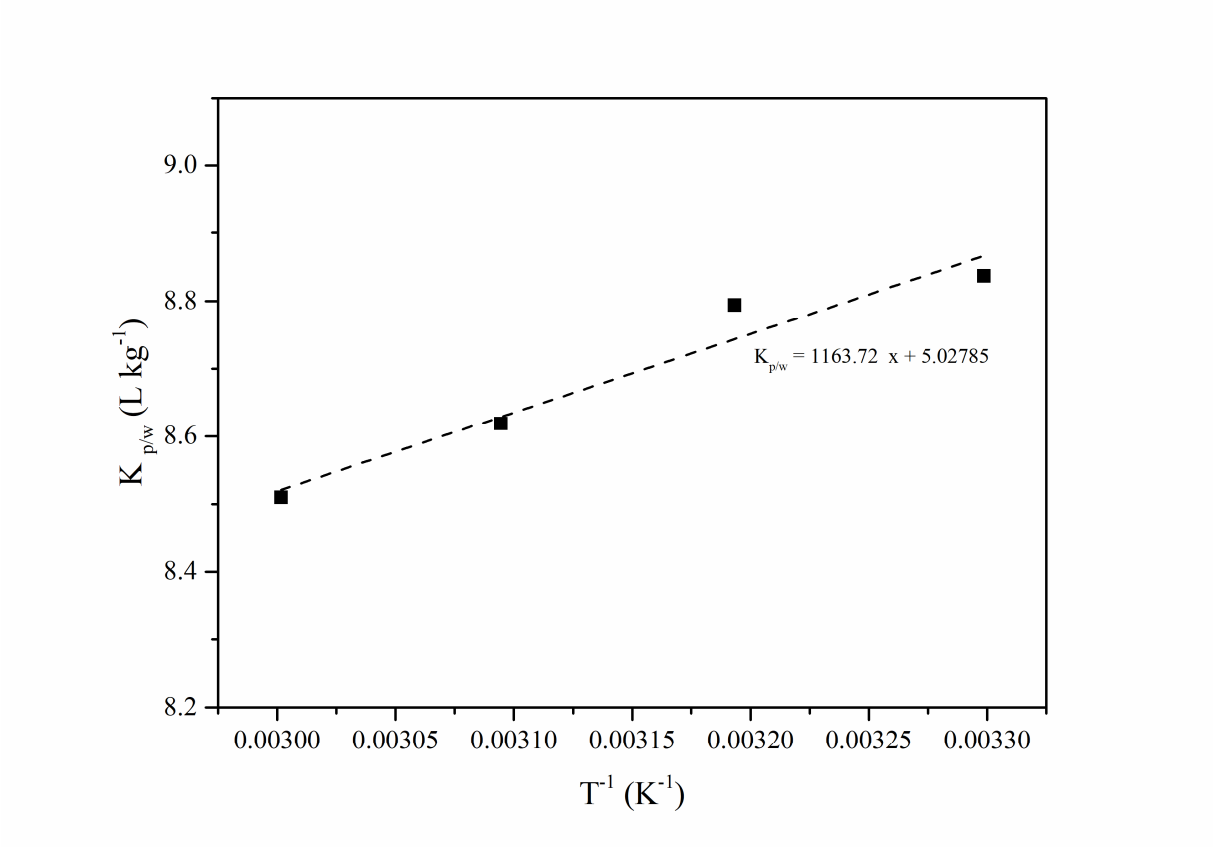

Figure A5-4 - Determined $K_{p/w}$ values of nPb plotted against the reciprocal temperature.

Table A5-4 - Results from aHDPE ILC experiments.

Compound	Rt (min)	log $K_{p/w}$
Oct2on	0.465	1.0
Benz	0.464	1.0
pXy	5.458	2.03
n-PB	18.059	2.54
Sty	4.090	1.91
2Cp	0.157	0.61
Atp	0.293	0.82
Benzal	0.170	0.63
MTBE	0.293	0.82
Nerol	0.262	0.78

t_R: retention time; log $K_{p/w}$: logarithmic distribution coefficient between HDPE and water [L kg^{-1}].

Table A5-5 - Experimental results for the complete dataset using different column lengths and chromatographic conditions.

	Column SI			Column SII			Column SIII			aHDPE			NaHDPE		
Substance	t_R	Rf	log $K_{p/w}$	t_R	Rf	log $K_{p/w}$	t_R	Rf	log $K_{p/w}$	t_R	Rf	log $K_{p/w}$	t_R	Rf	log $K_{p/w}$
Oct2on	0.3	3.5	1.8	0.5	4.9	1.9	0.7	6.6	1.9	0.5	5.4	2.0	0.3	2.8	1.7
Benz	0.3	3.5	1.8	0.5	5.1	1.9	0.7	6.8	1.9	0.5	5.3	2.0	0.4	3.9	1.9
pXy	4.7	63.8	3.1	4.9	54.1	2.9	5.0	54.5	2.8	5.5	76.9	3.2	3.2	43.4	2.9
nPb	19.1	264.6	3.7	23.1	260.6	3.6	24.2	267.9	3.5	18.1	257.4	3.7	10.1	140.7	3.4
cOcte	0.4	4.5	1.9	0.5	5.1	1.9	0.7	6.6	1.9						
1Hex	0.4	4.8	2.0	0.6	5.3	1.9	0.7	6.2	1.9						
Styr	2.0	25.8	2.7	2.1	23.0	2.5	2.3	24.2	2.5	4.1	57.3	3.0	3.8	52.5	3.0
Atz [a]	4.7	63.6	3.1	4.9	54.0	2.9	5.0	54.4	2.8						
12DCB	0.2	2.1	1.6	0.4	3.6	1.8	0.5	4.8	1.8						
MPE	0.7	8.3	2.2	0.9	9.0	2.1	1.0	10.3	2.1						
Phen[b]	0.6	6.5	2.1	0.8	7.6	2.1	0.9	8.7	2.0						
AP	0.3	3.5	1.8	0.5	5.1	1.9	0.7	6.4	1.9						
2CP	0.2	2.1	1.6	0.4	3.8	1.8	0.6	5.2	1.8	0.2	0.9	1.3	0.2	1.7	1.5
Bbf	0.2	2.0	1.6	0.5	4.2	1.8	0.5	4.9	1.8						
TEA	1.3	17.4	2.5	1.5	16.4	2.4	1.7	17.4	2.3						
Benzal	13.5	186.8	3.5	13.7	153.9	3.4	13.8	152.4	3.3	0.2	1.1	1.4	0.2	1.7	1.5
oXy	0.2	1.7	1.5	0.4	3.7	1.8	0.5	4.9	1.8						
ACN	18.5	256.0	3.7	20.4	229.9	3.5	20.5	227.2	3.5						
MTBE	2.2	28.9	2.7	2.4	25.7	2.6	2.5	26.6	2.5	0.3	2.9	1.8	0.2	1.5	1.5

Atp [c]	6.6	90.2	3.2	6.8	75.7	3.1	6.9	75.6	3.0	0.3	2.9	1.8	0.4	3.8	1.9
Caf	0.7	8.2	2.2	0.9	8.9	2.1	1.0	10.2	2.1						
Cph	58.2	807.7	4.2	58.3	658.5	4.0	58.5	649.0	3.9						
Ba	3.0	40.9	2.9	3.2	35.5	2.7	3.3	36.2	2.7						
Bzi	8.6	118.2	3.3	8.7	97.4	3.2	8.8	97.0	3.1						
Flu	0.9	11.3	2.3	1.1	11.2	2.2	1.2	12.3	2.2						
Glu	57.4	796.9	4.2	57.7	651.4	4.0	57.8	641.1	3.9						
Aa	52.1	722.8	4.1	52.3	590.2	4.0	52.4	581.1	3.9						
Ma	0.2	2.0	1.6	0.4	3.8	1.8	0.5	5.1	1.8						
Non2on	0.4	3.9	1.9	0.6	5.5	1.9	0.7	6.3	1.9						
Linalool	9.2	127.2	3.4	9.4	105.7	3.2	9.6	105.2	3.1						
Ner	19.4	267.9	3.7	19.7	222.1	3.5	20.3	224.1	3.4	0.3	2.5	1.7	0.2	2.1	1.6
Glut	2.1	28.3	2.7	2.4	26.2	2.6	2.4	26.1	2.5						

t_R: Retention time in minutes; Rf: Retention factor; log $K_{p/w}$: Logarithmic HDPE-water distribution coefficient; [a] 100 µg mL^{-1} in acetone; [b] 1% solution in ethanol; [c] 50 mg L^{-1} solution.

A5 S4 Statistics on ppLFER modelling

Table A5-6 - Calculated parameters for the ppLFER of Column SI.

	Coefficient	SE	p-value
c	1.61	1.41	0.32
e	1.27	1.91	0.54
s	-1.45	2.74	0.62
a	-2.20	2.20	0.37
b	-0.01	2.20	0.99
v	1.43	1.72	0.45

Table A5-7 - ANOVA results for the ppLFER of Column SI.

	DF	Sum of Squares	Mean Square	F-Value	Prob>F
Model	5	2.13097	0.42619	0.46437	0.78895
Error	4	3.6712	0.9178		
Total	9	5.80218			

Table A5-8 - Calculated parameters for the ppLFER of the aHDPE Column.

	Coefficient	SE	p-value
c	0.83	0.64	0.26
e	1.74	0.87	0.12
s	-2.32	1.24	0.13
a	-2.87	0.99	< 0.05
b	-1.60	1.00	0.18
v	2.58	0.78	< 0.05

Table A5-9 - ANOVA results for the ppLFER of the aHDPE Column.

	DF	Sum of Squares	Mean Square	F-Value	Prob>F
Model	5	5.41334	1.08267	5.75341	0.05742
Error	4	0.75271	0.18818		
Total	9	6.16606			

Table A5-10 - Calculated parameters for the ppLFER of the NaHDPE Column.

	Coefficient	SE	p-value
c	0.69	0.58	0.30
e	1.86	0.79	< 0.05
s	-1.88	1.13	0.17
a	-2.31	0.91	0.06
b	-1.53	0.91	0.17
v	2.22	0.71	< 0.05

Table A5-11 - ANOVA results for the ppLFER of the NaHDPE Column.

	DF	Sum of Squares	Mean Square	F-Value	Prob>F
Model	5	4.17933	0.83587	5.3106	0.06542
Error	4	0.62958	0.1574		
Total	9	4.80891			

References

[1] C. Fesch, W. Simon, S. B. Haderlein, P. Reichert*, and R. P. Schwarzenbach, "Nonlinear sorption and nonequilibrium solute transport in aggregated porous media: Experiments, process identification and modeling," *J. Contam. Hydrol.*, vol. 31, no. 3, pp. 373–407, 1998.

[2] E. Bi, T. C. Schmidt, and S. B. Haderlein, "Practical issues relating to soil column chromatography for sorption parameter determination.," *Chemosphere*, vol. 80, no. 7, pp. 787–93, Aug. 2010.

[3] F. Metzelder and T. C. Schmidt, "Environmental Conditions Influencing Sorption of Inorganic Anions to Multiwalled Carbon Nanotubes Studied by Column Chromatography," *Environ. Sci. Technol.*, vol. 51, no. 9, pp. 4928–4935, 2017.

[4] K. Kamide and T. Dobashi, *Physical Chemistry of Poylmer Solutions*, 1st ed. Elsevier Science, 2000.

[5] R. J. Young and P. A. Lovell, *Introduction to Polymers*, 3rd ed. CRC Press, 2011.

[6] A. Bhattarai, "Determination of the medium molar mass of sodium polystyrenesulphonate from viscosity measurement," *Sci. World*, vol. 10, no. 10, pp. 17–19, 2012.

[7] S. Endo, N. Watanabe, N. Ulrich, G. Bronner, and K.-U. Goss, "UFZ-LSER database v 2.1," *Leipzig, Germany, Helmholtz Centre for Environmental Research-UFZ. 2015*. [Online]. Available: https://www.ufz.de/index.php?en=31698&contentonly=1&lserd_data[mvc]=Public/start. [Accessed: 23-Dec-2015].

[8] F. Metzelder, M. Funck, and T. C. Schmidt, "Sorption of Heterocyclic Organic Compounds to Multiwalled Carbon Nanotubes," *Environ. Sci. Technol.*, vol. 52, no. 2, pp. 628–637, Jan. 2018.

Chapter 6 Conclusion and Outlook

6.1 General conclusions and Outlook

In this thesis, sorption properties of environmentally relevant plastic materials were successfully be determined, and an alternative methodology to determine sorption coefficients could be applied. As plastic materials have been substituting several conventional materials, like stone, glass or wood, their environmental impact is under an ongoing investigation [1, 2]. Especially the litter of plastic materials into the environment is of major concern and is being discussed even at the G7 states level [3]. An aspect into assessing their environmental impact is the investigation of the sorption behaviour for organic compounds. Sorption is not only relevant in the environment but also for several applications like passive-sampling devices, fresh water pipes or convenience products (i.e. cutlery). Therefore, a first step in this work was the examination of high-density polyethylene (HDPE, **Chapter 3**) and polystyrene (PS, **Chapter 4**) and their sorption behaviour in water, to enhance the knowledge on the environmental and technical behaviour, with regard to sorption of organic compounds. The initial assumption of linear sorption to HDPE [4] was disproved. In the observed concentration range, sorption was found to be non-linear and sorption isotherms were best fitted by the Freundlich model (FM). With this conclusion, the sorption mode for HDPE was found to be a combination of *ab*sorption and *ad*sorption, following the ratio of sorption coefficients of n-alkanes to cycloalkanes (K_n/K_c) suggested by Endo et. al [5]. Previous studies focused more on low-density polyethylene (LDPE) [6] and showed *ab*sorption to be the dominating sorption mode. The difference in crystallinity and density between HDPE and LDPE do therefore render differences in the sorption mode.

The developed HDPE ppLFER equations show that HDPE has no H-bond interactions in water. Negative A and B descriptors demonstrated the strong interactions of the organic compounds in water. Other descriptors like the HDPE molar volume in comparison with LDPE molar volume lead to the conclusion that sorption of PE is dependent on the plastics density and crystallinity [7], i.e. low density and low crystallinity leading to a higher sorption potential. It would suggest that non-polar amorphous plastic materials with a low density and low crystallinity have a higher potential for accumulation in water, than plastic materials with a high density and crystallinity [8]. The literature LDPE ppLFER [12] indicated a similar behaviour as the HDPE ppLFER, although showing differences like the molar volume, and shows that at least for similar plastic materials, in terms of monomeric unit, predictions are possible. Sorption behaviour of polypropylene (PP) might be more similar to the sorption of HDPE than LDPE,

due to their similar polymerization degree (chain branching) and monomeric unit [13]. Therefore, the HDPE ppLFER could easily be applied for PP.

As with HDPE, PS or Styrofoam, is another plastic material that is brittle but with a density close to HDPE and found in the aquatic environment. There it derives mostly from weathered insulation or in the form of cutlery and cups and the sorption properties of PS in water are of increasing interest [9–11]. Plastic materials like PS in general do not only have a high sorption affinity for hydrophobic, but also hydrophilic compounds as shown by the gathered ppLFER for PS. The ppLFER for PS rendered different descriptors, i.e. showing π-interactions, compared to the HDPE or LDPE ppLFER. This suggests that plastic materials with possible π-interactions like PS, in the aquatic environment will more likely sorb organic compounds due to the extra π-π- and η-π-interactions.

There are other mass production plastic materials that will need further investigations like polyethylene terephthalate (PET), polyvinylchloride (PVC) or polyacrylate (PA). Furthermore, material property changes caused by degradation through UV-B aging, mechanical abrasion or even biological degradation should be investigated [14]. To generate a large database of plastic materials, a fast and robust method to determine sorption for a large compound set is necessary.

A different experimental approach to **Chapter 3 and 4** was demonstrated in **Chapter 5** with the inverse-liquid chromatography (ILC), where environmentally relevant conditions, like salt content and lower contact times, could easily be accomplished. A similar approach was recently applied for multi-walled carbon nanotubes and LDPE [6, 15]. The column chromatography could successfully be used to investigate the sorption properties of HDPE in water with varying conditions. Data were compared with data generated in **Chapter 3,** which confirmed the robustness of the ILC approach. With the column chromatography, the influence of environmental conditions on sorption to HDPE could be observed.

HDPE material was degraded through UV-B light and distribution coefficients with aged HDPE rendered almost no change for non-polar compounds. Interestingly the sorption strength for more polar compounds decreased significantly, indicating the presence of oxygen-containing functional groups and water clusters on the HDPE surface [16]. For these compounds, there was almost no change in sorption strength of the aged HDPE material under pure water and salt water conditions and indicating a decreasing vector effect over time.

The **Chapters 3 and 4** demonstrated very well beneficial aspects of knowing the sorption behaviour of plastics in an aquatic environment. The derived sorption prerequisites for PS and PE (non-polarity and low density) demonstrated that i.e. PS will accumulate organic compounds in water to a higher degree than LDPE and HDPE. The big drawback though, is the significant amount of time and the consumption of material to determine the distribution. **Chapter 5** demonstrates therefore a faster but also effective approach to determine distribution in a dynamic system. Future research should focus on the determination of distribution in a variety of different sorption systems with changing conditions, i.e. changing the pH, contact time, temperature or anion and cation type. Deriving the sorption isotherm directly from the peak of the sorbate in the ILC chromatogram would allow for a fast determination of sorption isotherms. ILC could also be used for the fast comparison of different plastic materials (PET, PA, PP and PVC) for an efficient and fast development of new sorption phases. Therefore, ILC should be used more frequently in the future to generate a robust data base for partition estimation, since it only requires a classical HPLC system which is available in most laboratories. The fairly good availability and the potential for easy automation make it a useful research tool. Research for other materials than plastics is already focusing on this approach [17]. Especially with the ever-increasing distribution of plastic materials in the environment through other paths than disposal, e.g., degrading of car tires or cosmetic industry [18], generating fast and robust partition data is a key point. Within the next few years, the demand for sorption data on plastics will increase, since it is heavily discussed on a political level within the context of micro plastics [3, 19]. Recently, for example, a ban of plastic straws was initiated within the EU to decrease the amount of single-use plastic, and therefore decrease the possibility of environmental litter. With the latest project to remove plastic waste from the oceans, “Ocean Clean-up”, the public awareness for plastic materials and its dangers is rising [20]. The general idea there is, to remove the plastic litter from the great garbage patches in the world’s oceans. There are already recent studies investigating the amount of pollutants on plastic particles in the world’s gyres, suggesting a chemical risk to organisms [2]. Even large industrial companies are supporting projects like the Ocean Clean-up to remove plastic debris from the oceans and improve the overall quality of these [21].

This thesis made a valuable contribution to the understanding of the sorption properties directing sorption by nonpolar plastic materials in water and can aid studies regarding the risk assessment of plastic materials in the environment.

6.2 References

[1] D. Eerkes-Medrano, R. C. Thompson, and D. C. Aldridge, "Microplastics in freshwater systems: A review of the emerging threats, identification of knowledge gaps and prioritisation of research needs," *Water Res.*, vol. 75, pp. 63–82, 2015.

[2] Q. Chen *et al.*, "Pollutants in Plastics within the North Pacific Subtropical Gyre," *Environ. Sci. Technol.*, vol. 52, no. 2, pp. 446–456, 2018.

[3] G7Presidency, "Final Report by the Federal Government on the G7 Presidency 2015," Berlin, 2015.

[4] E. L. Teuten *et al.*, "Transport and release of chemicals from plastics to the environment and to wildlife," *Philos. Trans. R. Soc. B Biol. Sci.*, vol. 364, no. 1526, pp. 2027–2045, 2009.

[5] S. Endo, P. Grathwohl, and T. C. Schmidt, "Absorption or Adsorption ? Insights from Molecular Probes n -Alkanes and Cycloalkanes into Modes of Sorption by Environmental Solid Matrices," *Environ. Sci. Technol.*, vol. 42, no. 11, pp. 3989–3995, 2008.

[6] T. Hüffer, F. Metzelder, G. Sigmund, S. Slawek, T. C. Schmidt, and T. Hofmann, "Polyethylene microplastics influence the transport of organic contaminants in soil," *Sci. Total Environ.*, vol. 20, no. 657, pp. 242–247, 2019.

[7] T. H. Uber, T. Hüffer, S. Planitz, and T. C. Schmidt, "Characterization of sorption properties of high- density Polyethylene sheets using the poly-parameter linear-free energy relationships," *Environ. Pollut.*, vol. 248, no. C, pp. 312–319, 2019.

[8] A. A. Koelmans, A. Bakir, G. A. Burton, and C. R. Janssen, "Microplastic as a Vector for Chemicals in the Aquatic Environment: Critical Review and Model-Supported Reinterpretation of Empirical Studies," *Environ. Sci. Technol.*, vol. 50, no. 7, pp. 3315–3326, 2016.

[9] T. Hüffer, A. K. Weniger, and T. Hofmann, "Data on sorption of organic compounds by aged polystyrene microplastic particles," *Data Br.*, vol. 18, pp. 474–479, 2018.

[10] B. Xu, F. Liu, P. C. Brookes, and J. Xu, "Microplastics play a minor role in tetracycline sorption in the presence of dissolved organic matter," *Environ. Pollut.*, vol. 240, pp. 87–94, 2018.

[11] T. Hüffer and T. Hofmann, "Sorption of non-polar organic compounds by micro-sized plastic particles in aqueous solution.," *Environ. Pollut.*, vol. 214, no. 1, pp. 194–201, Apr. 2016.

[12] Y. Choi, Y. M. Cho, and R. G. Luthy, "Polyethylene-water partitioning coefficients for parent- and alkylated-polycyclic aromatic hydrocarbons and polychlorinated biphenyls," *Environ. Sci. Technol.*, vol. 47, pp. 6943–6950, 2013.

[13] A. Franck, B. Herr, H. Ruse, and G. Schulz, *Kunststoff Kompendium*, 7th ed. Vogel Business Media, 2011.

[14] T. Hüffer, A. K. Weniger, and T. Hofmann, "Sorption of organic compounds by aged polystyrene microplastic particles," *Environ. Pollut.*, vol. 236, pp. 474-4218–225, 2018.

[15] F. Metzelder, M. Funck, and T. C. Schmidt, "Sorption of Heterocyclic Organic Compounds to Multiwalled Carbon Nanotubes," *Environ. Sci. Technol.*, vol. 52, no. 2, pp. 628–637, Jan. 2018.

[16] D. Zhu, S. Kwon, and J. J. Pignatello, "Adsorption of single-ring organic compounds to

wood charcoals prepared under different thermochemical conditions," *Environ. Sci. Technol.*, vol. 39, no. 11, pp. 3990–3998, 2005.

[17] F. Metzelder, "Investigation of sorption properties of carbon nanomaterials using packed columns and inverse liquid chromatography Dissertation," University of Duisburg-Essen, 2018.

[18] S. Wagner, T. Hüffer, P. Klöckner, M. Wehrhahn, T. Hofmann, and T. Reemtsma, "Tire wear particles in the aquatic environment - A review on generation, analysis, occurrence, fate and effects," *Water Res.*, vol. 139, pp. 83–100, 2018.

[19] N. B. Hartmann *et al.*, "Are We Speaking the Same Language? Recommendations for a Definition and Categorization Framework for Plastic Debris," *Environ. Sci. Technol.*, vol. 53, no. 3, pp. 1039–1047, Feb. 2019.

[20] B. Slat *et al.*, *Feasibility Study - The Ocean Cleanup*. 2014.

[21] "AkzoNobel Partners with the Ocean Cleanup for Largest Clean-Up in History," *Focus Powder Coatings*, no. 6, p. 3, Jun. 2018.

Chapter 7 Appendix

7.1 List of Figures

7.2 List of Tables

7.3 List of Abbreviations and Symbols

A	Hydrogen bond acidity
12DCB	1,2-Dichlorobenzene
1Hex	1-Hexene
1Oct	1-Octene
a	Slope of linear fit
Aa	Ascorbic Acid
aHDPE	Aged high-density polyethylene
AIC	Akaike's information criterion
ANOVA	Analysis of variance
AP	Acetophenone
Atp	Atropine
Atz	Atrazine
B	Hydrogen bond basicity
Ba	Benzoic acid
BbF	Benzo[b]furan
Benz	Benzene
Benz	Benzene
Bezal	Benzaldehyde
Bzi	Benzil
Caf	Caffeine
cHept	Cycloheptane
cHex	Cyclohexane
cHexe	Cyclohexene
$C_{i,s}$	Sorbed sorbate concentration [ug kg^{-1}]
$C_{i,sat}$	Saturated aqueous solubility of the individual sorbate
$C_{i,w}$	Aqueous concentration [ug L^{-1}]
ClB	Chlorobenzene
cOct	Cyclooctane
cPente	Cyclopentene
Cph	Camphor
DNBE	Di-n-butyl ether
DNPE	Di-n-propyl ether
E	Excess molar refraction
e	Sorption potential [kJ mol^{-1}]
esw	Effective sorption potential [kJ mol-1]
Flu	Fluorene
FM	Freundlich Model
GC	Gas chromatography
GC-MS	Gas chromatography-mass spectrometry
Glu	Glucose
Glut	Glutaraldehyde
HDPE	High-density polyethylene
HOC	Hydrophobic organic carbons
HS	Headspace
iHex	Isohexane

ILC	Inverse Liquid chromatography
Ind	Indole
K_{aw}	Distribution coefficient between air and water [L kg^{-1}]
K_c	Distribution coefficient of cyclo-alkanes [L kg-1]
K_d	Distribution coefficient
K_F	Freundlich coefficient [(µg kg^{-1}) / (µg $L^{-1})^{1/n}$]
K_n	Distribution coefficient of n-alkanes [L kg^{-1}]
$K_{p/w}$	Distribution coefficient
L	Logarithmic hexadecane-air constant [L kg^{-1}]
LC	Liquid chromatography
LDPE	Low-density polyethylene
Lin	Linalool
LM	Linear model
LMM	Langmuir Model
log K_d	Logarithmic distribution coefficient [L kg^{-1}]
log $K_{p/w}$	Logarithmic polymer-water distribution coefficient [L kg-1]
log $K_{p/a}$	Logarithmic distribution coefficient between a polymer and air [L kg^{-1}]
log $K_{h/w}$	Logarithmic hexadecane/air coefficient
log K_{ow}	Logarithmic 1-octanol/water distribution coefficient [L kg^{-1}]
LSER	Linear solvation energy relationships
Ma	Methylamine
MMW	Medium molar mass
MP	Micro plastic particles
MPE	Methyl phenyl ether
MPE	Methyl phenyl ether
MRA	Multiple regression analysis
MS	Mass spectrometry
MTBE	Methyl tert-butyl ether
n	Freundlich exponent [-]
N	Number of data points
NaHDPE	Liquid column chromatography experiment with sodium chloride and high-density polyethylene
Naph	Naphthalene
Ner	Nerol
nHept	n-Heptane
nHex	n-Hexane
nOct	n-Octane
Non2on	2-Nonanone
nPB	n-Propylbenzene
Oct2on	2-Octanone
p	Number of fitting parameters
PA	Polyacrylate
PE	Polyethylene
PET	Polyethylene
PET	Polyethylene terephthalate

PMM	Polanyi-Manes model
PMMA	Poly(methyl methacrylate)
POM	Polyoxymethylene
PP	Polypropylene
Ppl	Phenolphthalein
ppLFER	Poly-parameter linear free-energy relationships
PS	Polystyrene
PSD	Passive-sampling-devices
PU	Polyurethane
PVC	Polyvinyl chloride
pXy	p-Xylene
Qmax	Maximum sorption capacity [ug kg^{-1}]
R	Retardation factor
R^2	Regression coefficient
ρ_b	Bulk density (kg m^{-3})
Rf	Retention factor
RMSE	Root mean squared error
RSD	Relative standard deviation
S	Dipolarity/polarizability
SE	Standard error of estimates
spLFER	Single-parameter linear free-energy relationships
Sty	Styrene
T	Absoluter temperature [K]
TCM	Trichloromethane
TDU	Thermal desorption unit
Tea	Triethylamine
TeCM	Tetrachloromethane
TetCe	Tetrachloroethene
T_g	Glass transition temperature
Tol	Toluene
tR	Retention time
TriCe	Trichloroethene
V	Molar volume
WSS_{res}	Weighted sum of squares residual
θ	Material pore volume (m^3)

7.4 List of Posters and Publications

Publications in peer-reviewed journals

Uber, T.H., Hüffer, T., Planitz, S., Schmidt, T.C. Characterization of sorption properties of high- density Polyethylene sheets using the poly-parameter linear-free energy relationships. *Environmental Pollution,* ***2019****,* 248, 312–319.

Uber, T.H., Hüffer, T., Planitz, S., Schmidt, T.C. Sorption of non-ionic organic compounds by polystyrene in water. *Science of the Total Environment*, submitted.

Poster presentations

Uber, T.H., Hüffer, T., Planitz, S., Schmidt, T.C. Characterization of sorption properties of polyethylene (PE) using the poly-parameter linear free-energy relationship model. *15th EuCheMS International Conference on Chemistry and the Environment*, *Leipzig,* ***2015.***

7.5 Curriculum Vitae

Der Lebenslauf ist in der Online-Version aus Gründen des Datenschutzes nicht enthalten.

7.6 Declaration of scientific contributions

The present thesis includes work that has been published in cooperation with co-authors, with my own contributions declared as follows:

Chapter 3

Tobias H. Uber, Thorsten Hüffer, Sybille Planitz, Torsten C. Schmidt

Characterization of sorption properties of high-density polyethylene using the poly-parameter linear free-energy relationships.

Envi. Poll 248 (2019) 312-319.

Declaration of own contribution: The experiments, including the batch experiments, IR analysis, TG analysis and density analysis were performed by THU (100 %). As an exception, medium molar mass measurements were performed by Philipp Korona (Westphalian University of Applied Sciences). TH, SP and TCS contributed to the discussion of the results. The draft and corrections to the manuscript were written by THU (100 %). SP and TCS supervised the study. The manuscript was revised by TH and TCS.

Chapter 4

Tobias H. Uber, Thorsten Hüffer, Sybille Planitz, Torsten C. Schmidt

Sorption of non-ionic organic compounds by polystyrene in water, Sci.Total Environ.

Submitted (2019).

Declaration of own contribution: The experiments, including the batch experiments, TG analysis and density analysis were performed by THU (100 %). As an exception, medium molar mass measurements were performed by Philipp Korona (Westphalian University of Applied Sciences) and IR measurements was performed by Heike Tewes (Westphalian University of Applied Sciences). TH, SP and TCS contributed to the discussion of the results. The draft and

corrections to the manuscript were written by THU (100 %). SP and TCS supervised the study. The manuscript was revised by TH and TCS.

Chapter 5

Tobias H. Uber, Titus Breski, Florian Metzelder, Sybille Planitz, Torsten C. Schmidt

Using inverse liquid chromatography to determine sorption properties of high-density polyethylene in water, unpublished manuscript.

Declaration of own contribution: ILC experiments were performed by THU and TB. TB performed the preliminary experiments and the data was evaluated by THU. The collected ILC data was interpreted by THU. Aging of the HDPE material was done by TB. TB, FM, SP and TCS contributed to the discussion of the results. The draft and corrections to the manuscript were written by THU (100 %). SP and TCS supervised the study. The manuscript was revised by TB, FM and TCS.

7.7 Erklärung

Hiermit versichere ich, dass ich die vorliegende Arbeit mit dem Titel

„Adsorption and desorption processes on polymers in aquatic systems"

selbst verfasst und keine außer den angegebenen Hilfsmittel und Quellen benutzt habe, und dass die Arbeit in dieser oder ähnlicher Form noch bei keiner anderen Universität eingereicht wurde.

Recklinghausen, im April 2019

Tobias Uber